DESIGN CONTROL DOCUMENT FOR THE
US-APWR
Chapter 4
Reactor

MUAP- DC004
REVISION 3
MARCH 2011

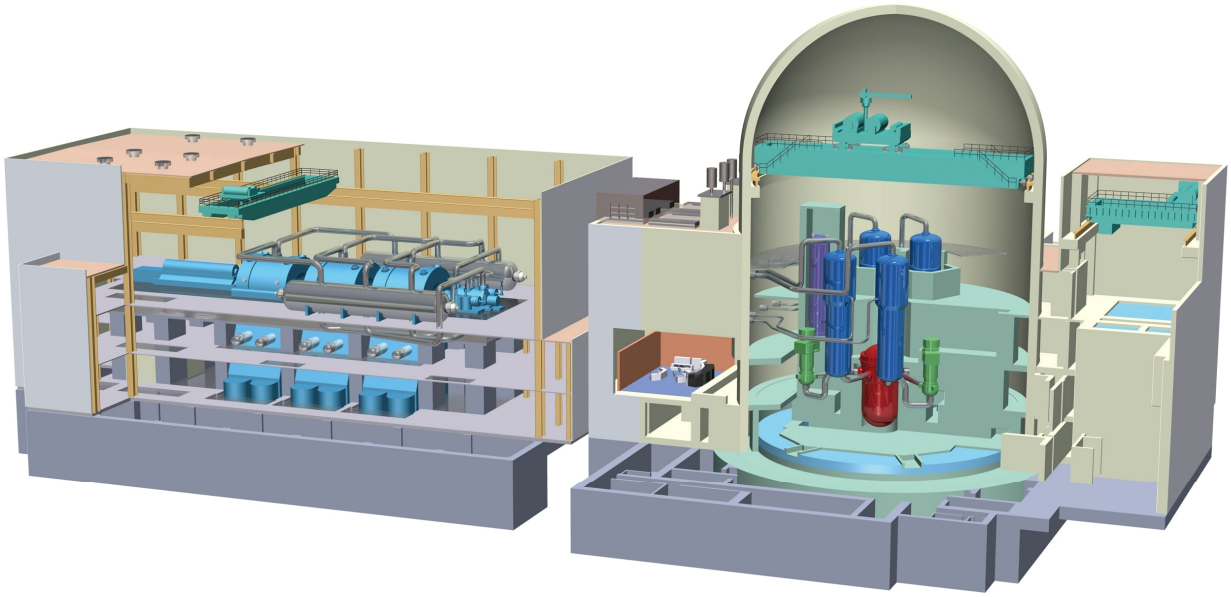

MITSUBISHI HEAVY INDUSTRIES, LTD.

Mitsubishi Heavy Industries, Ltd.

16-5, Konan 2-chome, Minato-ku

Tokyo 108-8215 Japan

CONTENTS

TABLES

FIGURES

ACRONYMS AND ABBREVIATIONS

AOO	anticipated operational occurrence
ASME	American Society of Mechanical Engineers
ATWS	anticipated transient without scram
BEF	best estimate flow
CFR	Code of Federal Regulations
COL	Combined License
CRDM	control rod drive mechanism
CRDS	control rod drive system
CVCS	chemical and volume control system
DAS	diverse actuation system
DCD	Design Control Document
DNB	departure from nucleate boiling
DNBR	departure from nucleate boiling ratio
ECCS	emergency core cooling system
EPRI	Electric Power Research Institute
GDC	General Design Criteria
ICCC	in-core control component
ICIS	incore instrumentation system
LOCA	loss-of-coolant accident
MD	movable neutron detector
MDF	mechanical design flow
MHI	Mitsubishi Heavy Industries, Ltd.
MMF	minimum measured flow
NPSH	net positive suction head
NRC	U.S. Nuclear Regulatory Commission
PCMI	pellet/cladding mechanical interaction
PCT	peak cladding temperature
PRA	probabilistic risk assessment
PWR	pressurized-water reactor
QAP	quality assurance program
RCCA	rod cluster control assembly
RCS	reactor coolant system
RG	Regulatory Guide
RIA	reactivity initiated accident
RTDP	revised thermal design procedure
RTP	rated thermal power
RV	reactor vessel

ACRONYMS AND ABBREVIATIONS (CONTINUED)

SG	steam generator
SIS	safety injection system
SLB	streamline break
SRP	Standard Review Plan
SSE	safe-shutdown earthquake
TC	thermocouple
TD	theoretical density
TDC	thermal diffusion coefficient
TDF	thermal design flow

4.0 REACTOR

Chapter 4 describes the fuel system design, nuclear design, thermal-hydraulic design, reactor materials, and the reactivity control system functional design.

4.1 Summary Description

This section provides an overview of the reactor system. The analytical techniques used in Chapter 4 are summarized and definitions of key technical terms used throughout Chapter 4 are also identified.

4.1.1 Reactor Overview

This subsection provides brief descriptions of the components which comprise the reactor, including the fuel assemblies, the reactor internals and the core control and monitoring components (Figure 4.1-1). Table 4.1-1 presents a summary of the principal US-APWR design parameters, together with design parameters for other typical licensed PWR plants for comparison purposes.

The US-APWR core consists of 257 mechanically identical fuel assemblies surrounded by the stainless steel neutron reflector described in Section 3.9.

The reactor internals provide support and alignment of the core, and direct the amount of coolant flow and its distribution within the reactor vessel. The upper reactor internals consist of the upper core support, upper core plate, upper support columns and control rod guide tubes. The lower core support plate is welded to the bottom of the core barrel, and supports all fuel assemblies, the neutron reflector, the flow diffuser plate and the energy absorber. The reactor internals are described in detail in Subsections 3.9.5 and 4.5.2.

The neutron reflector is located between the core barrel and the core, and forms the core cavity. Relative to conventional PWR baffle designs, the US-APWR neutron reflector improves neutron utilization and significantly reduces vessel irradiation.

The US-APWR fuel assembly utilizes a 17x17 array of 264 fuel rods, 24 control rod guide thimbles and one in-core instrumentation guide tube. The fuel rod and thimble components are bundled by grid spacers.

The fuel rods consist of slightly enriched cylindrical uranium dioxide pellets contained in a cylindrical tube made of zirconium-based alloy. During manufacture, the fuel rods are pressurized with helium and sealed with end plugs. The US-APWR axial active fuel length is approximately 14 ft (4200 mm). Some fuel rods may have fuel pellets containing gadolinia (Gd_2O_3) integral burnable absorber in full-length or part-length axial configurations. Detailed descriptions of the US-APWR fuel rod and fuel assembly design features are given in Section 4.2.

The US-APWR fuel design includes features that have been proven through extensive operating experience in Mitsubishi-fueled Japanese plants, as well as in United States and European plants. Such features include:

- ZIRLO™ fuel rod cladding,
- Zircaloy-4 grid spacers with a grid fretting-resistant design,
- a reconstitutable top nozzle, and
- an anti-debris bottom nozzle with a built-in filter.

The US-APWR fuel design uses 11 grid spacers that span the 14-ft active fuel length. The upper and lower grid spacers are made of nickel-chromium-iron Alloy 718 (Inconel 718), and the nine intermediate grid spacers are made of Zircaloy-4. The grid-to-grid distance for the US-APWR design is basically the same as that for the 12-ft Mitsubishi fuel with a nine grid spacer design, thus ensuring a similar resistance to failures due to fretting wear, the same proven coolant mixing and DNB performance as the 12-ft Mitsubishi fuel design. The intermediate grid spacer is designed based on current version in use in Mitsubishi-fueled reactors with advanced mixing vanes.

The fuel assembly top and bottom nozzles provide structural support and alignment within the core. The top nozzle has Inconel 718 hold-down springs to prevent fuel assembly lift during normal operation and transients. The top nozzle also provides alignment for insertion of control and instrumentation components. The bottom nozzle is designed to provide adequate flow and prevent debris from entering the fuel assembly.

Mitsubishi has manufacturing and operational experience for 23 nuclear plants with over 400 cycles of operation using over 17,000 fuel assemblies. Mitsubishi has a record of excellent fuel performance. The fuel assembly design features described above are within Mitsubishi's manufacturing and operational experience, and its analytical capabilities.

Sixty-nine rod cluster control assemblies (RCCAs) are used in a pattern in the core to provide relatively rapid reactivity control. Each RCCA consists of 24 rods connected to a central hub (a configuration called "spider assembly") that couples with the control rod drive mechanism, as described in Subsections 3.9.4 and 4.5.1. The rods are designed to be inserted into the fuel assembly guide thimble. Each rod contains Silver-Indium-Cadmium absorber material in stainless steel cladding.

Discrete burnable absorber rods or primary and/or secondary neutron sources may also be inserted into the fuel assembly guide thimbles. Discrete burnable absorbers are used to limit the required initial amount of soluble boron in the coolant and to provide compensatory reactivity control change to account for effects such as fuel burnup. Burnable absorbers are also used for local power peaking control.

The core power distribution is periodically monitored by using movable in-core neutron detectors and constantly surveyed by fixed neutron ex-core detectors. The in-core instrumentation is top-mounted, and detectors are inserted through the in-core instrumentation guide tube to monitor the entire fuel assembly active length. The strategically located in-core detector positions provide sufficient information to reconstruct detailed three-dimensional power distributions. The ex-core detectors provide on-line global axial and radial power distribution data and power changes, and provide input to

automatic control functions. Thermocouples at the outlets of a subset of fuel assemblies also provide core performance data.

4.1.2 Analytical Techniques

Table 4.1-2 contains a brief summary of the primary techniques and codes used for the analyses described in Chapter 4. Detailed descriptions are provided in the individual subsections as listed in the table.

4.1.3 Definitions

The terms linear heat rate (LHR) or linear power density is the thermal power generated per unit length of fuel; typical units used are kW/ft.

The average linear heat rate (ALHR) is the total thermal power generated in the fuel rods, divided by the total core active heated length.

The peak linear heat rate (PLHR) is the maximum linear heat rate produced by any fuel in the core.

The nuclear enthalpy rise hot channel factor ($F^N_{\Delta H}$) is the ratio of the maximum integrated rod power within the core to the average rod power.

The axial offset (AO) represents the power difference between the upper and bottom halves of the core and it is defined as (PT - PB) / (PT + PB) where PT is the integrated power in the top half of the core and PB is the integrated power in the bottom half of the core.

The heat flux hot channel factor or total peaking factor (F_Q) is the maximum local heat flux on the surface of a fuel rod divided by the average fuel rod heat flux. F_Q includes an allowance for fuel pellet and fuel rod manufacturing tolerances as well as the calculational uncertainty. Alternatively, F_Q can be described as the ratio between the peak and average linear heat rates.

Departure from nucleate boiling (DNB) is the onset of transition from nucleate boiling to film boiling. DNB ratio (DNBR) is the ratio of DNB heat flux to actual heat flux, and is used as an index of margin to DNB condition.

4.1.4 Plant Condition Categorizations

The plant conditions for design are categorized in Standard Review Plan (SRP) 15.0 and 4.2 (Reference 4.1-1), as follows:

- Normal operation.
- Anticipated operational occurrences (AOOs): those conditions that are expected to occur one or more times during the life of a nuclear power plant.
- Postulated accidents: accidents that are postulated but not expected to occur during the life of the nuclear power plant.

The reactor is designed so that it meets the following acceptance criteria for AOOs:

- Pressure in the reactor coolant and main steam systems should be maintained below 110 percent of the design values in accordance with the American Society of Mechanical Engineers (ASME) Boiler and Pressure Vessel Code (Reference 4.1-2).

- Fuel cladding integrity should be maintained by ensuring that the minimum departure from nucleate boiling ratio (DNBR) remains above the acceptable design DNBR on a 95/95 basis.

- The maximum fuel centerline temperature should be less than the fuel melting point so that the fuel cladding will not be mechanically damaged.

- An AOO should not generate a postulated accident without other faults occurring independently or result in a consequential loss of function of the reactor coolant system (RCS) or reactor containment barriers.

For postulated accidents,

- Pressure in the RCS and main steam system should be maintained below the acceptable design limits, considering potential brittle as well as ductile failures.

- Fuel cladding integrity will be maintained if the minimum DNBR remains above the design limits. If the minimum DNBR does not meet these limits, the fuel is assumed to have failed.

- The release of radioactive material should not result in offsite doses in excess of the guidelines of 10 CFR Part 100.

- A postulated accident, should not, by itself, cause a consequential loss of required functions of systems needed to cope with the fault, including those of the RCS and reactor containment barriers.

- In addition, for loss-of-coolant accidents (LOCA), the following 10 CFR 50.46 criteria also apply:

  - The calculated maximum fuel element cladding temperature, total oxidation, and hydrogen generation should not exceed the limits in SRP 15.0.

  - Calculated changes in core geometry shall be such that the core remains amenable to cooling.

Detailed classification of AOOs and postulated accidents is shown in Chapter 15.

4.1.5 Combined License Information

No additional information is required to be provided by a COL Applicant in connection with this section.

4.1.6 References

4.1.1 U.S. Nuclear Regulatory Commission, Standard Review Plan for the Review of Safety Analysis Reports for Nuclear Power Plants, NUREG-0800, March 2007.

4.1.2 Nuclear Power Plant Components, Article NB-7000, Protection Against Overpressure, ASME Boiler and Pressure Vessel Code, Section III.

4.1.3 Vogtle Electric Generating Plant, Updated Final Safety Analysis Report Revision12, November 5, 2004.

4.1.4 South Texas Project Electric Generating Station (STPEGS) Units 1 and 2, Updated Final Safety Analysis Report (UFSAR), Revision 12, September, 2004.

Table 4.1-1 Comparison of Principal Reactor Design Parameters (Sheet 1 of 3)

Parameter	US-APWR	Typical 12-ft 4-loop PWR (Ref. 4.1-3)	Typical 14-ft 4-loop PWR (Ref. 4.1-4)
Key Reactor Parameters			
Core thermal output (MWt)	4451	3565	3853
System pressure (psia)	2250	2250	2250
Inlet temperature (°F)	550.6	556.8	549.8 to 561.2
Core average temperature (°F)	588.8	592.2	586.9 to 597.8
Vessel average temperature (°F)	583.8	588.4	582.3 to 593.8
Vessel thermal design flow (10^6 lbm/hr)	168.2	139.4	145.0
Core bypass flow (%)	9.0	6.4	8.5
Reactor Structural Parameters			
Equivalent core diameter (cold, ft)	12.8	11.1	11.1
Thermal shield/reflector design	Neutron Reflector	Neutron Panel	Neutron Pad
Core barrel ID/OD (in)	175.98/181.97	148.0/152.5	148.0/152.5
Fuel Parameters			
Number of fuel assemblies	257	193	193
Fuel assembly array Number of fuel rods	17x17 264	17x17 264	17x17 264
Effective fuel length (in)	165.4	143.7	168
Assembly overall dimensions (in) Fuel rod pitch (in)	8.426 x 8.426 0.496	8.426 x 8.426 0.496	8.426 x 8.426 0.496
Uranium dioxide per fuel assembly, nominal (lb)	1350	1058	1352
Fuel rod OD (in)	0.374	0.360	0.374
Pellet-cladding gap (in)	0.0033	0.0031	0.0033
Cladding thickness (in)	0.0224	0.0225	0.0225

Table 4.1-1 Comparison of Principal Reactor Design Parameters (Sheet 2 of 3)

Parameter	US-APWR	Typical 12-ft 4-loop PWR (Ref. 4.1-3)	Typical 14-ft 4-loop PWR (Ref. 4.1-4)
Fuel pellet material	Sintered UO_2 Sintered $(U,Gd)O_2$	Sintered UO_2	Sintered UO_2
Fuel pellet diameter (in)	0.322	0.3088	0.3225
Fuel pellet density (%TD)	97	95	95
Number of grids per assembly	11	8	10
Fuel pellet length (in) Blanket pellet length (in)	0.453	0.370 0.462/0.500	0.387 (0.462)[a]
Rod Cluster Control Assemblies			
Neutron absorber material	Ag-In-Cd	Ag-In-Cd or Hafnium	Hafnium or Ag-In-Cd
Number of clusters	69	53	57
Number of absorber rods per cluster	24	24	24
Absorber diameter (in)	0.341	0.341	0.366
Cladding material thickness, for Ag-In-Cd (in)	Type 304 SS 0.0185	Type 304 SS 0.0185	Type 304 SS 0.0185
Key Core Design Limits & Conditions			
Total heat flux hot channel factor, F_Q	2.60	2.50	2.70
Fraction of heat generated in the fuel (%)	97.4	97.4	97.4
Maximum fuel centerline temperature during AOOs (°F)	≤4620	≤4700	≤4700
Maximum peak linear heat rate during AOOs[b],[c] (kW/ft)	≤21.9 (assuming overpower of 120%)	≤22.4 (assuming overpower of 120%)	≤22.0 (assuming overpower of 118%)
Minimum DNBR during AOOs Typical channel Cold wall (thimble) channel	≥1.35 ≥1.33	≥1.24 ≥1.23	≥1.26 ≥1.24
Correlation used for above DNBR values	WRB-2	WRB-2	WRB-1

Table 4.1-1 Comparison of Principal Reactor Design Parameters (Sheet 3 of 3)

Parameter	US-APWR	Typical 12-ft 4-loop PWR (Ref. 4.1-3)	Typical 14-ft 4-loop PWR (Ref. 4.1-4)
Effective heat transfer area on fuel surface[(b)] (ft^2)	91,360	57,505	69,700
Normal operation core average linear heat rate[(b)] (kW/ft)	4.65	5.69	5.20
Normal operation peak linear heat rate[(b)] (kW/ft)	12.1	14.2	14.0
Normal operation core average heat flux[(b)] (10^6 Btu/hr-ft^2)	0.162	0.206	0.181
Normal operation peak heat flux[(b)] (10^6 Btu/hr-ft^2)	0.421	0.515	0.489
Effective flow area for core cooling (ft^2)	68.0	54.1	51.3
Core average coolant mass velocity (10^6 lbm/hr-ft^2)	2.25	2.41	2.59
Core average coolant velocity (ft/s)	14.1	15.4	15.6

Notes:

(a) Annular pellets

(b) Based on densified active heated length

(c) See subsection 4.4.2.11.5

Table 4.1-2 Analytical Techniques Summary (Sheet 1 of 2)

Design Category	Analysis Techniques/Approach	Primary Code (s) Used	Referenced Sections
Fuel			
Key parameters such as rod interna pressure, cladding oxidation, fuel temperatures and cladding stress, strain	Fuel performance models using thermal, fission gas release, corrosion and hydrogen uptake based on extensive empirical data	FINE	Subsection 4.2.3 Subsection 4.4.2.11
Loads, stress and deflection of fuel assembly components	Static and dynamic analyses of fuel assembly components for events occurred during normal operation, AOOs and postulated accidents	Finite element method codes such as ANSYS or ABAQUS FINDS	Subsection 4.2.3
Nuclear			
Few-group microscopic and macroscopic cross-sections	Collapse of fine-group data and spatial homogenization, performed by 2D current coupling collision probability methods (CCCP)	PARAGON	Subsection 4.3.3.1
3D power distributions, peaking factors, fuel depletion, boron concentrations, reactivity coefficients, control rod worth, transient fission product behavior (Xe, Sm)	2-group diffusion theory applied with a nodal expansion method (NEM)	ANC	Subsection 4.3.2 4.3.3.1
Vessel Irradiation			
Fast neutron flux	Discrete ordinates Sn transport methodology	DORT	Subsection 4.3.2.8
Criticality			
Criticality of reactor, fuel assemblies, new and spent fuel racks, fuel handling	Monte-Carlo methodology	MCNP	Subsection 4.3.2.6 4.3.3.2
Thermal-Hydraulic			

Table 4.1-2 Analytical Techniques Summary (Sheet 2 of 2)

Design Category	Analysis Techniques/Approach	Primary Code (s) Used	Referenced Sections
Steady-state and transient conditions	Subchannel analysis of local fluid conditions in the core, solving mass, momentum and energy conservation equations for steady state/transient conditions	VIPRE-01M	Subsection 4.4.4.5

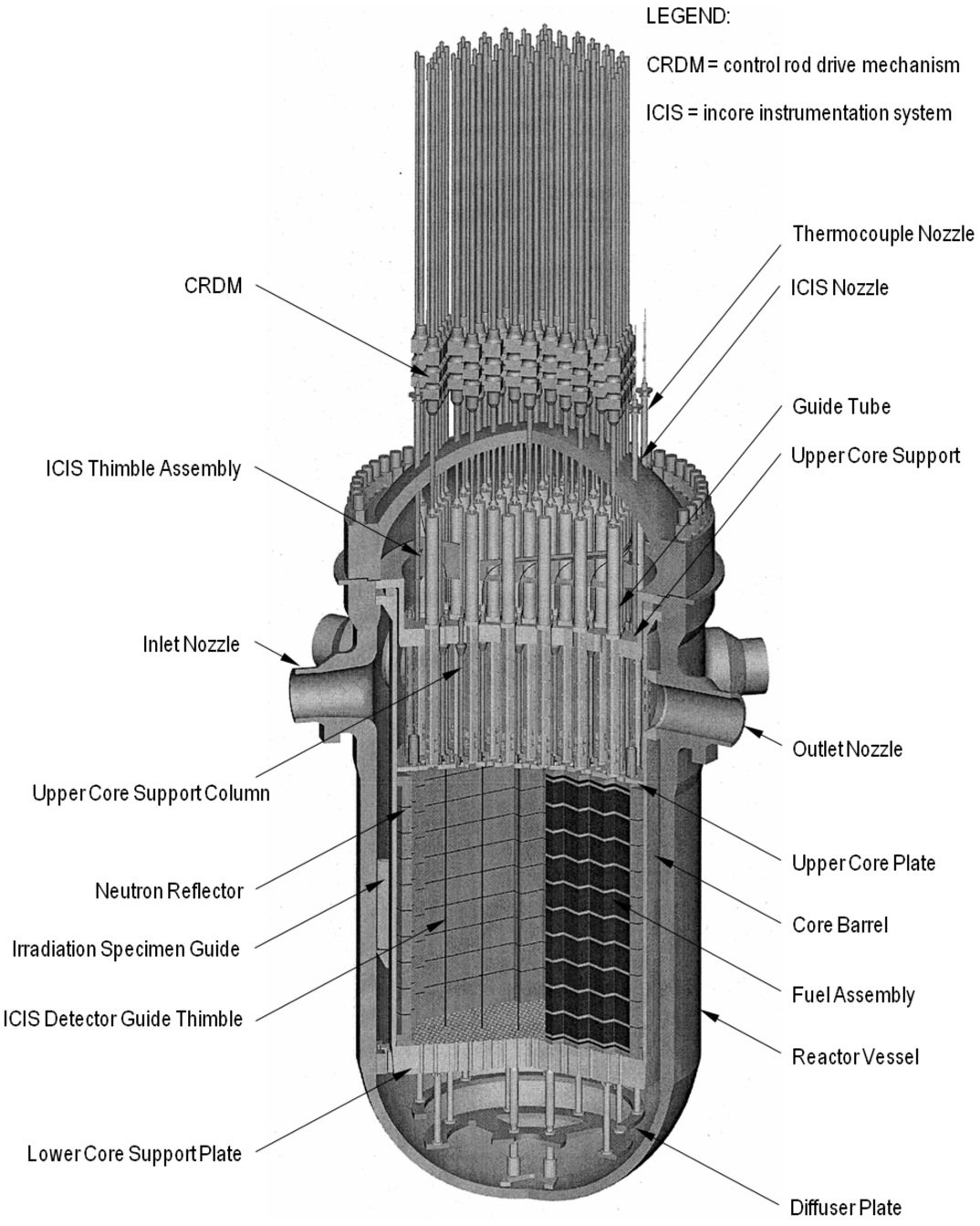

Figure 4.1-1 Reactor General Assembly

4.2 Fuel System Design

Design requirements for the fuel system are described in the NRC Standard Review Plan (SRP) 4.2 (Reference 4.2-1). These requirements are in compliance with General Design Criteria (GDC) 10, 27 and 35 of 10 CFR 50 Appendix A (Reference 4.2-2), with 10 CFR 50.46 (Reference 4.2-3) and with 10 CFR 100 (Reference 4.2-4). They are also consistent with Section C.I.4.2 of Regulatory Guide 1.206 (Reference 4.2-5).

The objectives of the fuel system design in safety analysis are to assure that:

a. the fuel system is not damaged as a result of normal operation and anticipated operational occurrences (AOOs),

b. fuel system damage is never so severe as to prevent control rod insertion when it is required,

c. the number of fuel rod failures is not underestimated for postulated accidents, and

d. coolability is always maintained.

Consideration related to anticipated transients without scram (ATWS) are discussed in Section15.8.

4.2.1 Design Bases

The design bases and associated design criteria for the Mitsubishi US-APWR fuel rod and fuel assembly design are described in detail in the “Mitsubishi Fuel Design Criteria and Methodology” topical report, MUAP-07008-P (Reference 4.2-6) and in the “US-APWR Fuel System Design Evaluation”, MUAP-07016-P (Reference 4.2-7). These design bases and criteria are consistent with the fuel design requirements identified in the NRC Standard Review Plan (Reference 4.2-1). The analysis methods presented in these topical reports have been established and justified for application up to the rod design burnup of 62,000MWD/MTU for the US-APWR.

Design bases for the US-APWR fuel rod, which are individually described in the following subsections, are established to prevent fuel rod failure and fuel system damage in terms of the fuel criteria, such as fuel temperature, internal pressure, cladding stress, cladding strain and fatigue usage. The design bases consider influences of irradiation behavior such as pellet density, fission product gas release, cladding creep, oxidation and other physical phenomena, on those parameters above.

As also described in the following subsections, the design bases for the US-APWR fuel assembly consider functional requirements for the fuel assembly and provide limiting loads and/or stresses on the fuel assembly components. The loads and stresses are those due to normal operation, AOOs and postulated accidents in addition to non-operational condition such as shipping and handling.

For purposes of safe shutdown, maintaining sub-criticality and adequate reactivity control of the reactor, design bases for in-core control components are established in terms of thermal-physical properties of absorber material, compatibility of the absorber and

cladding material, cladding stress-strain limits, and irradiation behavior of absorber material (Reference 4.2-7).

4.2.1.1 Cladding

The cladding material for the US-APWR fuel design is ZIRLO^{TM}. The ZIRLO alloy was developed by Westinghouse Electric Corporation (“Westinghouse”) for improved corrosion resistance.

4.2.1.1.1 Mechanical Properties

The ZIRLO alloy is a zirconium based alloy with improved corrosion properties, low neutron absorption cross section for good fuel economy, high strength and ductility under reactor operating conditions, and excellent chemical compatibility with the fuel. These properties are described in Appendix B of Reference 4.2-6. Mitsubishi currently uses ZIRLO cladding for high burnup fuel in Japan.

4.2.1.1.2 Stress-Strain Limits

4.2.1.1.2.1 Cladding Stress

The ASME Boiler and Pressure Vessel Code, Section III (Reference 4.2-8) criteria are applied for cladding stress. All cladding stresses except for pellet/cladding mechanical interaction (PCMI) related stress, are considered in the stress evaluation and are assessed according to ASME Section III limits.

Category	Limit
Primary Membrane	Sm
Primary Membrane + Bending	1.5 Sm
Primary Membrane + Bending + Local	1.5 Sm
Primary Membrane + Bending + Local + Secondary	3.0 Sm

The allowable stress intensity, Sm, is the minimum of two thirds of the cladding yield stress and one third of the cladding ultimate stress, with consideration of operating temperature and irradiation.

4.2.1.1.2.2 Cladding Strain

Cladding strain during normal operation is less than 1% relative to the un-irradiated condition. This criterion assures that the dimensional change of the cladding due to cladding creep during normal operation remains within the ductility limits for the cladding.

During power transients associated with AOOs, the total cladding strain change, elastic plus plastic, remains below 1% relative to the pre-transient condition. This criterion limits the cladding strain due to pellet/cladding mechanical interaction (PCMI).

4.2.1.1.3 Vibration and Fatigue

4.2.1.1.3.1 Vibration

The fuel rod is not damaged by fuel cladding fretting wear due to flow-induced vibration during normal operation. The maximum fretting wear depth that could occur on the cladding surface is limited to assure that fuel damage does not occur (Reference 4.2-6).

4.2.1.1.3.2 Fatigue

The cumulative fatigue usage over the life of the fuel is less than 1.0, with consideration of a safety factor of 2 applied to the stress amplitude or a safety factor of 20 applied to the number of cycles to failure, whichever is most limiting. The fatigue design curve is based on the work of Langer and O'Donnell (Reference 4.2-9) and is given in Reference 4.2-6.

4.2.1.1.4 Chemical Properties

Chemical properties of the ZIRLO cladding material are similar to those of Zircaloy-4 as discussed in Appendix B of Reference 4.2-6.

4.2.1.2 Fuel Material

4.2.1.2.1 Thermal-Physical Properties

To prevent fuel from overheating under normal operation and AOOs, the calculated fuel centerline temperature does not exceed the melting temperature of the fuel, with consideration of uncertainties. The melting temperature is 5072°F (2800°C) and 4892°F (2700°C) for un-irradiated uranium dioxide(UO_2) fuel and gadolinia-uranium dioxide($(Gd,U)O_2$) fuel respectively, and decreases with burnup by 58°F (32°C) per 10 GWD/MTU. The nominal density for the US-APWR fuel design is 97%TD. Additional details on the material properties of uranium dioxide fuel and gadolinia-uranium dioxide fuel are provided in Appendix B of Reference 4.2-6.

4.2.1.2.2 Fuel Densification and Fission Product Swelling

Fuel densification and swelling are modeled in the Mitsubishi FINE code and are verified by extensive data (Reference 4.2-6). The FINE code evaluates cladding stress, cladding strain, fatigue, fuel temperature, rod internal pressure, etc., using the fuel densification model and the swelling model.

4.2.1.2.3 Chemical Properties

Chemical compatibility of the fuel with other fuel rod materials and the reactor coolant is discussed in detail in Appendix B of Reference 4.2-6.

4.2.1.3 Fuel Rod Performance

4.2.1.3.1 Analytical Models

The FINE code incorporates all of the basic fuel rod performance models required to evaluate in-reactor fuel behavior. The FINE code fuel performance models are described in detail in Chapter 4 of Reference 4.2-6. A summary of these models is provided in Subsection 4.2.3. The uncertainties in the fuel performance models and in the fuel fabrication are taken into account to obtain conservative evaluations of the fuel rod performance.

4.2.1.3.2 Mechanical Design Limits

4.2.1.3.2.1 Cladding Collapse

On the basis of the extensive operating experience of Mitsubishi fuel in Japan, it is concluded that cladding collapse does not occur for pre-pressurized fuel rods with initial fuel pellet density of 95%TD or greater. Maintaining initial pellet density of 95%TD or greater, with current fabrication processes, results in a fuel pellet that is relatively stable with respect to fuel densification, so that any pellet-pellet gaps are too small for cladding collapse to occur. In addition, the initial helium pressurization reduces the differential between the system pressure and the rod internal pressure and provides additional resistance to cladding collapse. Therefore, cladding flattening does not occur. Cladding collapse is discussed in detail in References 4.2-6 and 4.2-7.

4.2.1.3.2.2 Rod Internal Pressure

The fuel rod internal pressure remains below the lowest of the following three rod internal pressure design limits.

- No cladding liftoff during normal operation
- No reorientation of the hydrides in the radial direction in the cladding
- A description of any additional failures resulting from departure of nucleate boiling (DNB) caused by fuel rod overpressure during transients and postulated accidents

These limits are described more completely in References 4.2-6 and 4.2-7.

4.2.1.4 Grid Spacer

Subsections 4.2.1.4.1 and 4.2.1.4.2 present the acceptance limits applied to the grid spacer for mechanical strength and for vibration and fatigue, respectively, to address the criteria for RCCA insertability for reactor safe shutdown and core coolability, and for proper support for the fuel rod.

4.2.1.4.1 Mechanical Limits and Material Properties

It is important for the grid spacer to maintain an appropriate restraint force for the fuel rods, proper geometrical configuration of the control rod guide thimbles and dimensional

stability to prevent excessive closure of the fuel rod to rod spacing and interference with other fuel assemblies and the neutron reflectors. The grid spacers made of nickel-chromium-iron alloy 718 (called “Inconel 718”) and Zircaloy-4 are appropriately designed, considering variations of the above characteristics caused by high temperature and irradiation.

The grid spacer is tough enough so as not to prevent control rod insertion, even if the combined loads resulting from earthquake and loss-of-coolant accident (LOCA) causes deformation of the grid spacer. Characteristics such as the buckling load, deformation after buckling and stiffness of the grid spacer are obtained by impact tests accounting for the operating temperatures at a 95% confidence level.

The grid spacer spring does not fail throughout the fuel lifetime due to fatigue that results from flow-induced vibration of the fuel rod.

The upper and lower grid spacers are made of Inconel 718, which shows sufficient stability in terms of chemical reactions such as corrosion and hydrogen absorption (Reference 4.2-7). Oxidation and hydriding of Zircaloy-4, the material used for the intermediate grid spacers, are restricted within limits that are determined to prevent degradation of mechanical properties (Reference 4.2-7).

4.2.1.4.2 Vibration and Fatigue

Cladding fretting wear limits are provided in Subsection 4.2.1.1.3.1. The grid spacers provide sufficient grid spring contact force to support the fuel rod throughout its fuel life, thus minimizing the impact of fuel rod vibration on cladding fretting wear (References 4.2-6 and 4.2-7). Vibration of the fuel rod is also limited to preclude fatigue of the grid spacer spring.

4.2.1.5 Fuel Assembly

With respect to functional requirements including safe shutdown and coolability of the reactor, the structural integrity of the fuel assemblies is maintained by satisfying appropriate design limits for stresses and loads associated with normal operation, AOOs and postulated accidents in addition to non-operational conditions such as shipping and handling. As discussed in Subsections 4.2.1.5.1 through 4.2.1.5.3, acceptance limits for the stresses and the loads to maintain the above requirements are established for the fuel assembly components such as the top and bottom nozzles, control rod guide thimbles, grid spacers, and joints of the components (References 4.2-6 and 4.2-7).

4.2.1.5.1 Loads Applied by Core Restraint System

To keep the fuel stack in the proper position and to prevent fuel assembly damage due to impact following liftoff, fuel assembly liftoff does not occur due to worst case hydraulic load during normal operation and AOOs, except for pump-over-speed condition. This design basis requires that the force applied by the holddown spring be properly designed (Reference 4.2-6). Thermal-hydraulic design is discussed in Section 4.4.

The following design criteria are applied to maintain coolable geometry of the core and to provide for the safe shutdown of the reactor. The criteria assure that significant structural

deformation of the fuel assembly will not occur under anticipated loads during normal operation and AOOs (Reference 4.2-7).

- The fuel assembly experiences neither excessive distortion nor damage by compressive loads due to interference with the top nozzle and the upper core plates during irradiation. This criterion requires that the clearance between the top nozzle and the upper core plate is maintained throughout the fuel assembly lifetime.

- To supply the expected thermal power and maintain fuel rod integrity during irradiation, the fuel rods do not experience excessive bowing nor be damaged by excessive compressive loads. Therefore, the clearance between the fuel rod and the top and bottom nozzles does not close during irradiation due to the differential axial growth and thermal expansion of the fuel rods and the control rod guide thimbles.

- The stresses in the top nozzle and the control rod guide thimbles, except for the dashpot region, are less than the acceptance limit based on ASME Section III (Reference 4.2-8) under the loads imposed by a RCCA scram during normal operation.

- The stresses in the bottom nozzle and the dashpot region of control rod guide thimbles during normal operation and reactor scram are less than the acceptance limit based on ASME Section III (Reference 4.2-8). The maximum loads are defined by summation of the loads during normal operation, the impact force of the RCCA on the top nozzle and the reaction force when the RCCA is decelerated in the dashpot region.

- Fatigue usage factors for the top and bottom nozzles and the control rod guide thimbles are less than 1.0 considering cyclic loading during normal operation and AOOs. The evaluation of the fatigue usage factors includes a safety factor of 2 on stress amplitude or a safety factor of 20 on the number of cycles, whichever most limiting.

- Significant fretting wear does not occur at the contact points other than those between the fuel rod and the grid spacer.

The stress intensity limits defined by ASME Section III (Reference 4.2-8) are described in Subsection 4.2.1.1.2.1.

For the Zircaloy-4 components, the allowable stress intensity, Sm, is the minimum of two thirds of the yield stress and one third of the Zircaloy-4 ultimate stress with consideration of reactor operating temperature. For conservatism, the un-irradiated mechanical properties are used. For the stainless steel components, the allowable stress intensity, Sm, is defined by ASME Section III (Reference 4.2-8).

Oxidation and hydrogen absorption in Zircaloy-4 material such as the control rod guide thimbles are restricted within acceptance limits that are determined to prevent degradation of mechanical properties (Reference 4.2-7).

4.2.1.5.2 Analysis of Combined Shock (including LOCA) and Seismic Loading

As stated in Appendix A of Reference 4.2-1, core coolability and safe shutdown of the reactor are maintained with consideration of the combination of earthquake and postulated accident loads (Reference 4.2-6). The following criteria are applied to prevent structural deformation of the fuel assembly and its components.

Under combined earthquake and postulated accident loads:

- Deformation of the grid spacer does not prevent the control rods from being inserted into the fuel assembly,
- The stresses in the control rod guide thimbles and the top and bottom nozzles are less than the allowable stress intensity based on Appendix F of ASME Section III (Reference 4.2-8),
- The control rod guide thimble does not experience buckling due to axial loads caused by earthquake and postulated accidents, and
- Combined cladding stresses resulting from response to earthquake and postulated accidents are less than 90% of cladding yield stress at operating temperature.

4.2.1.5.3 Loads Applied in Fuel Shipping and Handling, Including Misaligned Handling Tools

To assure that the fuel assembly does not experience excessive deformation during shipping and handling, the following design criteria are applied (References 4.2-6 and 4.2-7).

- Under axial loading during shipping and handling, stresses in the top and bottom nozzles and the control rod guide thimble are less than the allowable stress intensity based on ASME Section III (Reference 4.2-8).
- Under axial loading during shipping and handling, the maximum forces in the joints between the top nozzle and the control rod guide thimbles, and between the grid spacers and the guide thimbles are less than the acceptance limits of loads experimentally obtained.
- Under lateral loading during shipping and handling, inelastic deformation of the grid spacer spring is not increased.
- The grid spacer spring is not damaged due to vibration during shipping.

4.2.1.6 In-Core Control Components

The functions and kinds of in-core control components used in the US-APWR are described below.

- Rod cluster control assembly: For reactor shutdown and reactivity control
- Burnable absorber assembly: For reactivity control
- Neutron source assembly: For supplying neutrons at reactor startup and for sensitivity increase of neutron detectors in order to monitor sub-criticality
- Thimble plug assembly: For limiting bypass flow in the reactor

These in-core control components are inserted into the control rod guide thimbles of the fuel assemblies and do not interfere with reactor cooling.

Design bases for the in-core control components are determined in terms of the following aspects:

- Thermal-physical properties of absorber material,
- Compatibility of the absorber and cladding material,
- Cladding stress-strain limits, and
- Irradiation behavior of absorber material.

Cladding stress of all in-core control component claddings meets stress intensity limits in ASME Section III. Sm is determined to be two thirds of Sy, taking into account the mechanical property of cold-worked type 304 stainless steel.

4.2.1.6.1 Rod Cluster Control Assembly

Design bases for the control rod and the rod cluster control assembly (RCCA) including those aspects are as follows:

- The absorber temperature during usage is less than its melting point.
- Adequate clearance in diameter between the control rod cladding and the control rod guide thimble is maintained throughout the lifetime of the rod cluster control assembly.
- The absorber material has sufficient compatibility with the cladding material.
- Taking into account irradiation behavior of the control rod cladding and the contained absorber materials, and acceleration by stepped movement of control rod driving mechanism (CRDM), the cladding stress meets stress intensity limits in ASME Section III (Reference 4.2-8) during normal operation, AOOs and postulated accidents.
- The absorber material and its nuclear reaction products have low chemical reactivity with the coolant in case of cladding failure.

- Cladding of the control rod does not fail due to fatigue during the lifetime of the rod cluster control assembly.

To assure safe shutdown and coolabilty of the reactor, and efficient performance:

- Insertion of the control rod is not interrupted by misalignment of the control rod guide thimbles.
- It is possible for the control rods to be inserted to the fuel assembly during an earthquake and a postulated accident.
- No significant wear in the control rod cladding occurs during the rod cluster control assembly lifetime.

4.2.1.6.2 Burnable Absorber Assembly

Taking into account the four aspects of irradiation and material behavior, as given in Subsection 4.2.1.6, the design bases for the burnable absorber rod and the burnable absorber assembly are as follows.

- The absorber temperature during usage is less than its softening point.
- Diametrical clearance is adequately maintained in between the burnable absorber rod cladding and the control rod guide thimble during the burnable absorber assembly lifetime.
- The absorber material has sufficient compatibility with the cladding material.
- Taking into account irradiation behavior of the burnable absorber rod cladding and the contained absorber materials, the cladding stress meets stress intensity limits in ASME Section III (Reference 4.2-8) during the normal operation, AOOs and postulated accidents.
- The absorber material and nuclear reaction products have low chemical reactivity to the coolant in case of cladding failure.
- A significant wear in the burnable absorber cladding does not occur during the lifetime.

4.2.1.6.3 Neutron Source Assembly

Taking into account the four aspects of irradiation and material behavior given in Subsection 4.2.1.6, the design bases for the primary and secondary neutron source rods and their assemblies are as follows.

- The temperature of the primary and the secondary sources during usage is less than their melting point.
- The neutron source material has sufficient compatibility with the cladding material.

- Cladding stresses caused by differential pressure between the inside and outside of both neutron source rods meet stress intensity limits in ASME Section III (Reference 4.2-8) during normal operation, AOOs and postulated accidents.

- The primary and secondary source materials and their nuclear reaction products have low chemical reactivity to the coolant in case of cladding failure. Alternatively, sufficient prevention in structure is adopted.

- No significant wear in the cladding of the neutron source occurs during the neutron source assembly lifetime.

4.2.1.6.4 Thimble Plug Rods and Assembly

Thimble plug rods, which are solid rod structures, do not require special design criteria.

4.2.1.7 Surveillance Program

The US-APWR fuel assembly is designed and manufactured based on the substantial database obtained from the testing and fuel surveillance programs on Mitsubishi conventional fuel assemblies, which has been used for verification of fuel performance and validation of the design bases, as described in Reference 4.2-6.

A surveillance program for the US-APWR fuel assembly will be established for verification of the fuel performance and validation of the design bases. This surveillance program will specify the inspection items, inspection criteria, methodology, schedule, number of fuel assemblies and in-core control components such as burnable absorbers and RCCAs, so as to be sufficient for identifying gross problems of structural integrity, fuel rod failure, rod bowing, dimension changes, or crud deposition. This program will also include criteria for additional inspection requirements for irradiated fuel assemblies or in-core control components, if abnormal behavior is observed during operation or in visual inspections as described in Subsection 4.2.4.5.

4.2.2 Description and Design Drawings

The fuel assembly design specifications are given in Table 4.2-1 (Reference 4.2-6 and ”US-APWR Fuel System Design Parameters List”, MUAP-07018-P, Reference 4.2-10).

A fuel assembly consists of 264 fuel rods arranged in a 17x17 square array, together with 24 control rod guide thimbles, an in-core instrumentation guide tube, 11 grid spacers, a top nozzle and a bottom nozzle. The control rod guide thimbles guide the in-core control components, such as the control rods, the burnable absorber rods, the neutron source rods and the thimble plug rods, into the fuel assembly. The in-core instrumentation tube directs the movable neutron detector into the fuel assembly from a center hole of the adapter plate in the top nozzle. The in-core instrumentation guide tube is located at the center of the square array, whereas the control rod guide thimbles are symmetrically arrayed according to arrangement of the control rods in the rod cluster control assembly. The cross section of the fuel assembly array is shown in Figure 4.2-1. The fuel assembly full length schematic view is shown in Figure 4.2-2.

To preclude contact between the fuel rod and the nozzles, the fuel rods are loaded into the fuel assembly with an initial clearance between the fuel rod ends and the top and bottom nozzles. The fuel rods are supported by 11 grid spacers. The top and bottom grid spacers are made of Inconel 718, and the intermediate grid spacers are fabricated from Zircaloy-4.

The fuel assembly is loaded into the core barrel and supported by the lower core support plate. The upper core plate is installed over the fuel assemblies after their loading. Fuel assembly alignment is provided by engagement between alignment holes in the top and bottom nozzles and guide pins attached to the lower core support plate and the upper core plate. The upper core plate compresses the holddown spring of the fuel assembly to fix the axial location of the fuel assembly.

4.2.2.1 Fuel Rod

The fuel rods consist of cold-worked and stress relieved ZIRLO fuel cladding (referred to simply as “cladding” below) loaded with sintered uranium dioxide pellets and/or sintered gadolinia-uranium dioxide pellets, a coil spring (called the “plenum spring”) in the upper plenum, a lower plenum spacer, and end plugs welded at the top and bottom ends to seal the rod, as shown in Figure 4.2-3. ZIRLO is a zirconium based alloy for improved corrosion resistance. The sintered uranium dioxide pellets and sintered gadolinia-uranium dioxide pellets are produced by compression molding powdered uranium dioxide, or a mixture of powdered uranium dioxide and gadolinia, respectively, and then sintered in an atmosphere of hydrogen or a hydrogen/nitrogen mixture. The pellets are cylindrical with a hollow (called a “dish”) at the center of each end surface which is chamfered. The dishes accommodate the axial swelling and thermal expansion of the pellet during irradiation. The chamfer acts to strengthen the pellet ends to reduce the incidence of small defects close to the pellet surface and to suppress deformation of the end surfaces when the pellets expand.

Between the pellet stack and both end plugs there are an upper and a lower plenum that accommodate the increase in internal gas content due to the release of gaseous fission products with irradiation. The plenum spring placed in the upper plenum prevents the pellets from moving during shipping and handling of fuel assemblies. A stainless steel spacer in the lower plenum provides additional cladding support. The cladding wall thickness and the radial gap between the pellets and cladding are determined so that the integrity of the fuel rod is fully maintained during normal operation including AOOs, where thermal expansion of the pellet exceeds that of the cladding. The axial clearance between the fuel rod and the top nozzle and between the fuel rod and the bottom nozzle are determined to allow for the difference between the fuel rod and assembly in the axial dimensional change due to irradiation growth and thermal expansion during normal operation.

To reduce pellet/cladding interaction and prevent collapse during normal operation, the fuel rods are pressurized with helium through a pressurization hole provided in the top end plug which is then closed off by welding to yield a sealed structure.

4.2.2.2 Fuel Assembly

As shown in Figure 4.2-2, the fuel assembly structure consists of the bottom nozzle, the top nozzle, the fuel rods, the control rod guide thimbles, the in-core instrumentation guide tube and the grid spacers.

4.2.2.2.1 Bottom Nozzle

A schematic view of the bottom nozzle is shown in Figure 4.2-4. The bottom nozzle has the following functions:

- Positioning the fuel assemblies properly inside the core barrel
- Introducing the primary coolant inside the fuel assembly
- Preventing fuel rods from passing through the bottom nozzle during fuel life
- Acting as a filter for debris
- Bearing the axial loads of the fuel assembly, including its weight

The bottom nozzle consists of a top plate, four legs and side panels between the legs. The top plate and side panels are called the “adapter plate” and “skirt”, respectively. All of these parts are made of stainless steel. The bottom nozzle is connected to the control rod guide thimbles by thimble screws that pass through the insert and into the thimble end plug, as shown in Figure 4.2-5.

In addition to guiding the primary coolant into the fuel assembly, the flow holes on the adapter plate are designed in both their position and their diameter, to prevent fuel rods from passing through the flow holes and going out of the fuel assembly during fuel life.

As shown in Figure 4.2-4, an anti-debris bottom nozzle with a built-in debris filter is used in the US-APWR fuel assembly. Thin plates are placed and welded in grooved slits in the adapter plate, providing a filter for debris passing through the flow holes. The thin plates, made of Inconel 718, are called “blades”. This type of debris filter can trap smaller debris than the conventional debris filter bottom nozzle. The bottom nozzle skirt also catches debris that flows out from the bottom of the adapter plate into gaps between the fuel assemblies.

Axial loads on the fuel assembly are transmitted through the bottom nozzle from the lower core support plate. Alignment holes in two diagonally opposite legs of the bottom nozzle properly guide the fuel assembly in the core by engaging with guide pins on the lower core support plate. Lateral loads on the fuel assembly are transmitted through the guide pins from the lower core support plate.

4.2.2.2.2 Top Nozzle

The top nozzle is the uppermost structural component of the fuel assembly. The parts of the top nozzle are holddown springs, top plate, enclosure, clamps and adapter plate, as

shown in Figure 4.2-6. While the holddown spring is made of Inconel 718, the other parts are made of type 304 stainless steel.

The top nozzle has the following functions and mechanisms.

- Housing for the in-core control components
- Fixing the holddown springs to prevent liftoff of the fuel assembly due to hydraulic force of the primary coolant
- Removing the heat generated in the fuel assembly by guiding the primary coolant flow out of the assembly
- Preventing fuel rods from passing through the top nozzle during fuel life
- Allowing for assembly re-constitution to be able to replace the fuel rods if there is fuel leakage

The in-core control components are positioned in the space formed by the top plate, enclosure and the adapter plate.

The top nozzle has four sets of holddown springs, attached to the top nozzle by two diagonally opposite clamps. Each set of the holddown springs is attached to the clamp by means of a spring screw.

There are alignment holes in the two diagonally opposite corners of the top nozzle that do not have the holddown spring clamps. The alignment holes engage with the guide pins attached to the upper core plate. The indexing hole in one corner of the top plate assures that the fuel assembly is loaded in the proper position in the core. The identification number engraved on the opposite corner clamp is used for visual confirmation of correct assembly loading.

The nozzle sleeves are mechanically connected to holes for the control rod guide thimble holes in the adapter plate, as shown in Figure 4.2-7. This enables removal and replacement of the top nozzles for replacing fuel rods in the case of leakage. To remove the top nozzle, a tool is inserted into the holes for the control rod guide thimbles to rotate the lock parts at the holes. After removing the top nozzle, any fuel rod in the assembly can be gripped and withdrawn for examination or replacement. The re-construction of the top nozzle is completed by setting the top nozzle on the top nozzle sleeves and rotating the lock parts.

Positions of the flow holes in the adapter plate are designed to prevent fuel rods from passing through the top nozzle during fuel life.

4.2.2.2.3 Control Rod Guide Thimble and In-core Instrumentation Guide Tube

The control rod guide thimble is a structural member of the fuel assembly and has the function of guiding in-core control components, such as the control rods, the burnable absorber rods or the neutron source rods, when they are inserted into the fuel assembly, and then holding them in place. The control rod guide thimble is fabricated from

Zircaloy-4. The lower part of the control rod guide thimble has a reduced diameter and small holes to provide a buffer effect when the control rods are dropped. This configuration reduces the impact force on the top nozzle when the RCCA drops. The bottom end of the control rod guide thimble is welded to an end plug which has a small flow hole to avoid the stagnation of the primary coolant in the control rod guide thimble during operation.

The bottom grid spacer is spot-welded to an insert tube which is made of type 304 stainless steel. As shown in Figure 4.2-5, the control rod guide thimbles are positioned within the insert and connected with the bottom nozzle adapter plate by thimble screws.

The top nozzle sleeve for the re-constructible top nozzle is linked to the top of a control rod guide thimble by three bulge joints, as shown in Figure 4.2-7.

Mechanical testing of the locking and unlocking mechanism to connect the top nozzle with the control rod guide thimble has been carried out to verify that these designs satisfy the design requirements.

The grid spacers, except for the bottom, are connected to the control rod guide thimbles by bulge joints. The schematic view of the connection is shown in Figure 4.2-8.

The in-core instrumentation guide tube has a uniform diameter and has the function of guiding the in-core neutron detector which is inserted from the top nozzle into the fuel assembly. The instrumentation tube is also made of Zircaloy-4 and both ends are inserted into the top and bottom nozzles. The instrumentation tube is connected to the top grid spacer and the intermediate grid spacers by a single-stage bulge joint identical to that used to attach the control rod guide thimbles to the grid spacers.

4.2.2.2.4 Grid Spacer

As shown in Figure 4.2-2, the fuel rods are supported by the grid spacers. The grid spacers have a 17x17 lattice structures and are made by interlocking thin straps made of Inconel 718 or Zircaloy-4. The grid spacer holds the fuel rod by means of two grid spacer springs and four dimples as shown in Figure 4.2-8. It also has the function of maintaining the clearance between the fuel rods, the control rod guide thimble and the in-core instrumentation guide tube so as to maintain the nuclear and thermal-hydraulic performance.

The top and bottom grid spacers are fabricated from Inconel 718 to provide the restraint force on the fuel rod. The restraint force is designed to prevent grid fretting wear of the fuel rod cladding and fuel rod bowing during the assembly lifetime.

The nine intermediate grid spacers are fabricated from Zircaloy-4 to improve neutron economy. The intermediate grid spacers hold the fuel rods by the grid spacer springs and dimples in the same manner as the top and bottom grid spacers. Straps of the Inconel 718 and Zircaloy-4 grid spacers are respectively brazed or welded together.

The intermediate grid spacers have mixing vanes on the top of inner straps to increase the mixing of the primary coolant and increase the heat removal efficiency. The top and bottom grid spacers do not have mixing vanes.

The outermost straps of all grid spacers are provided with guide vanes and guide tabs to avoid the interference with the adjacent fuel assemblies and the neutron reflector during loading and unloading of the fuel assemblies.

4.2.2.3 In-Core Control Components

The in-core control components specifications are given in Table 4.2-2. Except for their length, the geometry and material of the US-APWR in-core control components are the same as those of the current Mitsubishi in-core control components.

4.2.2.3.1 Control Rods and Rod Cluster Control Assemblies

As shown in Figure 4.2-9, the rod cluster control assembly consists of the spider assembly and the control rods attached to the spider assembly. The rod cluster control assemblies are inserted into the control rod guide thimbles of the fuel assemblies in specific positions in the reactor.

The control rod contains an alloy for neutron absorption composed of 80 % silver, 15 % indium and 5 % cadmium, and a coil spring made of type 302 stainless steel in a cladding made of type 304 stainless steel.

Both ends of the control rod are plugged by end plugs and welded. The diametrical clearance between the cladding and the absorber is determined to accommodate the difference in thermal expansion between the cladding and the absorber, to prevent excessive loads on the cladding. The bottom end plug, which is made of type 308 stainless steel, has bullet tip shape to reduce water resistance and expedite smooth control rod insertion during scram. The top end plug is made of the same material as the bottom end plug. The top end plug consists of two structurally different sections: a section with a screw for connecting to the spider assembly, and a section with a smaller diameter that provides flexibility at the root of the control rod fixing point.

The spider assembly consists of a spider body, a spring, a spring retainer and a bolt for attaching the spring to the spider body. The spider body is a single-piece machined structure, with vanes extended from the center of the body in a radial pattern. A control rod is hung at the tip of each vane. A groove is machined in the upper part of the spider body for connection with the handling tool and CRDM. A coil spring is contained and axially fixed by the bolt and the spring retainer inside the spider body. The retainer can move toward the inside of the spider body, so that energy can be absorbed, when the rod cluster control assembly impacts on the adapter plate of the top nozzle. The components of the spider assembly, except for the spring retainer and the coil spring, are made of type 304 stainless steel. The spring retainer and the coil spring are made of type 630 stainless steel and Inconel 718, respectively.

All of the rod cluster control assemblies are withdrawn from the fuel stack during normal operation. Reactor scram is achieved by gravitational drop of the rod cluster control assemblies together with the drive rods.

The design lifetime of the control rod and cluster control assembly is 15 years.

4.2.2.3.2 Burnable Absorber Rods and Assemblies

As shown in Figure 4.2-10, the burnable absorber assembly consists of the burnable absorber rods, the thimble plug rods and the holddown assembly for attaching the burnable absorber rods.

The burnable absorber contains an annular tube made of borosilicate glass in a cladding made of type 304 stainless steel. The borosilicate glass gradually depletes the neutron absorber material with irradiation; this characteristic of the absorber allows its use for long term reactivity control and operational flexibility. The annular glass tube is axially supported from inside by a thin spacer tube made of type 304 stainless steel.

Both ends of the cladding are plugged by end plugs and welded. Both end plugs are made of type 308 stainless steel. As with the control rod top end plug, the burnable absorber top end plug has two structurally different sections, one of which is screw-shaped, to connect the burnable absorber rod to the holddown assembly and the other of which has a reduced diameter.

The holddown assembly is composed of a base plate, a spring guide, a holddown spring and a holddown bar. The assembly is located between the adapter plate of the top nozzle and the upper core plate in the reactor. Components of the holddown assembly other than the holddown spring are made of type 304 stainless steel. The holddown spring is made of Inconel 718. The base plate has holes with female screws to fix the burnable absorber and the thimble plug rods, and flow holes for the coolant. The spring guide supports the holddown spring and prevents the holddown bar from rotating. In order to prevent the burnable absorber assembly from lifting due to hydraulic force of the coolant, the holddown spring provides compression force via the holddown bar which is compressed downward by the upper core plate. Both ends of the holddown bar are bent so as not to interfere with the top nozzle.

4.2.2.3.3 Neutron Source Rods and Assemblies

As shown in Figure 4.2-11, the primary source assembly consists of a primary source rod, the thimble plug rods and the holddown assembly. The primary source assembly is used for supplying neutrons at reactor startup and for sub-criticality monitoring during the first fuel loading.

A duplex structure consisting of an outer cladding and a capsule is used in the primary neutron source rods. The outer cladding of the primary neutron source rod encases a capsule that contains californium as the neutron source, and a spacer tube for positioning the capsule. The outer cladding, the capsule and the spacer tube are made of type 304 stainless steel. Each end of the outer cladding is plugged by an end plug and welded. Both end plugs are made of type 308 stainless steel.

While californium undergoes α decay with emission of an α particle, its spontaneous fission also radiates neutrons. Although helium gas is released due to the a decay, the internal pressure of the outer cladding is not increased, since the source is contained in the capsule.

As shown in Figure 4.2-12, the secondary source assembly consists of four secondary source rods, the thimble plug rods and the same holddown assembly as the burnable absorber and primary source assemblies. The secondary neutron source assembly is used for supplying neutrons at reactor startup and for sub-criticality monitoring during fuel loading.

While the primary neutron source is radioactive from the beginning, the secondary neutron source becomes radioactive during reactor operation and then is able to function as the neutron supplier during reactor startup. The secondary neutron source assembly is used instead of the primary source assembly after the initial reactor startup.

The secondary neutron source rod also has a duplex structure composed of an outer cladding and a capsule including the secondary neutron source. The capsule is made of type 304 stainless steel and contains mixed antimony and beryllium pellets, a spring clip made of type 401 stainless steel and a spacer tube made of type 304 stainless steel. The capsule is inserted into the outer cladding made of type 304 stainless steel. The outer cladding is plugged by the plugs and welded. Material for the secondary neutron source is antimony and beryllium mixed with volume ratio of 50 % each.

4.2.2.3.4 Thimble Plug Rods and Assemblies

The thimble plug assembly can be installed into fuel assemblies that are not equipped with other in-core control components such as the rod cluster control, burnable absorber and neutron source assemblies. The thimble plug assembly has a structure in which thimble plug rods are fixed to the same holddown assembly as other holddown type of in-core control components. The thimble plug rods are also used in other in-core control assemblies for plugging the control rod guide thimbles where the control rods, burnable absorber rods and neutron source rods are not installed.

4.2.3 Design Evaluation

The US-APWR fuel system design is based on the design of the Mitsubishi 17x17 fuel rod, assembly and in-core control components, which has demonstrated high reliable performance, as shown by the significant irradiation experience in Japan (Reference 4.2-6).

Design evaluations of the fuel rod, fuel assembly and in-core control components of the US-APWR are summarized in this subsection. The detailed evaluation methodology of the fuel rod design and fuel assembly design, including material properties, is described in References 4.2-6 and 4.2-7.

The fuel rod design considers all events expected during normal operation and AOOs. The fuel rod power as a function of the irradiation time, i.e., the fuel rod power history, is an important parameter in the assessment of fuel rod behavior. Some of the characteristic power histories are known to be most limiting with respect to margin to fuel rod design limits. The limiting histories may be the highest or lowest power rods in a cycle or the highest burnup fuel rods in a cycle, depending on the fuel rod design criterion to be assessed. In general, a single fuel rod power history is not limiting for all fuel criteria, so the characteristic power histories are typically assessed in the fuel rod design. These power histories bracket the range of fuel rod power histories for the fuel region, and

provide the bases for assessing fuel rod performance relative to the established specified acceptable fuel design limits (SAFDLs). The material properties of each part of the fuel are used in the fuel rod design (Reference 4.2-6).

The nuclear design and thermal-hydraulic design related to the fuel rod design are discussed in Sections 4.3 and 4.4, respectively.

The fuel assembly design considers all events expected during shipping and handling, normal operation, AOOs and postulated accidents. The anticipated maximum loads on the fuel assembly components and joints are taken into account in the design evaluation. The stress evaluation is performed based on ASME Section III (Reference 4.2-8) criteria.

The design of in-core control components and their rods takes into consideration thermal-physical properties, compatibility of the absorber or source materials and the cladding, cladding stress limits, and irradiation behavior of the absorber or source materials during normal operation, AOOs and postulated accidents.

The AOO events considered for the fuel rod transient evaluations are categorized in Chapter 15 to specify the limiting event for fuel system integrity. The postulated accident events associated with fuel, such as RIA events and LOCA events are evaluated in Chapter 15 as well. A dose analysis is performed for the postulated accidents where rod failure occurs, such as RIA and LOCA. In the Transient and Accident Analysis, material properties and phenomenological models such as specific heat and heat capacity, are taken into account.

4.2.3.1 Cladding

4.2.3.1.1 Fuel Rod Vibration and Fretting Wear

Fretting wear of the fuel rod cladding is evaluated by long-term hydraulic flow tests and analytical evaluations. The fuel rod vibration characteristics and measured wear depths are obtained from the hydraulic flow tests and are used as reference data for the analytical evaluation. The analytical evaluation to predict fretting wear in the fuel rod cladding has been developed as a semi-empirical model, and has been verified by comparison with results obtained in long term hydraulic flow tests. The cladding stress and fatigue evaluations account for the cladding wear.

In the US-APWR fuel assembly, fuel rod vibration caused by coolant flow has no significant effect on fuel rod integrity due to the low amplitude of the rod vibration (Reference 4.2-7). The grid spacer springs are designed so that there is no gap between the springs and fuel rod throughout the fuel lifetime.

Crevice corrosion has not been observed in the irradiation experience of the current Mitsubishi fuel.

4.2.3.1.2 Fuel Rod Internal Pressure

The rod internal pressure is maintained below the cladding liftoff pressure, at which the pellet-cladding gap increases due to outward cladding creep. Cladding liftoff is prevented to eliminate the possibility of a thermal feedback in which the gap opening leads to increased pellet temperatures, which accelerate the fission gas release and thus further

increase the internal pressure. In the US-APWR fuel design, the rod internal pressure is evaluated using the FINE code (Reference 4.2-6).The evaluation takes into account the uncertainties in the fuel fabrication and the fuel performance models. The US-APWR fuel rod, with upper and lower plenums has enough free volume to accommodate the fission gas release. The internal pressure of the limiting rod is well below the liftoff pressure (Reference 4.2-7), which allows a wide variety of operation from the viewpoint of rod internal pressure evaluation.

During operation an oxide layer forms on the cladding surface. The formation of the oxide layer generates hydrogen and some portion of this hydrogen is absorbed in the cladding. The cladding hydrogen content that exceeds its solubility limit precipitates as hydrides of low ductility, which may lead to a reduction in the cladding ductility. The hydrides are oriented in the circumferential direction under low circumferential stresses, but are reoriented in the radial direction under high circumferential stresses. Cladding cracks can be then initiated along the radially oriented hydrides due to the embrittlement of the hydrides. If the fuel cladding temperature during normal operation is assumed to be no more than approximately 750°F (400°C), the hydrogen reorientation stress is no less than approximately 11500psi (80MPa) (Reference 4.2-11). In Appendix B of Reference 4.2-6, it is shown that hydride reorientation does not occur if the rod internal pressure is below approximately 3900psi (27MPa).

For departure from nucleate boiling ratio (DNBR), there is at a 95% probability at a 95% confidence level that the hot rod in the core does not experience DNB or boiling transition condition during normal operation or AOOs. The probability that excessive DNB propagation may occur is low. To evaluate the above, the probability that a high pressure rod occurs and the probability that rods is in DNB condition is considered. This evaluation leads to the result that the probability of DNB propagation occurrence is quite low (Reference 4.2-7). The evaluation for the postulated accidents is also discussed in Reference 4.2-7.

4.2.3.1.3 Cladding Stresses

The ASME Section III (Reference 4.2-8) pressure vessel criteria are used to determine the cladding stress design limits. All cladding stresses, except for those due to pellet/cladding mechanical interaction (PCMI), are considered in the stress evaluation and are assessed according to ASME Section III (Reference 4.2-8). Cladding stresses take into account the differential pressure across the cladding wall, thermal stresses, hydraulic and seismic vibration, fuel rod bowing, grid spacer contact and cladding ovality. The stresses due to PCMI stress are excluded in the cladding stress evaluation because they are addressed in the cladding strain criterion and the no fuel melting criterion. The category of each stress is summarized as follows.

- Primary Membrane : Stress due to differential pressure
- Bending : Stress due to ovality, hydraulic and seismic vibration and fuel bowing
- Local : Stress due to grid spacer contact force
- Secondary : Thermal stress due to temperature difference across the cladding

The stress due to differential pressure and the thermal stress are evaluated by the FINE code. The stresses due to hydraulic and seismic vibration are derived from vibration analysis and basic equations. The stresses due to ovality, fuel bowing and grid spacer contact force are assessed based on basic equations as well.

The total stress is determined by summing these different contributions to the stresses. The stress intensity is evaluated as the differential stress between the maximum stress and minimum stress, as specified by the ASME Section III (Reference 4.2-8) criteria. The total stress of the limiting rod in the US-APWR fuel rod design during normal operation and AOOs is below the allowable stress intensity (Reference 4.2-7).

4.2.3.1.4 Chemical Reaction

The use of ZIRLO cladding significantly reduces cladding corrosion and material wastage attributable to mass transfer, compared with Zircaloy-4, as shown in Reference 4.2-6. During normal operation and AOOs, the cladding surface temperature is limited to be less than the temperature at which an accelerated corrosion could occur.

Hydrogen generated due to cladding corrosion is partially absorbed into the cladding. The evaluated hydrogen absorption of the limiting rod is less than the hydrogen absorption limit to maintain the cladding ductility. High temperature mechanical properties data for un-irradiated cladding show that the cladding retains its ductility up to the hydrogen absorption limit (Reference 4.2-6).

Primary hydriding is prevented by maintaining the level of moisture and other hydrogenous impurities at a very low level during pellet manufacturing as shown in Reference 4.2-6. The quality controls for moisture content in pellet manufacturing have been strengthened to assure that these requirements are satisfied.

Examination of un-irradiated cladding indicates that there is a possibility of an iodine chemical attack on the cladding at high iodine levels and high tensile stresses. The excellent operating experience of Mitsubishi fuels in Japan, as described in Appendix A of Reference 4.2-6, indicates that there is little likelihood of fuel failure due to chemical attacks. The chemical compatibility of ZIRLO with fission products has also been verified by the irradiation experience. In addition, no significant crud deposition has been observed. The crud deposition is taken into account in the thermal design as discussed in Section 4.4.

4.2.3.1.5 Cladding Fatigue

The cumulative number of strain fatigue cycles is less than the design fatigue lifetime, which includes a safety factor of 2 on the stress amplitude or a safety factor of 20 on the number of cycles, whichever is most limiting. The Langer-O'Donnel model (Reference 4.2-9) is used as the fatigue design curve. Fatigue tests on irradiated fuel cladding give results consistent with Langer-O'Donnel best fit model, and this design curve, with the specified safety factors, is applicable to high burnup fuel design. The cumulative fatigue damage is assessed by summing the fatigue usage over the fuel rod's life. The usage is determined by dividing the number of anticipated load cycles by the number of cycles to failure obtained from the fatigue design curve at the load condition, using the cladding stresses calculated by the FINE code.

In the fatigue evaluation, the number of anticipated load cycles is assumed.

In the US-APWR design evaluation, the fatigue usage of the limiting rod is assessed and cumulated. This estimated cumulative fatigue usage has margin to the limit, as described in References 4.2-6 and 4.2-7.

4.2.3.1.6 Fuel Rod Bowing

Fuel rod bowing is a phenomenon observed in irradiated fuel assemblies. It leads to spacing closure between adjacent fuel rods. While the mechanism is not yet fully understood, it is related to the as-fabricated bowing of the fuel rods, the restraint force due to the grid spacers and the differential irradiation growth of the fuel rods and the control rod guide thimbles.

Significant fuel rod bowing may influence thermal-hydraulic characteristics, such as the departure from nucleate boiling ratio (DNBR).

The rod to rod spacing on all four faces of each fuel assembly has been measured in visual inspections of irradiated fuel assemblies. The mean values and standard deviations of rod to rod spacing are obtained for each span (the longitudinal space between consecutive grid spacers), and then the spacing closure is estimated from the worst span data. The design envelope for the spacing closure at the worst span of each fuel assembly is established as a function of fuel assembly burnup.

The variance consistent with the EOL value of the design envelope is used for estimating the DNB penalty, as discussed in Section 4.4.

The span length and the grid spring restraint force on the fuel rods in the US-APWR fuel assembly are appropriately designed to reduce fuel the rod bowing and the consequent DNB penalty to an acceptable level.

4.2.3.1.7 Consequences of Power Coolant Mismatch

The evaluation for consequences of power coolant mismatch (DNB) is discussed in Chapter 15.

4.2.3.1.8 Irradiation Stability of Cladding

The irradiation behavior of fuel cladding, such as cladding creep and growth, are taken into account in the fuel rod design using the fuel rod performance models described in Reference 4.2-6.

4.2.3.1.9 Creep Collapse and Creepdown

The Mitsubishi fuel design uses high density fuel pellets of more than 95 %TD density, which are stable with respect to fuel densification. In addition, the fuel rods are initially pressurized with helium. The combination of stable fuel and pre-pressurized fuel rods has been quite effective in eliminating the formation of axial gaps in the fuel column due to densification, and in avoiding cladding collapse. As described in Appendix A of Reference 4.2-6, Mitsubishi fuel has experienced no incident of cladding collapse since the adoption of the 95 %TD pellet density and initial pressurization with helium in the fuel design for

more than 30 years. Mitsubishi uses fuel pellets with a higher initial density of 97 %TD for the US-APWR fuel rod design. The US-APWR pellet design is even more stable with respect to fuel densification due to this additional reduction in the fuel's initial porosity, and therefore have greater margin to cladding collapse than the Mitsubishi design with the 95 %TD pellet density.

On the basis of the extensive operating experience of Mitsubishi fuel in Japan, cladding collapse does not occur for fuel rods with initial fuel pellet density of 95 %TD or greater and with initial fuel rod pressurization with helium. Maintaining current pellet fabrication process controls with initial pellet density of 95 %TD or greater and with current initial helium pressurization levels is therefore sufficient to prevent cladding collapse, as evaluated in Reference 4.2-7.

4.2.3.2 Fuel

The dimensional behavior of fuel during irradiation such as densification and swelling, are taken into account in the fuel rod design using the fuel rod performance models described in Reference 4.2-6.

The uranium dioxide pellets have high resistance to corrosion and solubility in high-temperature water, dimensional stability such as a stable crystal structure and volume over a wide range of the oxygen to uranium ratio below melting point. There would be no significant chemical interaction between the pellets and the coolant water if there were any leakage of the primary coolant into the fuel rod due to cladding damage during irradiation. There are no significant effects of changing the pellet density from 95%TD to 97%TD is quite low because the crystal structure and lattice parameters are the same at both densities.

The thermal behavior of the fuel during operation is affected by the fuel's densification and swelling, due to solid and gaseous fission products, thermal expansion, and thermal conductivity. These effects are accounted for in the fuel design, as described in Reference 4.2-6. The 95%TD density of the fuel is high enough to prevent the formation of any significant axial gaps in the fuel column. The fuel centerline temperature is limited to be less than the melting temperature of fuel during normal operation and AOOs.

Solid and gas bubble swelling of the fuel and fission gas release during irradiation are accounted for in the fuel rod design, as described in Reference 4.2-6.

4.2.3.3 Fuel Rod Performance

The fuel rod analysis accounts for the following factors in order to predict the fuel rod behavior during operation:

- Thermal models: coolant temperature and cladding temperature, crud layer thickness, gas mixture thermal conductivity including thermal conductivity in the Knudsen domain, clad-to-fuel gap conductance, pellet thermal conductivity, pellet RIM formation as fuel restructuring;

- Gas release models: fission gas release, helium absorption and release;

- Pellet dimensional change models: densification, solid and gaseous fission product (gas bubble) swelling;
- Cladding models: cladding corrosion, hydrogen absorption, rod growth, creep, cladding fuel side oxidation;
- Mechanical analysis for the cladding stresses and strains; and
- Rod internal pressure.

These phenomenological models have been verified by comparison with measured data. An extensive database has been used for verification of the models for the fuel temperature, fission gas release, pellet density change, helium gas content, cladding corrosion, hydrogen pickup, rod growth and cladding creep models. The predicted results for the rod free void volume and rod internal pressure have been compared with the measured data to demonstrate the integrated performance of these models, including the basis for the model uncertainties used in the fuel rod analysis. These comparisons are described in Reference 4.2-6.

4.2.3.3.1 Fuel-Cladding Mechanical Interaction

Fuel rod initial helium pre-pressurization is an effective approach to maintain fuel integrity with respect to the cladding stresses, cladding strains and fatigue during operation. Due to the dimensional changes of the pellets and the cladding, such as swelling and densification of pellet, thermal expansion of the pellets and the cladding, and creep of cladding, pellet-cladding contact occurs during irradiation.

Pellet/cladding mechanical interaction (PCMI) is limited by two criteria, as follows.

- Cladding strain increments during AOOs must remain below 1%. Cladding ductility is maintained until at least 1% cladding strain based on mechanical test data for irradiated and un-irradiated cladding material (Reference 4.2-6),
- Fuel centerline melting does not occur.

During normal operation, the calculation of the cladding strain takes into account the cladding creepdown due to the pressure differential between the coolant system pressure and the rod internal pressure, and the outward deformation due to pellet swelling after pellet-cladding contact occurs. The cladding strain during normal operation due to PCMI is dominant and determined by the pellet densification, swelling and thermal expansion as well as by the cladding creep. The power variation during normal operation is generally very moderate, and zirconium based alloy cladding easily deforms due to creep. A strain increment of 1% relative to the un-irradiated state is conservatively used as the criterion to limit PCMI during normal operation. For power transients associated with AOOs, the change in the cladding strain from normal operation to the maximum power of the AOO is evaluated as the total tensile strain change (elastic and inelastic). This strain is principally due to the pellet expansion resulting from the pellet thermal expansion and fission gas bubble swelling. The local power increase during the AOOs causes both the PCMI and

the gas bubble swelling. The strain change is evaluated by the FINE code. The US-APWR fuel rod design meets the above criteria during normal operation and AOOs.

Manufacturing and model uncertainties are taken into account in the peak centerline temperature evaluation as described in Section 4.4. The US-APWR fuel centerline temperature is well below the melting point during normal operation and AOOs.

For postulated accidents, the total number of fuel rods that is predicted to exceed the melting temperature, with consideration of uncertainties, is accounted for in the radiological dose calculations.

4.2.3.3.2 Failure and Irradiation Experience

The failure and irradiation experience of Mitsubishi fuel are described in Appendix A of Reference 4.2-6.

4.2.3.3.3 Fuel and Cladding Temperature

The evaluation for fuel temperature with respect to overheating of the fuel pellets is discussed in Section 4.4 including the maximum linear heat generation rate. The evaluation for cladding temperature with respect to overheating of the cladding is discussed in Chapter 15.

4.2.3.3.4 Potential Effects of Temperature Transients

There is a possibility of propagation of fuel failures due to departure from nucleate boiling (DNB) during overpower transients associated with AOOs when the rod internal pressure exceeds the coolant system pressure. This possibility of DNB propagation is accounted for in the analysis of the consequences of the AOOs. As described above, the possibility of DNB propagation for US-APWR fuel is low (Reference 4.2-7). As described in Section 4.4, DNB during transients is avoided at a 95% probability at a 95% confidence level.

The distance between the grid spacers, or span length, and the grid spacer spring restraint force on the fuel rods have been designed to suppress rod bowing during normal operation and temperature transient events. The axial compressive stress of the fuel rod produced by the friction force between the grid spacer and the fuel rod is not sufficient to cause rod bowing (Reference 4.2-7).

4.2.3.3.5 Energy Release and Potential Effects of Fuel Burnout

Under DNB conditions, steam blanketing at the fuel rod surface degrades heat transfer causing the cladding temperature to rise. There is a potential for increasing chemical reactions between cladding and coolant. The energy release and potential effects of fuel burnout (DNB) are taken into account in Chapter 15.

4.2.3.3.6 Energy Release and Pressure Pulse Effects

The evaluation for energy release and pressure pulse effects with excessive fuel enthalpy or violent expulsion of fuel is discussed in Section 15.4. The corrosion level in the US-APWR fuel design is limited by the hydrogen absorption limit and is within the corrosion level shown in the diagram in Appendix B of Reference 4.2-1.

4.2.3.3.7 Fuel Rod Behavior during Coolant Flow Blockage Event

The evaluation for fuel rod behavior during coolant flow blockage event such as bursting/rupture and ballooning/swelling of cladding is taken into account in Subsection 15.6.5, including the limit of cladding embrittlement limits and the metal/water reaction rate calculation.

4.2.3.4 Grid Spacer

Taking into consideration that the excessive restraint force causes fuel rod bowing, the spring force of the grid spacers is properly designed, considering the decrease of the spring force due to stress relaxation during operation. The force is evaluated to be sufficient enough to prevent grid fretting wear of the fuel rod, as described in Subsection 4.2.3.1.1. In terms of the rod-to-rod spacing, data obtained from the irradiated fuel assemblies with the grid spacers made of Inconel 718 and Zircaloy-4 do not show significant closure of the spacing (Reference 4.2-7).

The irradiation growth of the Zircaloy-4 grid spacer is evaluated based on data from irradiated fuel assemblies (Reference 4.2-7), which shows that there is no significant interference with adjacent fuel assemblies or core baffle plates.

Grid spacer impact tests for the intermediate grid spacers have been performed. The purpose of the tests is to determine the dynamic stiffness and the buckling load of the grid spacer. Conservative temperatures, to represent the coolant temperature at the intermediate grid spacer locations, have been used in the impact tests. The impact test results for the dynamic stiffness and the buckling load are used for the time-response analysis of the fuel assembly in seismic event and LOCA. The grid spacer is designed to maintain sufficient integrity and the geometrical configuration of the control rod guide thimbles to assure control rod insertability during postulated accidents.

Inconel 718 is resistant to corrosion and hydrogen absorption. The measured oxide thickness and absorbed hydrogen for irradiated Zircaloy-4 grid spacers are lower than acceptance limits (Reference 4.2-7).

Fatigue tests on Inconel 718 and Zircaloy-4 grid springs have confirmed that the cycle and amplitude of vibration during irradiation do not cause fatigue failure due to fatigue of the grid springs (Reference 4.2-7).

4.2.3.5 Fuel Assembly

4.2.3.5.1 Loads Applied by Core Restraint System

Loads on the fuel assembly during normal operation are holddown spring force, hydraulic lift force, buoyant force, self-weight, and reaction force from the lower core support plate. Evaluation for the US-APWR fuel assembly and its components confirms that the design meets the required strength.

The irradiation experience for conventional fuel assemblies shows stable performance in terms of in-core characteristics, such as irradiation growth of both the fuel assembly and the fuel rod, fuel assembly bowing, distortion, and holddown spring relaxation (Reference

4.2-7). This irradiation experience is applicable to the US-APWR fuel assembly, which basically uses the same assembly design. Evaluations are as follows.

- The fuel assembly experiences neither significant vibration nor liftoff due to the worst-case hydraulic load from the coolant during normal operation and AOOs except for the pump-over-speed condition. Confirmation by hydraulic tests for the conventional fuel assemblies and their actual in-reactor performance supports this evaluation. To maintain the proper holddown force for the fuel assembly, the holddown spring is designed so that additional plastic deformation of the holddown spring does not occur in the event of liftoff at pump-over-speed conditions (References 4.2-6 and 4.2-7).

- The US-APWR fuel assembly initial clearance in axial direction between the top nozzle of the fuel assembly and the upper core plate is designed to assure that this clearance is maintained throughout the fuel assembly lifetime (Reference 4.2-7). The initial clearance between both nozzles and the fuel rod is designed to accommodate the differential irradiation growth and thermal expansion of the fuel assembly and the fuel rods.

- Stresses of components such as the nozzles and control rod guide thimbles meet the acceptance limit based on ASME Section III (Reference 4.2-8).

- Fatigue usage factors for the nozzles and the control rod guide thimbles are less than 1.0, based on the postulated number of scrams during the fuel assembly lifetime.

- Fretting wear observed at contact points other than those between the fuel rod and grid spacers is negligible.

- Existing data measured on irradiated fuel assemblies show that oxide thickness and hydrogen absorption in Zircaloy-4 material maintain below their acceptance limits.

4.2.3.5.2 Analysis of Combined Shock (Including LOCA) and Seismic Loading

The structural deformation of the fuel assembly is evaluated analytically for the combined seismic event and loss-of-coolant accident, in accordance with Appendix A of Reference 4.2-1. The analysis confirms that core coolability and safe shutdown of the reactor are maintained with consideration of the combination of earthquake and postulated accident loads.

For safe-shutdown earthquake condition, the time-dependent horizontal displacement of the fuel assembly and impact force and deformation of the grid spacers are analyzed by a group interactive vibration analysis modeling of the fuel assemblies array (Reference 4.2-14). The horizontal response due to a postulated accident is analyzed in the same manner.

Based on the data from structural tests of the conventional fuel assemblies, the vibration characteristics of the US-APWR fuel assembly, such as stiffness, frequency and damping are determined and used in the above evaluation.

Compared with experimentally obtained integrity of the grid spacer, the grid spacer deformation resulting from the analysis is confirmed to be insignificant so that there is no obstruction to control rod insertion to prevent safe reactor shutdown during postulated accidents (Reference 4.2-15).

The stresses in the fuel assembly components except for the grid spacer are evaluated at the most severe earthquake and postulated accident conditions. The stress in the major components is confirmed to be lower than the allowable stress intensity in ASME Section III (Reference 4.2-8) so that the design of fuel assembly satisfies the design requirement in the combined seismic and LOCA loading (Reference 4.2-15). The stress of the fuel rod cladding is confirmed to be less than 90% of cladding yield stress at operating temperature (Reference 4.2-15), as specified in Appendix A of Reference 4.2-1.

The axial load on the fuel assembly is confirmed to be lower than buckling load of the control rod guide thimble (Reference 4.2-15).

The evaluation for insertability of the rod cluster control assembly is summarized as follows.

The US-APWR fuel assembly, which uses 11 grid spacers, has grid-to-grid spacing equivalent to the conventional 12 ft fuel assembly, which has 9 grid spacers. This grid-to-grid spacing contributes to the lateral stiffness of fuel assembly and compensates for the reduction in the stiffness due to increasing the fuel stack length from 12 ft to 14 ft. For the US-APWR fuel assembly, the displacement due to the vibration in the combined earthquake and LOCA events (Reference 4.2-15), and the assembly bowing during irradiation are evaluated to be comparable to current 12 ft fuel assembly, which confirms that control rod insertability is maintained.

As another countermeasure for incomplete control rod insertion (IRI), the US-APWR fuel assembly design uses a longer region with an enlarged inner diameter in the dashpot region of the control rod guide thimble.

4.2.3.5.3 Loads Applied in Fuel Handling, Including Misaligned Handling Tools

The design limit during shipping is established as a load based on acceleration, which is monitored by acceleration indicators installed in the shipping cask. The design limit during handling is established as a load by an indicator equipped with the handling tool. Tensile tests of the linkages, which are the bulge joints in the grid spacers, the top nozzle and the control rod guide thimbles, confirm that the design meets the required strength during shipping and handling (Reference 4.2-7).

In addition to requiring low speeds in the upward and downward motion of the fuel assembly, a crane for handling the fuel assembly has an interlock mechanism to prevent overloading to the fuel assembly. Therefore, the fuel assembly is not subjected to severe force in the case of misaligned handling tools.

4.2.3.6 In-Core Control Components

4.2.3.6.1 Rod Cluster Control Assembly

The absorber temperature during normal operation and AOOs is evaluated to be less than the melting point (Reference 4.2-7). The diameters of the control rod cladding and the absorber are appropriately designed. Swelling of the absorber and the difference in thermal expansion of the cladding and the absorber do not cause significant stress of the cladding. Swelling of the cladding and the difference in thermal expansion of the cladding and the control rod guide thimble do not result in closure of the diametrical clearance between them during operation (Reference 4.2-7).

In the event of cladding failure, the Ag-In-Cd absorber material has low chemical reactivity with the coolant and has sufficient compatibility with the cladding material.

The cladding stresses due to the stepped movement of the CRDM and the differential pressure between inside and outside of the control rod satisfy ASME Section III (Reference 4.2-8) criteria during normal operation and AOOs. Because the nuclear reaction proceeds without gas release from the Ag-In-Cd absorber, the internal pressure of the control rod does not increase during operation, and the control rod's operating history has no impact on the cladding stress evaluation.

A section of the top end plug has a reduced diameter for stiffness flexibility, to expedite smooth control rod insertion into the guide thimble and also to prevent significant wear by reducing the mutual contact force between the control rod and the guide thimble. Chromium plating of the cladding surface also contributes to increase wear resistance of the cladding. This design has been already applied to the conventional rod cluster control. The irradiation experience has shown its effectiveness.

A material with high corrosion resistance, such as austenitic stainless steel, is used in the components of the rod cluster control assembly, including the control rod cladding, that are directly exposed to the coolant with high temperature and rapid flow velocity. The material has high ultimate tensile strength and is therefore capable of remaining watertight. The cladding would maintain its integrity if there was a cladding leak, with subsequent waterlogging.

4.2.3.6.2 Burnable Absorber Assembly

The borosilicate glass of the absorber material generates heat by γ-heating and the (n, α) reaction of the boron. The highest temperature that is obtained by solving the heat conduction equation is less than the softening point of borosilicate glass (Reference 4.2-7).

The diameters of the cladding and the absorber are designed so that the swelling of the absorber and the difference in thermal expansion of the cladding and the absorber do not cause significant stress in the cladding. Swelling of the cladding and the difference in thermal expansion of the cladding and the control rod guide thimble do not result in closure of the diametrical clearance between them during operation (Reference 4.2-7).

In the event of cladding failure, the absorber material has low chemical reactivity with the coolant and has sufficient compatibility with the cladding material.

The burnable absorber makes use of the neutron absorption of the ^{10}B in the borosilicate glass, which produces helium gas. The released helium gas increases the burnable absorber rod internal pressure, which essentially reaches its maximum value within one cycle of operation. The internal pressure of the burnable absorber rod is less than the reactor system pressure at all times during operation. The cladding stress is conservatively evaluated at BOL, when the differential pressure between the inside and outside of the cladding is at a maximum. The evaluation shows that the cladding stress meets the ASME Section III (Reference 4.2-8) criteria. Furthermore, the cladding stress due to the internal pressure meets the stress criteria in ASME Section III (Reference 4.2-8), even if the external pressure is lost in LOCA.

A material with high corrosion resistance such as austenitic stainless steel is used in the components of the burnable absorber assembly that are directly exposed to the coolant with high temperature and rapid flow velocity. The material has enough strength with high ultimate tensile stress to remain watertight. The cladding would maintain its integrity if there was a cladding leak, with subsequent waterlogging.

Full insertion of burnable rod into the control rod guide thimble during operation induces no turbulent flow and prevents significant wear of the burnable absorber rod.

4.2.3.6.3 Neutron Source Assembly

The primary and secondary neutron sources generate heat by γ-heating. The temperature within the sources is obtained by solving the heat conduction equation. The temperatures of the primary and secondary neutron sources are confirmed to be lower than the melting point of the primary source material, and the mixed antimony and beryllium pellets, respectively.

Both of the neutron source rods feature a duplex cladding design, with a very low probability for exposing the source material to the coolant. However, the neutron source material has low chemical reactivity with the coolant in case of cladding failure and has sufficient compatibility with the cladding material.

The stress in the primary neutron source rod cladding due to the loads during normal operation, AOOs and postulated accidents satisfy the stress criteria in ASME Section III (Reference 4.2-8).

The secondary neutron source rod has a duplex structure that consists of a capsule containing the neutron source and an outer cladding encasing the capsule. The stresses in the capsule and the outer cladding, due to the differential pressure between inside and outside of each cladding, are evaluated. Both the capsule and the cladding that encases the capsule are pressurized during fabrication. The internal pressure of the capsule also increases due to helium gas release during irradiation. Taking into account irradiation behavior including the gas release of the neutron source and swelling of cladding, the stresses on the cladding of the capsule and the outer cladding meet the ASME Section III stress criteria (Reference 4.2-8). Even if the external pressure after a postulated accident such as LOCA is reduced to containment pressure, the stress in the cladding meets the

stress criteria in ASME Section III (Reference 4.2-8), Appendix F, as shown in Reference 4.2-7.

Material with high corrosion resistance, such as austenitic stainless steel, is used in the components of the neutron source assembly that are directly exposed to the coolant with high temperature and rapid flow velocity.

4.2.4 Testing and Inspection Plan

4.2.4.1 Quality Assurance

Testing and inspection for the US-APWR fuel system comply with 10 CFR 50, Appendix B (Reference 4.2-12) and are based on the requirements of ASME NQA-1-1994,"Quality Assurance Requirements for Nuclear Facility Applications"(Reference 4.2-13).

Mitsubishi issues drawings and specifications for each product that include the testing and inspections to be performed to assure product quality.

When testing and inspection are performed by others than Mitsubishi, the procedures and requirements used for these activities are reviewed by Mitsubishi.

The US-APWR fuel system testing and inspection programs are essentially the same as the programs successfully used for Mitsubishi fuel utilized in Japanese nuclear power plants for many years.

4.2.4.2 Quality Control

The quality of the fuel assemblies and in-core control components is fully controlled. Some of the important inspection items such as pellet visual appearance, fuel rod welds and fuel rod leak tightness are inspected on all products. A sampling method is used for other inspection items, generally based on a 95 % probability at a 95 % confidence level. Destructive tests or nondestructive tests, including radiographic inspections, are used as appropriate.

Various methods are used to inspect the dimensions, weight and visual appearance of each part of the fuel assembly and in-core control components. The quality control program specifies the method to be used and requires that test reports be retained in prescribed forms.

4.2.4.2.1 Pellets

The enrichment, uranium content, chemical composition, impurities, O/U ratio, hydrogen content, dimensions and density of the pellets are inspected by sampling. The visual appearance, including cracks, chips, and surface condition, are inspected on all pellets. Dimensional inspections include the pellet diameter, height, dish diameter, dish depth, chamfer dimensions, and pellet squareness. The pellet sintering conditions are specified based on the UO_2 powder characteristics. For pellets containing gadolinia, additional inspections such as gadolinia content and homogeneity are specified.

4.2.4.2.2 Fuel Rods

The fuel rod components (cladding, upper and lower end plugs and plenum spring) are inspected before assembling the fuel rod. The material composition, mechanical properties, and visual appearance are inspected. For the cladding, additional inspections such as surface defects, wall thickness variation, straightness, corrosion resistance, and content and distribution of hydrides are also required.

The following inspections are performed for the fuel rod:

- Each rod is tested in a vacuum container by detecting whether any helium leaks from the rod.
- The fuel rod welds (circumferential boundary and seal of the pre-pressurization hole in the upper end plug) are inspected. The circumferential weld is inspected by visual inspection and ultrasonic testing. The seal weld is inspected by X-ray to confirm the weld depth.
- Dimensions of the rod are inspected. In addition to the rod length and straightness, the plenum length is measured by an eddy current method.
- Active gamma ray scanning is used to confirm the fuel enrichment.
- The existence of any gaps between the pellets is detected by an eddy current technique.
- The helium pressure inside the rod is measured after pressurization.

4.2.4.2.3 Fuel Assemblies

The fuel assembly components (grid spacers, top and bottom nozzles, holddown spring, spring screw, control rod guide thimbles and in-core instrumentation guide tube) are inspected before assembling. Fuel assembly inspection includes visual appearance and dimensions (length, straightness, the fuel rod spacing and the gaps between the fuel rods and nozzles). The bulge portion of the guide thimbles is also inspected for its dimensions and whether there are any cracks.

4.2.4.2.4 In-Core Control Components

Inspection of in-core control components is based on their visual appearance, dimensions, weights and other specified items to confirm to meet their specifications.

Each in-core control component is checked for compatibility with the fuel assembly by an insertion test. For the control rod assembly compatibility with the CRDM is confirmed at the manufacturing site using a gauge that has a latching mechanism identical to that of CRDM.

4.2.4.2.5 Process Control

The Mitsubishi process control specifications identify restrictions in the fuel fabrication to prevent the occurrence of any error that could affect the quality of the fuel. The primary objective is to assure rigorous identification of the pellet enrichment and fuel rod identification.

The uranium dioxide powder is controlled in a labeled container that specifies the container serial number, project name and enrichment. The handling manual specifies the procedures to prevent contamination of foreign materials. The fabrication line is fully cleaned up prior to changing to a different enrichment powder.

After sintering, the pellet trays are kept in the same manner as the powder. Testing by sampling confirms the characteristics of the pellets. The trays are labeled and the information is controlled as an item in the computerized fuel fabrication data base.

Laser marking is used to place a barcode label on each cladding tube during fuel rod fabrication. The contents of each fuel rod (pellets, plenum spring, and helium pre-pressurization) can be confirmed using the rod's barcode identifier.

Pellets with gadolinia and the gadolinia fuel rods are fabricated in a separate line from uranium dioxide fuel rods. The sealed gadolinia fuel rod is then transferred to the assembly area. The gadolinia rods can also be identified by a unique end plug shape.

4.2.4.2.6 Control of Measuring and Test Equipment

Testing and inspection require the validation of the tools, gauges, instrumentation, and other measuring and test equipments used in manufacturing. These are inspected by comparison with the authorized standards at specified intervals. The precision of the measurement is specified before the inspection. The calibration records are kept. Audits by outside organizations or a different section of the company are performed and the proper usage of the tools and gauges is periodically confirmed.

4.2.4.3 Onsite Inspection

A fuel-shipping container is used to transport the new fuel assemblies from the manufacturing location to the nuclear plant. After arrival, the condition of each fuel assembly is inspected. Written procedures are used for the new fuel inspection. Before opening the shipping container, the identification of the fuel is checked and the container is confirmed to be sealed and undamaged. The container is then opened and it is confirmed that it was not subject to any significant shock during transportation, by checking the shock indicators attached to the shipping container internals. The visual appearance of the fuel assemblies is performed to confirm that no significant dimensional change occurred during shipping.

In-core control components such as control rods, burnable absorbers and thimble plugs, are transported in the shipping container, either inserted into the fuel assemblies or separately from the fuel assemblies. In the latter case these components are loaded in the shipping container using supports fitted to their shape. Their condition is confirmed after arrival at the plant.

The new fuel assemblies and the in-core control components are then moved to the new fuel storage area inside the plant. The in-core control components are stored in the fuel assemblies in the storage area.

The control rod assembly is functionally tested at the plant site after core loading. Each control rod assembly is dropped at the full flow/hot condition to confirm that the drop time is within the specified limit. Since the control rod is a movable component which must move freely to control reactivity, the control rod capability for partial movement is also inspected. The rod drop test is periodically performed at each refueling outage to confirm rod capability to meet its functional requirements.

4.2.4.4 Coolant Radiation Monitoring

Radioactivity in the reactor coolant is monitored by periodic sampling of the coolant. Analysis is performed for iodine, noble gases and cesium. If any anomaly is found sampling is done more frequently. The US-APWR technical specification limits the radiation level for continued plant operation, but the plant will be shutdown at much lower radiation level, set in each plant operation control document. Detailed radiological monitoring and sampling systems are described in Sections 9.3 and 11.5.

4.2.4.5 Inservice Surveillance

Several monitoring systems are used during plant operation to obtain information related to core reactivity, radiation levels, and water chemistry. If the radiation level increases, it is monitored to determine the degree of fuel degradation and whether a plant shutdown is required. At normal refueling outages the irradiated fuel assemblies are visually inspected and some of them are dimensionally checked to confirm their integrity and verify consistency with the assembly condition assumed for their subsequent irradiation. Some of the US-APWR fuel assemblies loaded in the initial core will be closely examined to confirm their performance.

If a coolant radiation level change suggests leakage in the loaded fuel, at the beginning of the fuel inspection the fuel assembly containing the defective rod(s) will be identified by a sipping method. After the leaking fuel assembly is identified, techniques such as ultrasonic testing will be used to identify the leaking rod(s). Additional efforts to identify the cause of the fuel failure and determine countermeasures to eliminate the failure mechanism will continue inside and outside the plant.

4.2.5 Combined License Information

No additional information is required to be provided by a COL Applicant in connection with this section.

4.2.6 References

4.2-1 U.S. Nuclear Regulatory Commission, Standard Review Plan for the Review of Safety Analysis Reports for Nuclear Power Plants, NUREG-0800, Section 4.2, March 2007.

4.2-2 General Design Criteria for Nuclear Power Plants, NRC Regulations Title 10, Code of Federal Regulations, 10 CFR Part 50, Appendix A.

4.2-3 Acceptance Criteria for Emergency Core Cooling Systems for Light-Water Nuclear Power Reactors, NRC Regulations Title 10, Code of Federal Regulations, 10 CFR 50.46.

4.2-4 Reactor Site Criteria, NRC Regulations Title 10, Code of Federal Regulations, 10 CFR Part 100.

4.2-5 Combined License Applications for Nuclear Power Plants (LWR Edition), NRC Regulatory Guide 1.206. Section C.I.4.2.

4.2-6 Mitsubishi Fuel Design Criteria and Methodology, MUAP-07008-P Rev.2 (Proprietary) and MUAP-07008-NP Rev.2 (Non-Proprietary), July 2010.

4.2-7 US-APWR Fuel System Design Evaluation, MUAP-07016-P Rev.3 (Proprietary) and MUAP-07016-NP Rev.3 (Non-Proprietary), August 2010.

4.2-8 American Society of Mechanical Engineers Boiler and Pressure Vessel Code Section III.

4.2-9 W. J. O'Donnel and B. F. Langer, Fatigue Design Basis for Zircaloy Components, Nuclear Science and Engineering 20, pp.1-12, 1964.

4.2-10 US-APWR Fuel System Design Parameters List, MUAP-07018-P Rev.0 (Proprietary) and MUAP-07018-NP Rev.0 (Non-Proprietary), December 2007.

4.2-11 D.Hardie and M.W.Shanahan, Stress Reorientation of Hydrides in Zirconium 2.5 % Niobium, Journal of Nuclear Materials 55, pp.1-13, 1975.

4.2-12 Quality Assurance Criteria for Nuclear Power Plants and Fuel Reprocessing Plants, NRC Regulations Title 10, Code of Federal Regulations, 10 CFR Part 50, Appendix B.

4.2-13 Quality Assurance Requirements for Nuclear Facility Applications, ASME Boiler and Pressure Vessel Code NQA-1 1994.Edition.

4.2-14 FINDS: Mitsubishi PWR Fuel Assemblies Seismic Analysis Code, MUAP-07034-P Rev.3 (Proprietary) and MUAP-07034-NP Rev.3 (Non-Proprietary), July 2010.

4.2-15 Evaluation Results of US-APWR Fuel System Structural Response to Seismic and LOCA Loads, MUAP-08007-P Rev.2 (Proprietary) and MUAP-08007-NP Rev.2 (Non-Proprietary), December 2010.

Table 4.2-1 Fuel Assembly Design Specifications

Fuel Assemblies	
Fuel Rod Array	17 x 17
Number of Fuel Rods	264
Number of Control Rod Guide Thimbles	24
Number of In-Core Instrumentation Guide Tube	1
Number of Grid Spacers	11
Fuel Rods	
Outer Diameter	0.374 in (9.50 mm)
Cladding Thickness	0.0224 in (0.570 mm)
Active Fuel Length	165.4 in (4,200mm)
Fuel Enrichment	Max. 5 wt%
Gadolinia Content	Max. 10 wt%
Pellet Diameter	0.322 in (8.19 mm)
Pellet Density	97% TD
Plenum	Upper & Lower
Materials	
Cladding	ZIRLO
Top & Bottom Grid Spacers	Inconel 718
Intermediate Grid Spacers	Zircaloy-4
Control Rod Guide Thimbles and In-Core Instrumentation Guide Tube	Zircaloy-4
Nozzles	Stainless Steel
Holddown Springs	Inconel 718

Note: Inconel 718 is a nickel-chromium-iron alloy 718.

Table 4.2-2 In-core Control Component Assembly Specifications

Rod Cluster Control Assembly	
Number of Control Rods per Assembly	24
Absorber Material	Ag (80%)-In (15%)-Cd(5%)
Absorber Length	163.5 in (4153 mm)
Absorber Outer Diameter	0.341 in (8.66 mm)
Cladding Material	Type 304 Stainless Steel
Cladding Thickness	0.0185 in (0.47 mm)
Cladding Outer Diameter	0.381 in (9.68 mm)
Burnable Absorber Assembly	
Number of Absorber Rods per Assembly	Max. 24
Absorber Material	Borosilicate-Glass
Absorber Length	159.4 in (4050 mm)
Cladding Material	Type 304 Stainless Steel
Cladding Thickness	0.0185 in (0.47mm)
Cladding Outer Diameter	0.381 in (9.68mm)
Primary Source Assembly	
Number of Source Rods per Assembly	1
Neutron Source Material	Californium 252
Neutron Source Capsule Outer Diameter	0.330 in (8.38 mm)
Neutron Source Capsule Length	1.5 in (38 mm)
Cladding Material	Type 304 Stainless Steel
Cladding Thickness	0.0185 in (0.47mm)
Cladding Outer Diameter	0.381 in (9.68mm)
Secondary Source Assembly	
Number of Source Rods per Assembly	4
Neutron Source Material	Antimony–Beryllium
Neutron Source Outer Diameter	0.292 in (7.42 mm)
Neutron Source Length	88.0 in (2235 mm)
Cladding Material	Type 304 Stainless Steel
Cladding Thickness	0.0185 in (0.47mm)
Cladding Outer Diameter	0.381 in (9.68mm)

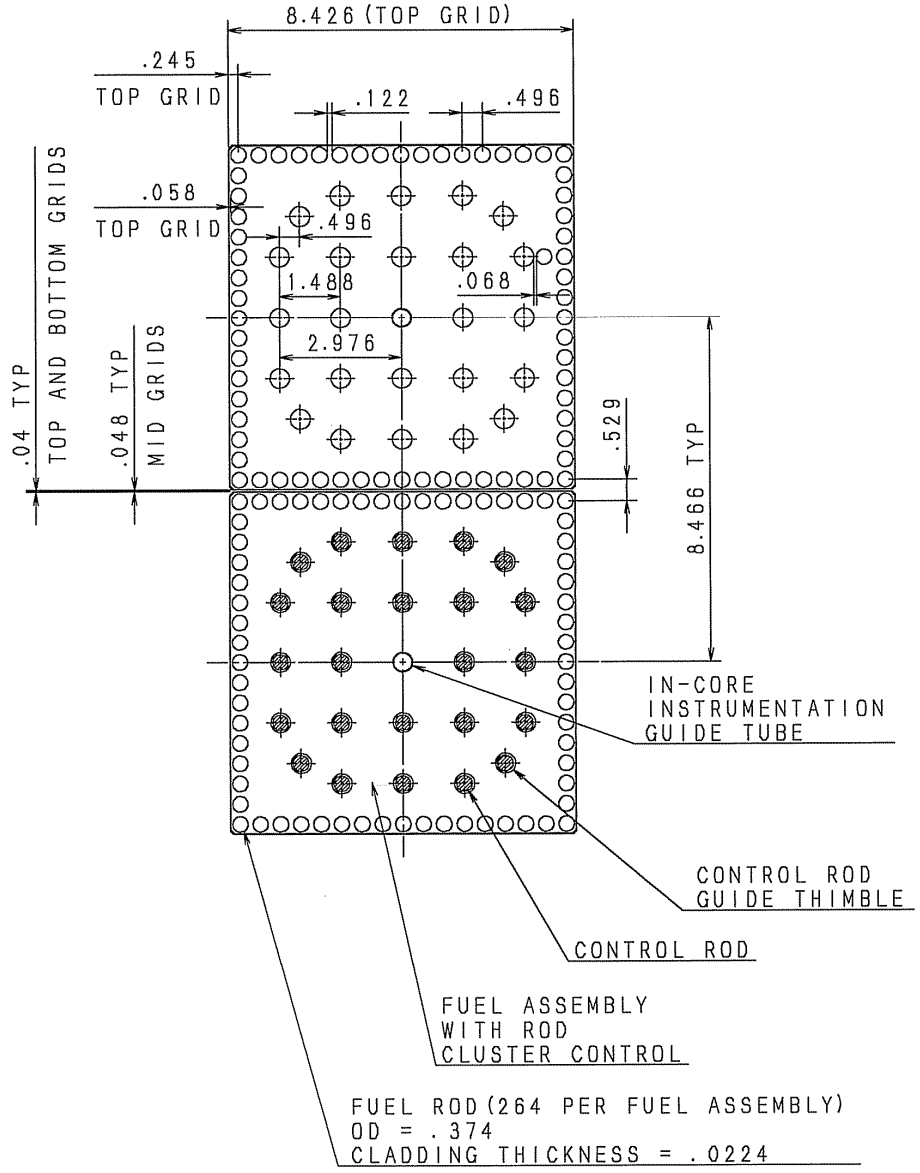

Figure 4.2-1 Cross Section of Fuel Assembly Array

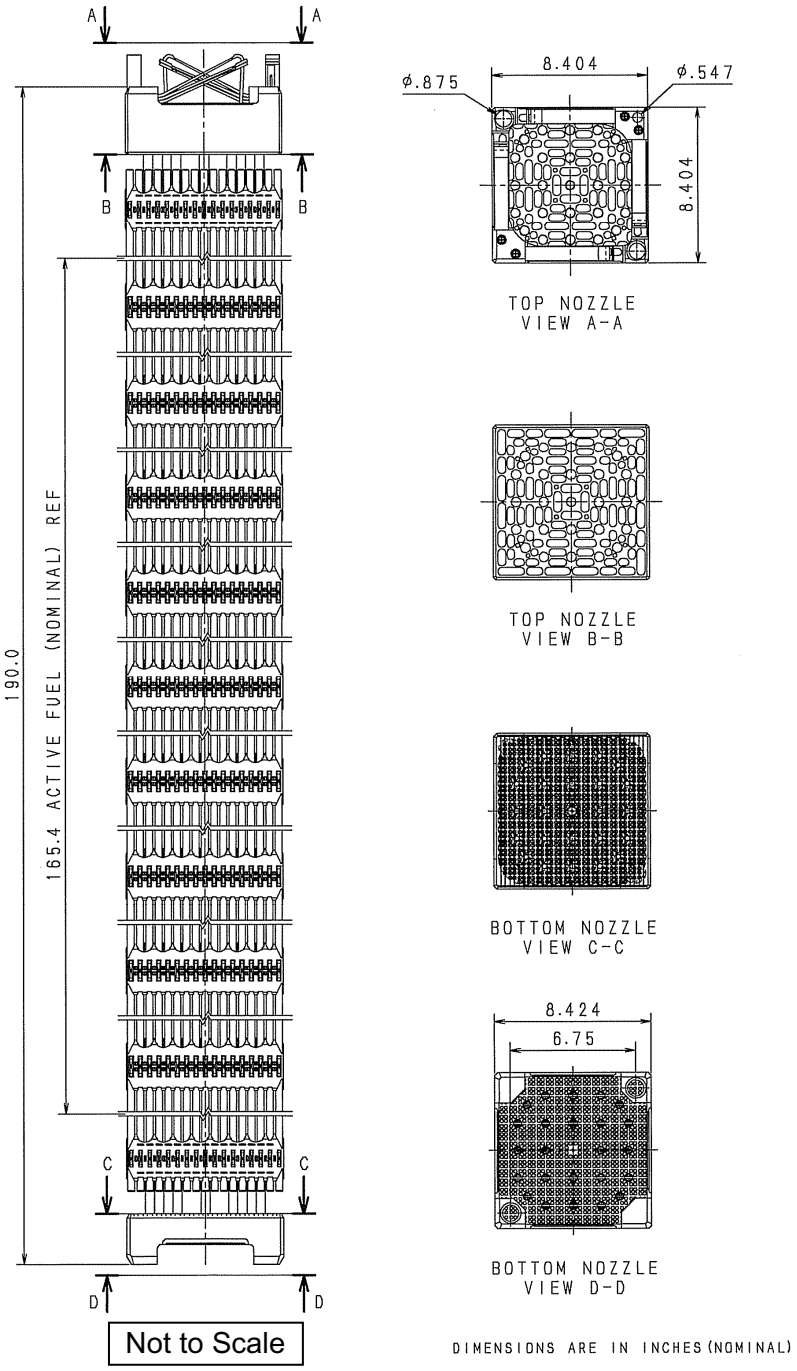

Figure 4.2-2 Fuel Assembly Full-Length Schematic View

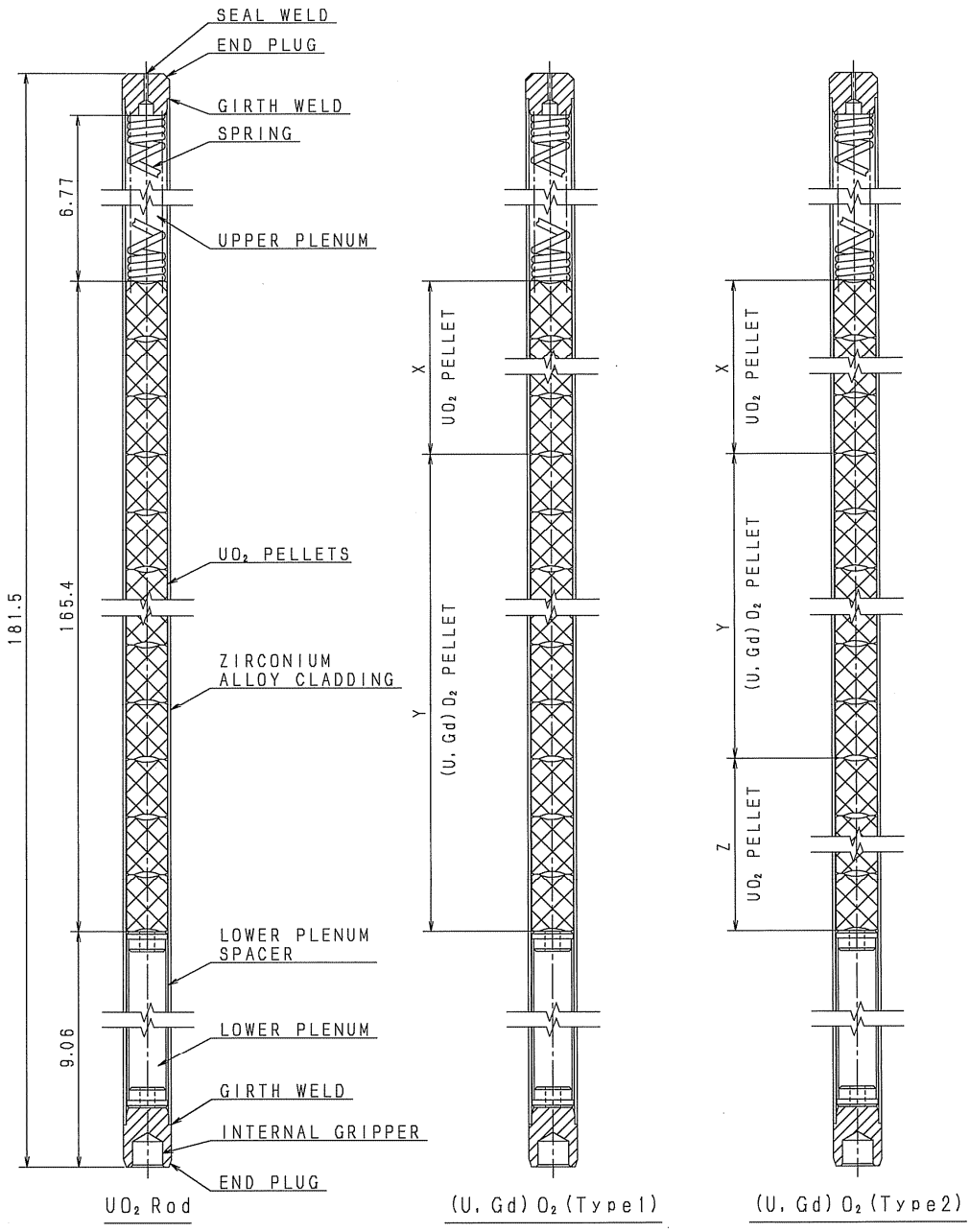

X,Y,Z dimensions depend on core design
Dimensions are in inches (Nominal)

Figure 4.2-3 Schematic View of Fuel Rod

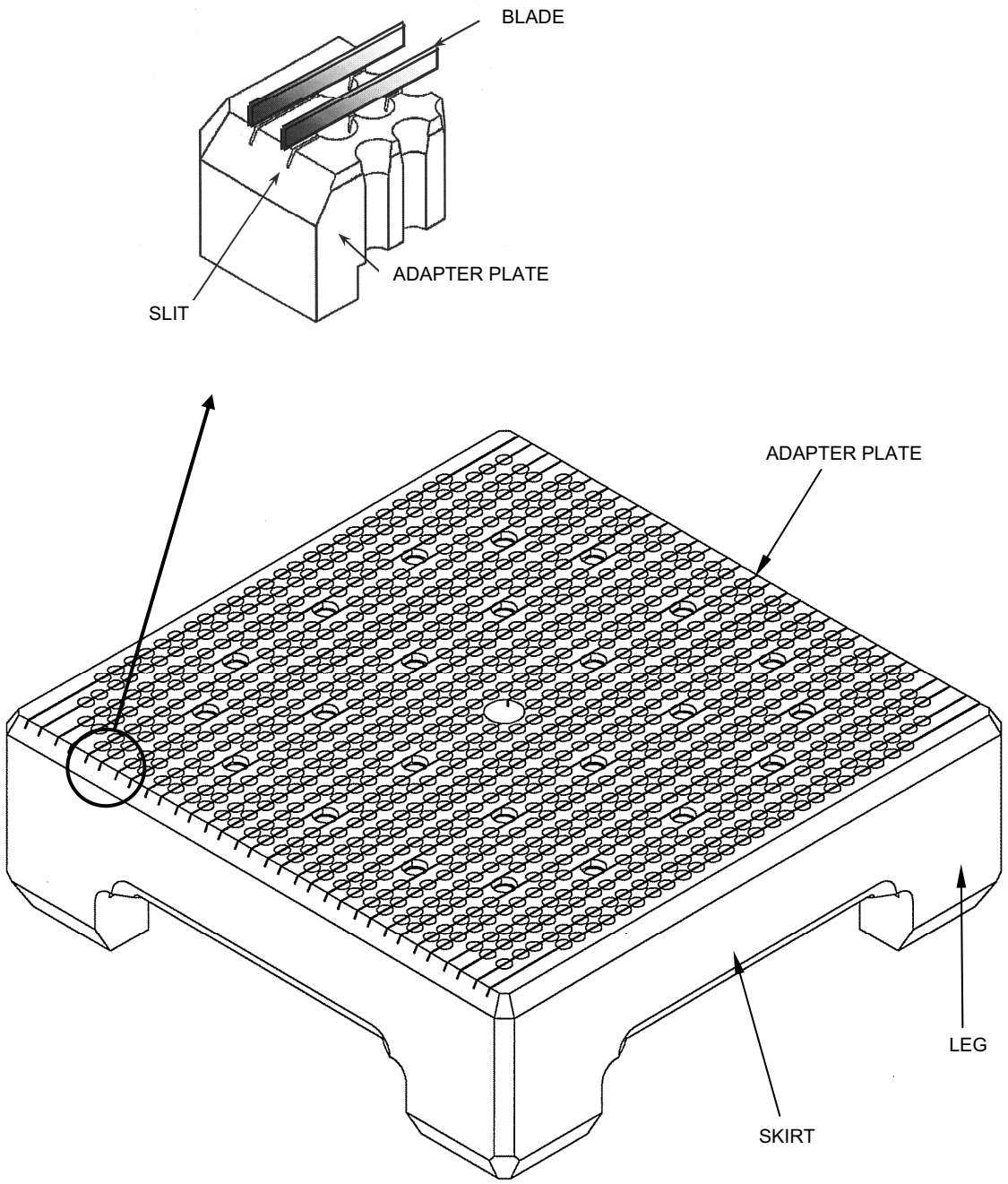

Figure 4.2-4 Schematic View of Bottom Nozzle

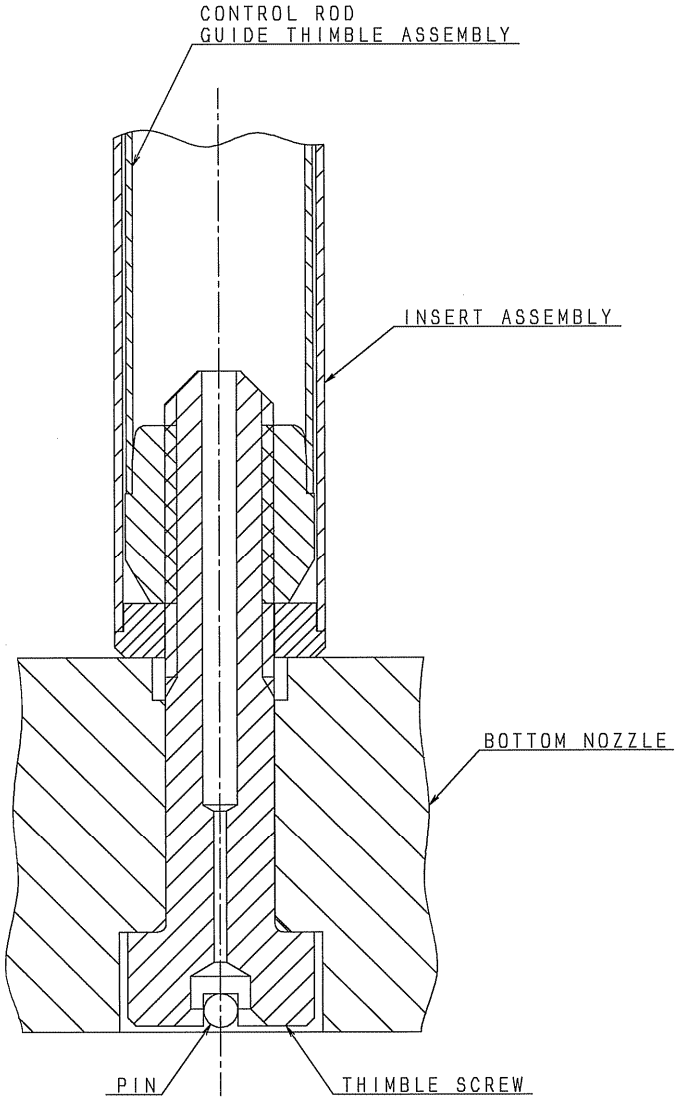

Figure 4.2-5 Control Rod Guide Thimble to Bottom Nozzle Joint

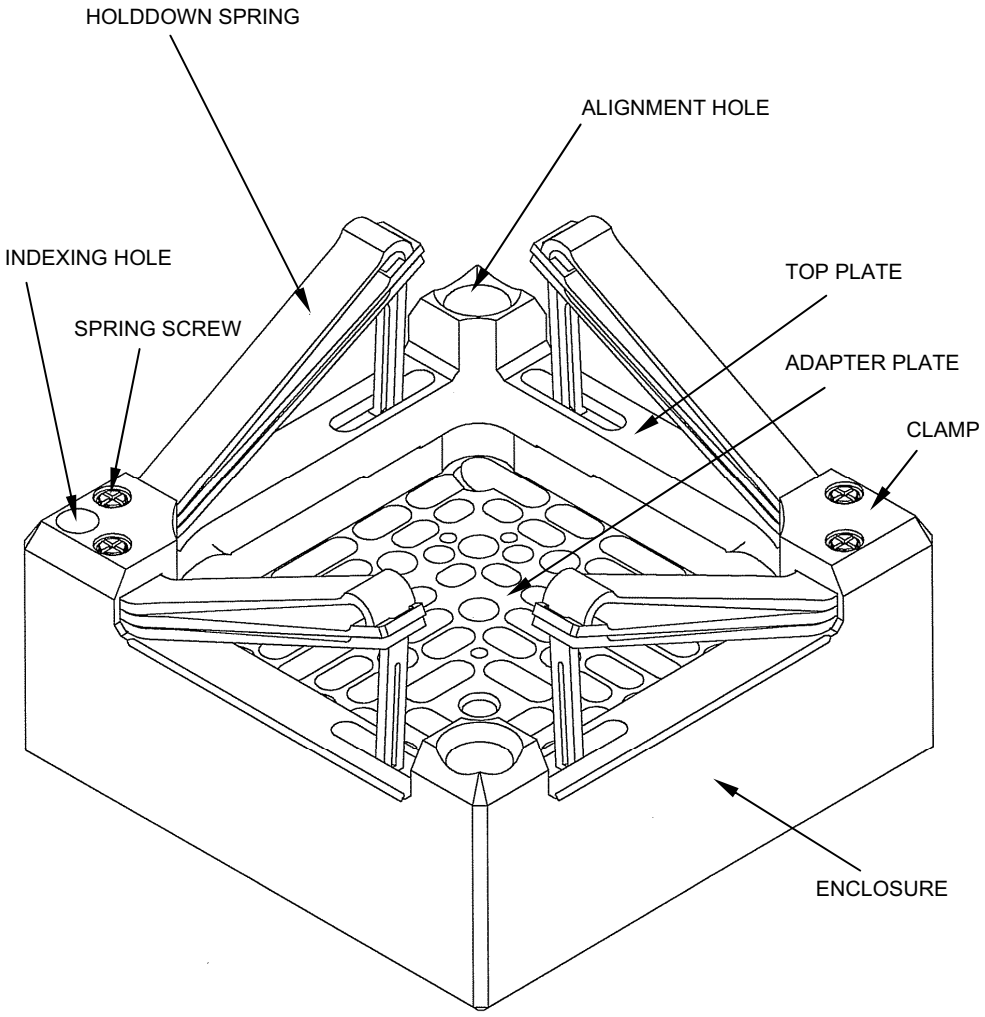

Figure 4.2-6 Schematic View of Top Nozzle

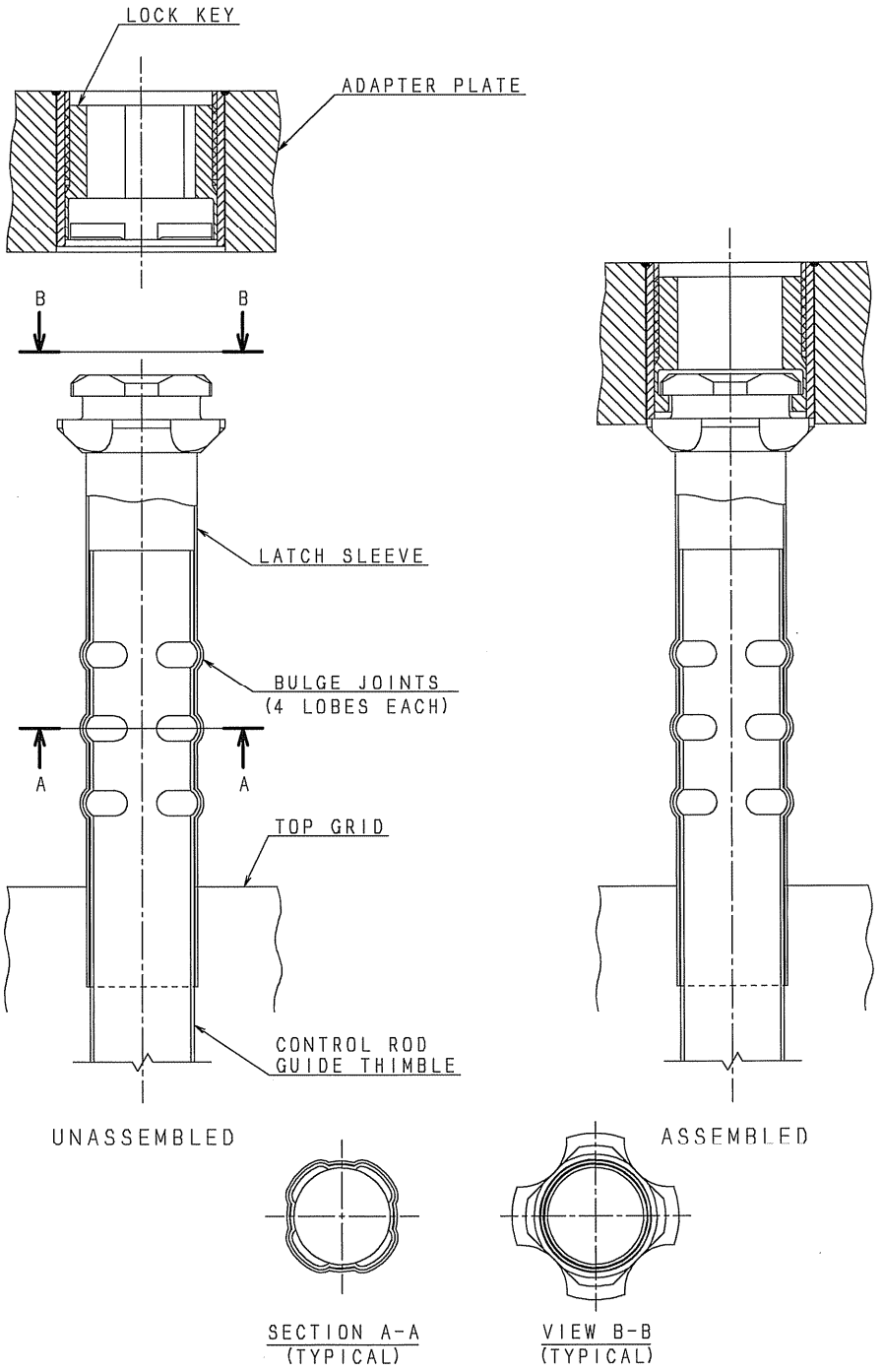

Figure 4.2-7 Control Rod Guide Thimble to Top Nozzle Joint

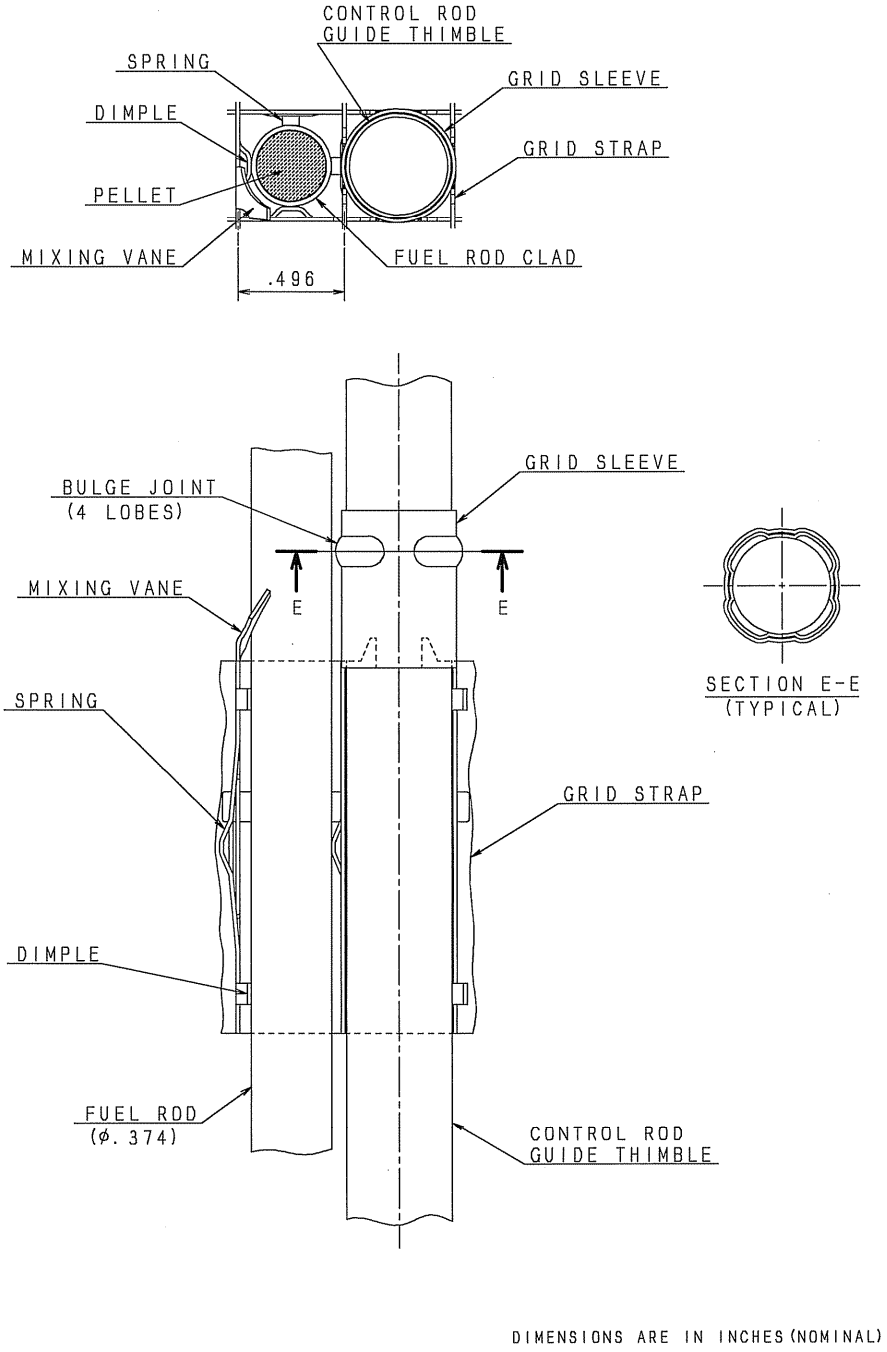

Figure 4.2-8 Control Rod Guide Thimble to Intermediate Grid Spacer Joint

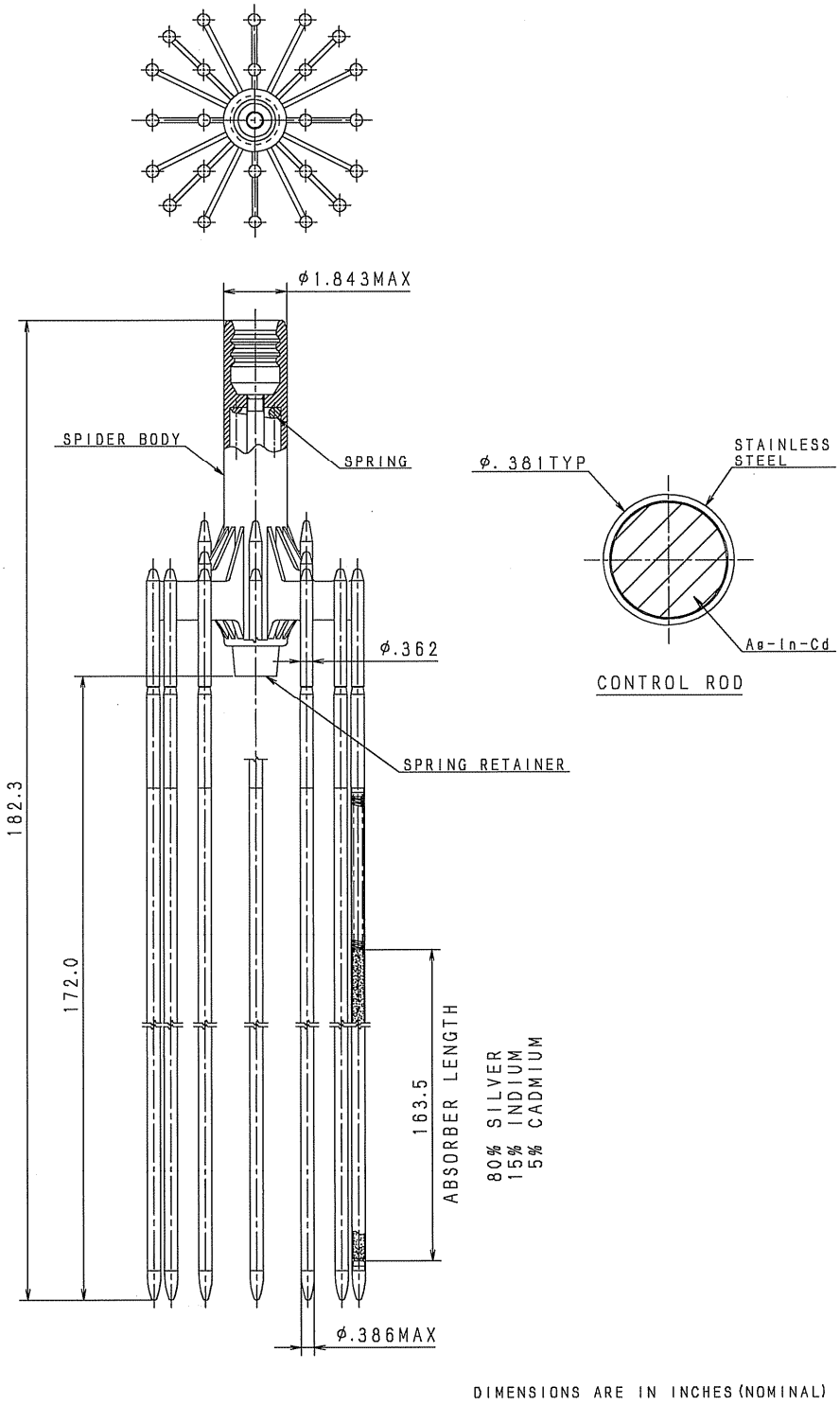

Figure 4.2-9 Schematic View of Rod Cluster Control Assembly

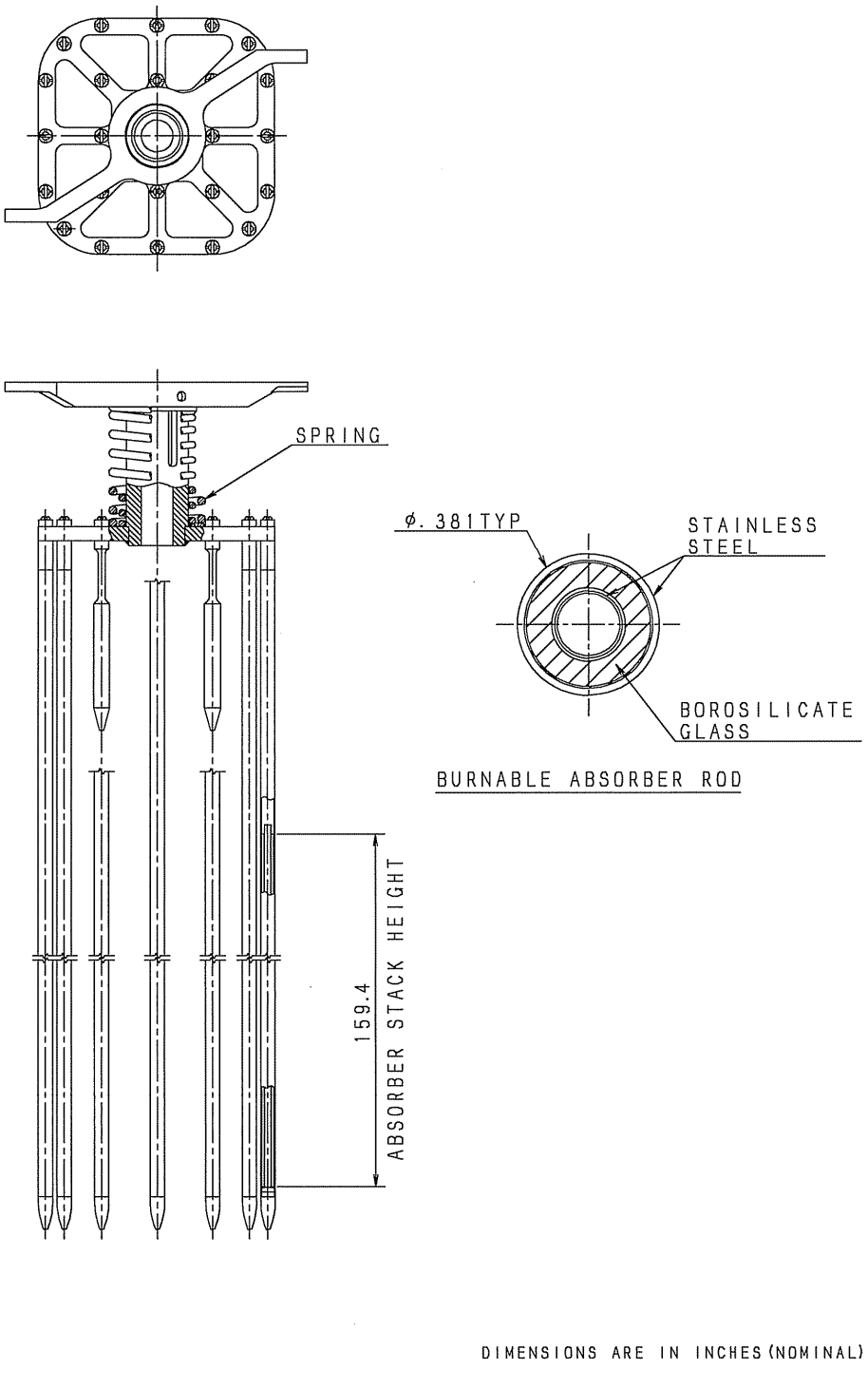

Figure 4.2-10 Schematic View of Burnable Absorber Assembly

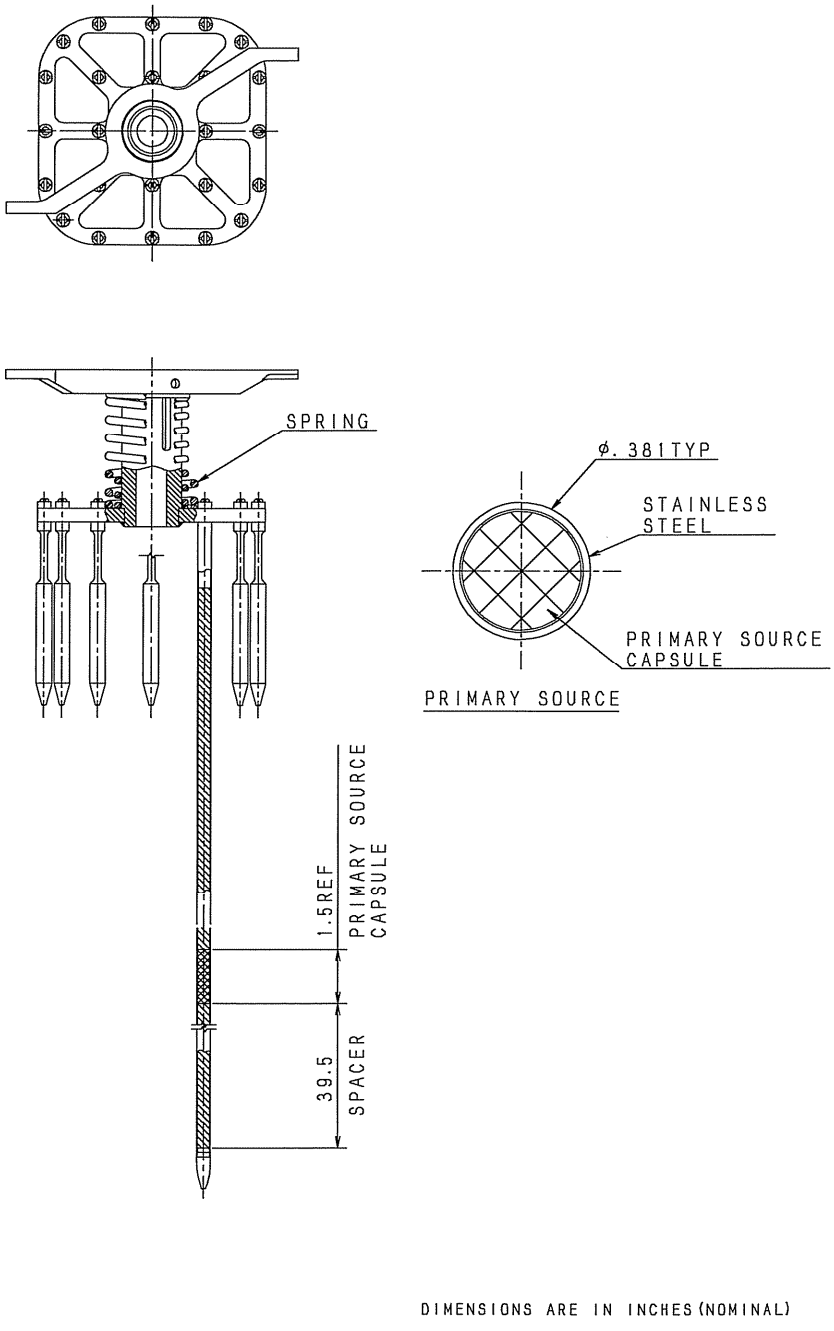

Figure 4.2-11 Schematic View of Primary Source Assembly

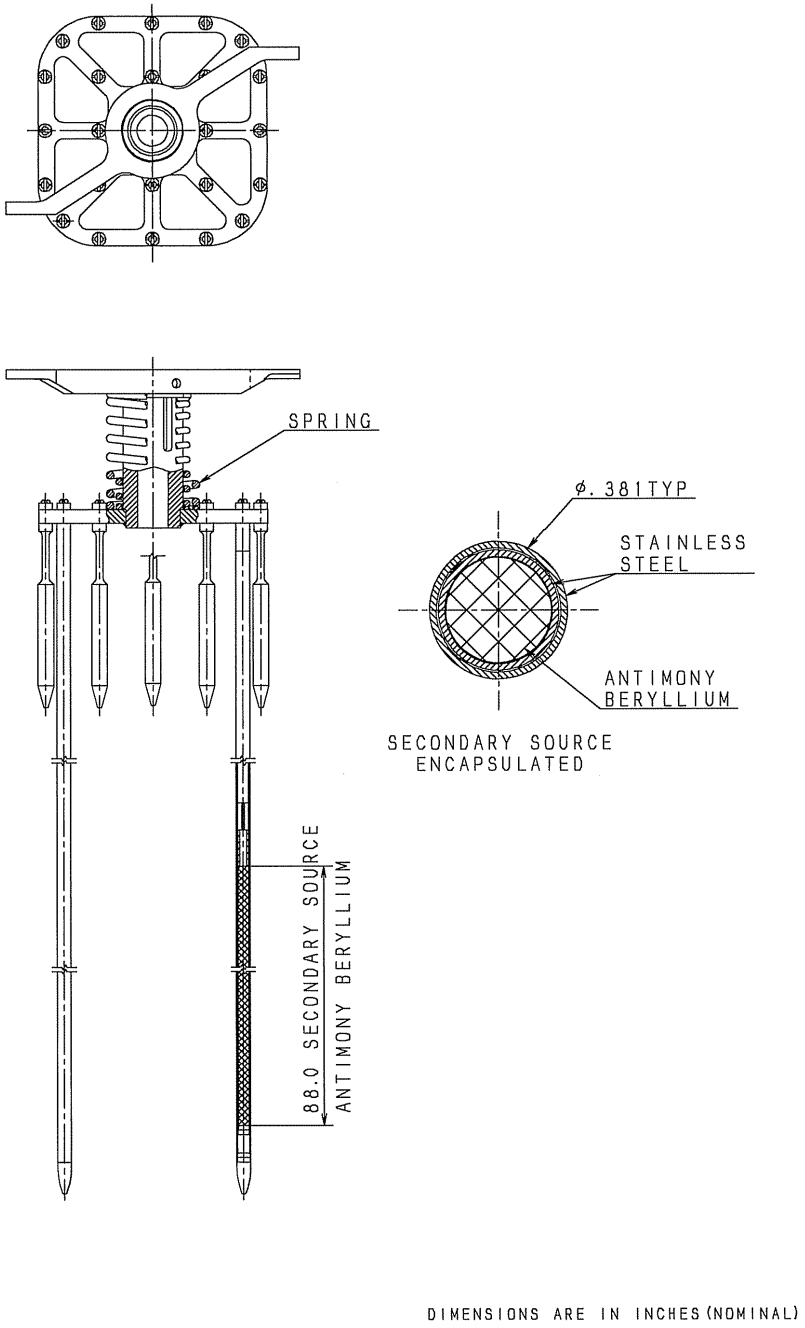

Figure 4.2-12 Schematic View of Secondary Source Assembly

4.3 Nuclear Design

This section begins by describing the bases for the nuclear design for the US-APWR. It describes the design, addressing power distribution, reactivity coefficients, control requirements, control rod patterns and reactivity worths, criticality of the reactor during refueling, stability of the reactor, and irradiation of the reactor vessel. It then describes the analytical methods used in the nuclear design.

4.3.1 Design Bases

The nuclear design of the US-APWR fuel and reactivity control system implements the design bases and functional requirements related to applicable General Design Criteria (GDC) (Reference 4.3-1). Analysis acceptance criteria, which are in accordance with guidance in Standard Review Plan 4.3 (Reference 4.3-2), are met using approved analytical techniques.

The following subsection describes how the nuclear design bases of the fuel and reactivity control systems satisfy the above analysis acceptance criteria and GDC. Specifically, the following GDC are considered in the nuclear design of the reactor: GDC 10, 11, 12, 25, 26, 27, and 28. Reference is also made to GDC 13 and 20 as applicable.

The plant conditions on which the nuclear design is based are described in Section 4.1.

Design bases for control of power distributions, negative core reactivity effects, shutdown margin, maximum controlled reactivity insertion rate and stability are presented and discussed in detail in the following subsections.

Limitations on excess reactivity, fuel burnup, core design lifetime, fuel replacement program and burnable absorber requirement are not direct or explicit design criteria, except in cases where they are quantified in order to satisfy other design bases.

A maximum fuel rod average burnup of 62,000 MWD/MTU is used to satisfy acceptable fuel design limits that are related to high burnup effects, as described in Reference 4.3-3.

At the beginning of each fuel cycle, sufficient initial excess reactivity is available in the core to meet core design lifetime (cycle length) and design discharge burnup requirements. A fuel replacement program (such as that described in Subsection 4.3.2.1) is implemented to meet safety-related criteria for each operating cycle.

The initial excess reactivity of the core is specified to allow full-power operation throughout the cycle lifetime with equilibrium xenon, samarium and other fission products present. Other negative reactivity control features such as chemical shim and/or burnable absorbers are also used to compensate for excess reactivity, and burnable absorbers help to control power distribution within the core. End of full-power design life occurs when control rods are almost completely withdrawn and the chemical shim concentration is at a very low value (e.g., approximately 10 ppm boron). Although the initial excess installed reactivity is not explicitly a design basis, all design bases must be met while satisfying the desired operating requirements described above.

4.3.1.1 Control of Power Distributions

4.3.1.1.1 Design Basis

In accordance with GDC 10, the reactor core and associated coolant, control, and protection systems are designed with appropriate margin to assure that specified acceptable fuel design limits are not exceeded during any condition of normal operation, including the effects of anticipated operational occurrences (AOO). Specific design basis requirements are:

- Fuel management will not result in operational duties (fuel rod power and burnup) that would exceed the assumptions for fuel rod integrity analysis as described in Section 4.2.

- The reactor core will not operate with a power distribution that would result in departure from nucleate boiling (DNB), as discussed in Section 4.4.

- The peak linear heat rate (PLHR) will not cause fuel melting, as discussed in Section 4.4.

- The fuel will be operated within the bounds determined by the body of the safety analysis under normal operating conditions.

4.3.1.1.2 Discussion

Adverse power distribution conditions are used as input to the initiation of all safety analyses. Radial and axial power distributions within the core are based upon the entire anticipated spectrum of allowable operation maneuvers during normal plant operation as described in Subsection 4.3.2.2. Power distribution uncertainties, as described in Subsection 4.3.2.2, are applied to predicted power distributions.

Reactor power distributions and global reactor conditions are monitored and controlled in accordance with GDC 13 and 20 to satisfy the above requirements, as described in Sections 7.2 and 7.7.

4.3.1.2 Negative Reactivity Feedback

4.3.1.2.1 Design Basis

In accordance with GDC 11, the reactor core is designed so that in the power operating range the net effect of the prompt inherent nuclear feedback characteristics compensates for a rapid increase in reactivity.

4.3.1.2.2 Discussion

Inherent physical characteristics of the reactor fuel and moderator design provide the required negative reactivity feedback to compensate for rapid reactivity insertions and associated increases in reactor power. Slightly enriched uranium has inherent Doppler negative reactivity effects due to increased fuel temperature that acts in a very short

timeframe. In addition, an increase in moderator temperature and reduction in moderator density provide additional, but slower, negative reactivity feedback.

The magnitude of both of these phenomena typically varies with reactor power and thermal and hydraulic conditions, and are therefore described in terms of reactivity coefficients for specified conditions. During normal conditions, the reactivity coefficients of the fuel and moderator temperature are negative. Early in fuel cycle life, when excess installed reactivity is large, the negative moderator reactivity feedback coefficient is assured by the use of burnable absorbers and/or control rods, which limit any competing effects of boron removal during moderator density changes. Typically, the use of burnable absorbers will be required for power distribution control and to maintain acceptable chemical shim concentrations. Although burnable absorber distribution and quantity are not an explicitly part of the design basis, the nuclear design will specify the burnable absorber requirements that meet applicable design criteria.

4.3.1.3 Shutdown Margin

4.3.1.3.1 Design Basis

In accordance with GDC 26, two independent reactivity control systems based on different design principles are provided. One of the systems uses control rods, based on a positive means for inserting the rods, and is capable of reliably controlling reactivity changes to assure that under conditions of normal operation, including AOOs, and with an appropriate margin for malfunctions such as stuck rods, specified acceptable fuel design limits are not exceeded. The second reactivity control system is capable of reliably controlling the rate of reactivity changes resulting from planned, normal power changes to assure acceptable fuel design limits are not exceeded. One of the systems is capable of holding the reactor core subcritical under cold conditions.

In addition, in accordance with GDC 27, reactivity control systems have a combined capability, in conjunction with boron addition by the emergency core cooling system, of reliably controlling reactivity changes under postulated accident conditions, with appropriate margin for stuck rods.

4.3.1.3.2 Discussion

The rod cluster control assembly (RCCA) and chemical shim in the moderator provide the two required independent systems for shutdown margin control. The RCCAs are divided into banks to provide two functions: 1) control banks to provide power distribution control and reactivity changes that compensate for Doppler and moderator effects due to changes in core power level from full power to no-load conditions, and 2) shutdown banks to provide additional negative reactivity. The RCCAs provide the minimum shutdown margin required under normal operation conditions and have a sufficient reactivity insertion rate to prevent fuel damage, assuming the highest worth RCCA does not insert upon reactor trip.

The chemical shim system typically provides most of the normal operation reactivity control during fuel depletion. The chemical and volume control system (CVCS) is also designed to compensate for reactivity insertion changes due to fission product inventory changes (e.g. xenon burnout) and to compensate for reactivity changes to maintain the

reactor sufficiently subcritical in cold shutdown. The mechanical and chemical shim control systems therefore satisfy the requirements for two independent means to maintain the shutdown margin.

Reactor power distributions and global reactor conditions are monitored and controlled in accordance with GDC 13 and 20 to satisfy the above requirements, as described in Sections 7.2 and 7.7.

Due to the lack of a specific criterion, a five percent sub-criticality margin is assumed for the refueling operation, which is consistent with the requirements of 10 CFR 50.68 (Reference 4.3-4). This criterion is fulfilled with the boron concentration for refueling specified in the technical specifications and with control rods inserted. Use of the specified boron concentration is enough to keep the reactor sub-critical even without the control rods. Criticality monitoring is performed during refueling.

4.3.1.4 Maximum Controlled Reactivity Insertion Rate

4.3.1.4.1 Design Basis

In accordance with GDC 25, the protection system is designed to assure that specified acceptable fuel design limits are not exceeded for any single malfunction of the reactivity control systems, such as accidental withdrawal (not ejection) of control rods.

Maximum reactivity insertion rates from RCCAs withdrawal or by chemical shim dilution are limited by system design (such as CVCS specifications), component design (such as RCCA drive mechanism capabilities), and the material/dimensional characteristics of the RCCAs.

During normal operation, maximum controlled reactivity insertion rates are limited by adherence to technical specifications. For accidental/inadvertent control rod group withdrawal of two banks, the maximum reactivity change rate is set such that limits of DNBR and PLHR are met.

In accordance with GDC 28, the reactivity control systems are designed with appropriate limits on the potential amount and rate of reactivity increase to assure that the effects of postulated reactivity accidents can neither (1) result in damage to the reactor coolant pressure boundary greater than the limited local yielding nor (2) sufficiently disturb the core, its support structures or other reactor internals to impair significantly the capability to cool the core.

4.3.1.4.2 Discussion

The maximum reactivity addition of a control bank (or banks) is primarily determined by the reactivity worth of the control rod bank(s) worth, the maximum withdrawal rate, and unfavorable axial power distributions. Xenon distributions are also considered, but the xenon burnout rate is much slower than the reactivity insertion rate for normal operation and accidental bank withdrawal.

Based on the analysis of bounding accidents and conditions, the maximum RCCA withdrawal speed is limited to 45 inches per minute. Combined with RCCA component

specifications that limit the maximum reactivity insertion rate (e.g., pcm/inch) and maximum CVCS charging/letdown rates, safety criteria are shown to be met.

In postulated reactivity accidents, such as rod ejection, the pressure in the reactor coolant system (RCS) and main steam system is maintained below acceptable design limits. In addition to the RCCA component and material specification, the core design limits the maximum reactivity worth of individual control rods. The rod ejection accident is discussed in detail in Subsection 15.4.8.

Reactor power distributions and global reactor conditions are monitored and controlled in accordance with GDC 13 and 20 to satisfy the above requirements, as described in Sections 7.2 and 7.7.

4.3.1.5 Stability

4.3.1.5.1 Design Basis

GDC 12 requires that the reactor core and associated coolant, control, and protection systems are designed to assure that power oscillations which can result in conditions exceeding specified acceptable fuel design limits are not possible or can be reliably and readily detected and suppressed.

4.3.1.5.2 Discussion

Core power stability can be categorized as total core power stability and incore power distribution stability in the axial and horizontal (X-Y plane) dimensions.

Undesired changes, or oscillations, in total power output of the core are reliably detected by protection systems. Loop temperature sensors and nuclear instrumentation protect design margin to fuel limits by initiating a reactor trip based on system setpoints for total core power and power (flux) rates. Reactor power, steam generator, and turbine control systems provide diverse protection against total core power oscillations. These diverse and redundant layers of protection make it unlikely that design power levels will exceed acceptable limits. Specifically, the reactor protection system over power ΔT ($OP\Delta T$) and over temperature ΔT ($OT\Delta T$) trip functions protect fuel against damage using loop temperature, pressurizer pressure, and measured axial offset inputs.

Mitigation of incore power distribution oscillations due to spatial xenon effects is provided by inherent design characteristics. Spatial stability in the X-Y plane is especially strong, and exciting significant oscillations in the horizontal plane is not likely as long as RCCA control is performed as required by the technical specifications. Axial power distribution oscillations due to xenon-induced reactivity effects may occur, especially late in the fuel cycle, due to the relatively flat axial power distribution and the axial oscillations can be readily controlled by use of the manual control rod system. The core monitoring system processes information provided by axially segmented ex-core detectors. Both radial and axial power distributions are monitored.

Reactor power distributions and global reactor conditions are monitored and controlled in accordance with GDC 13 and 20 to satisfy the above requirements, as described in Sections 7.2 and 7.7.

4.3.2 Description

4.3.2.1 Nuclear Design Description

The US-APWR core consists of 257 mechanically identical fuel assemblies surrounded by a stainless steel radial neutron reflector designed to improve neutron utilization, which reduces the fuel cycle cost and significantly reduces reactor vessel irradiation compared to previous PWRs with baffle/barrel designs. Other core components include burnable absorbers and RCCAs.

The US-APWR fuel assembly utilizes a 17x17 array of 264 fuel rods, 24 control rod guide thimbles and one in-core instrumentation guide tube. A cross sectional view of the 17x17 fuel assembly is shown in Figure 4.3-1.

The fuel rods consist of slightly enriched cylindrical uranium dioxide pellets contained in a cylindrical tube made of zirconium-based alloys and sealed with end plugs. The US-APWR axial active fuel length is approximately 14 ft. Detailed descriptions of the US-APWR fuel rod and fuel assembly design features are given in Section 4.2.

The resulting low linear power density of 4.65 kW/ft allows flexible core and fuel management with improved thermal margins. Even under the constraints of fuel enrichment less than 5 wt% and maximum fuel rod burnup of 62,000 MWD/MTU, both initial and reload cores are anticipated to operate up to 24 months assuming a cycle burnup of 23,000 MWD/MTU and refueling outage length of 0.5 months. The operation length of initial and reload cores depends on the energy requirements.

Both integral and non-integral burnable absorbers are used for power distribution and excess reactivity control. Some fuel rods have fuel pellets containing Gadolinia (Gd_2O_3) integral burnable poison in full-length or part-length axial configurations. In order to reduce the peak linear heat rate, the uranium enrichment of the Gadolinia fuel pellets is lower than the uranium enrichment of the uranium rods loaded in the same assembly (Subsection 4.4.1.2). Non-integral burnable absorber clusters with rods containing borosilicate glass burnable poison may also be inserted into the control rod guide thimbles of fuel assemblies. The burnable absorbers are strategically located within the fuel assembly to provide a favorable power distribution. Figure 4.3-1 shows the burnable absorber distributions within a fuel assembly for a typical initial core (hereafter referred to as “initial core” in Section 4.3).

The initial core typically uses three different uranium fuel rod enrichments to obtain a favorable radial power distribution throughout the cycle lifetime. Each fuel region, composed of fuel assemblies with the same uranium fuel rod enrichment, has approximately the same number of fuel assemblies. The fuel assemblies and burnable absorbers are arranged in the core to flatten the core power distribution. Figure 4.3-2 shows a typical initial core loading pattern for 24 month operation.

Loading patterns for reload cores can vary significantly depending on cycle burnup requirements and other operational constraints. The US-APWR is anticipated to operate for up to 24 months between refuelings. “Low leakage” loading patterns are typically used for fuel economy. Irradiated fuel assemblies, with one or two cycles of burnup, are loaded on the core periphery to reduce core peripheral power and therefore neutron leakage.

Fresh fuel assemblies are loaded into the core center. Because power is concentrated in the core center, additional power distribution control strategies are employed to meet power distribution limits. Burnable absorbers are used for both global and local power distribution control. Fuel assemblies may contain different numbers of fuel rods containing Gadolinia, and Gadolinia content may vary between assemblies. Further, Gadolinia may be used only in pellets of the central region of the fuel stack to obtain a part-length absorber for additional axial power distribution control.

The core average enrichment is determined by the amount of fissile material required to allow the full power operation throughout the cycle lifetime. The choice of enrichment for both the initial core and reloads includes consideration of the depletion of initial fissile material, U-235, and buildup of both parasitic fission products and fissile material such as Pu-239 and Pu-241, as shown in Figure 4.3-3.

Control rods and soluble boron in the coolant are provided as two independent shutdown mechanisms and are also designed to control reactivity during reactor operation.

The control rod system has enough reactivity to compensate for rapid reactivity fluctuations during operation and also for the transition from full power to the hot zero power condition. In addition, the hot shutdown margin with the most reactive control rod stuck provides adequate sub-criticality to minimize any consequences of over cooling events. In order to guarantee adequate shutdown margin, the control rod banks use insertion limits during operation. The RCCA is composed of 24 control rods of Ag-In-Cd alloy, and cladding in stainless steel. Figure 4.3-4 shows the fuel assembly and control rod assembly configuration in the US-APWR core.

The CVCS is designed to provide boron concentration changes in the RCS to compensate for the slow reactivity changes due to fuel burnup, fission product poisoning due to xenon and samarium, burnable absorber depletion, and the cold-to-operating moderator temperature reactivity defect. The negative reactivity insertion by soluble boron addition is rapid enough to overcome the reactivity rise due to the decay of built-up xenon. In addition, the boron concentration is controlled to maintain sufficient sub-criticality during refueling. Figure 4.3-5 shows the soluble boron concentration versus core depletion for the initial core.

A reactor core description and the main nuclear design parameters of the US-APWR are shown in Tables 4.3-1 and 4.3-2, respectively. Table 4.3-2 contains information important to evaluate global core performance, including reactivity coefficients, delayed neutron fractions and neutron lifetimes.

4.3.2.2 Power Distribution

The three dimensional power distributions of US-APWR are calculated with the analytical methods described in Subsection 4.3.3.1. Confirmation of the accuracy of power distribution calculations is given in Reference 4.3-5 and in Subsection 4.3.2.2.3. Additionally, as described in Subsection 14.2.12.2, detailed physics tests are planned at the beginning of the initial core, some of which will provide data for confirming the accuracy of power distribution calculations and methods.

Power distributions are calculated for a spectrum of power levels with the corresponding fuel temperature, and moderator temperature and density feedback. Effects of the xenon and samarium are also considered. In nuclear calculations, normal flow with the same flow per channel is considered.

4.3.2.2.1 Power Distribution Characteristics

Although power distributions are generated with 3D methods, the main features of radial and axial power distributions are analyzed for typical steady state conditions during cycle lifetime and presented below.

The radial power distribution is determined mainly by the fuel assembly and burnable absorber patterns at the beginning of cycle. The control rod pattern and amount of insertion also affects the radial power distribution. Figures 4.3-6 through 4.3-8 show typical initial core unrodded one-eighth-core normalized radial power distributions at hot full power, equilibrium xenon (EqXe) conditions for beginning of cycle (BOC), middle of cycle (MOC) and end of cycle (EOC), respectively. Rodded cases, with control rods at their rod insertion limits (RIL) at hot full power, are shown in Figure 4.3-9 through Figure 4.3-11 for BOC, MOC and EOC. In order to show the relative small effect of the xenon on the radial power distribution, Figure 4.3-12 shows the non-xenon (NoXe) power distribution for BOC, at hot full power and unrodded condition.

Figures 4.3-13 through 4.3-15 show typical rodwise power distributions, corresponding to the assembly with the highest relative power presented in the Figures 4.3-6 through 4.3-8, respectively.

The axial power distribution is mainly affected by control rod insertion, burnup history, power level, xenon distribution and axial fuel specifications such as the axial distribution of burnable absorber. Figure 4.3-16 shows typical initial core normalized axial power distributions for representative operating conditions mentioned above. The axial power distribution is controlled by the operator through the difference in power of the core top and bottom halves, called the axial flux difference (ΔI). The power level of the core top and bottom halves are obtained from ex-core detector signals situated outside the reactor parallel to reactor axis. There are four ex-core detectors placed in 90 degree symmetry. The ex-core detector signals are periodically calibrated with the in-core measurements. The calibrated flux difference is mainly used for providing the shape penalty function to the OTΔT DNB protection and the OPΔT overpower protection.

Figures 4.3-6 through 4.3-8 show the assembly-wise burnup distributions while Figure 4.3-17 shows a typical axial burnup distribution for the initial core. Radial power distribution within the fuel pellet is described in Reference 4.3-3.

The hot channel factors have been historically used to quantify relative power distributions. The most important hot channel factors are the nuclear enthalpy rise hot channel factor and heat flux hot channel factor or total peaking factor.

The ratio of the maximum integrated rod power within the core to the average rod power, $F^N_{\Delta H}$, is the nuclear enthalpy rise hot channel factor. $F^N_{\Delta H}$ is of particular interest for nuclear calculations because the moderator density is directly proportional to enthalpy. Typical initial core values of $F^N_{\Delta H}$ are shown in Figure 4.3-18.

The maximum local heat flux on the surface of a fuel rod divided by the average fuel rod heat flux, F_Q, is the heat flux hot channel factor or total peaking factor. F_Q includes an allowance for fuel pellet and fuel rod manufacturing tolerances. F_Q can be expressed as the product of two components:

$$F_Q = F_Q^N \times F_Q^E$$

where,

The first component, F^N_Q, is the nuclear heat flux hot channel factor, assuming nominal fuel pellet and rod parameters. This is the maximum local linear heat rate divided by the average heat rate.

The second component, F^E_Q, is the engineering heat flux hot channel factor. F^E_Q accounts for increases in heat flux due to the effects of manufacturing tolerances. Local variations in pellet density and diameter and enrichment are considered for the fuel. The fuel rod surface area is considered for the cladding. Combined statistically, the net effect is a factor lower than 1.03. Conservatively, 1.03 is adopted for F^E_Q.

Historically, the effect of fuel pellet densification has been considered for impact on local peaking factors. However, modern PWR fuel manufacturing practices have essentially eliminated significant fuel densification impacts on reactor design and operation, so for Mitsubishi fuel a densification power spike factor of 1.0 is appropriate, as described in Reference 4.3-3.

4.3.2.2.2 Limiting Power Distributions

As stated in Section 4.1, the plant conditions are categorized as normal operation conditions, AOOs and postulated accidents.

Normal operation conditions are expected as routine during the course of power operation, power maneuvers, and shutdown of the plant. There is a margin between any plant parameter and the value of the parameter which would require either automatic or manual protective action. The correct and timely action of the reactor operator is implicitly included in the definition of normal operation. The power distribution is maintained within appropriate values since the reactor operator follows operational procedures and takes any necessary actions alerted by the plant instrumentation.

Since normal operation conditions are considered as the starting point of AOOs and postulated accidents, a conservative set of initial conditions is selected for the analysis of each fault condition. The normal operation and shutdown conditions, their permissible deviations, and the operational transients are described in Section 15.0.

Radial power distribution is stable and easily controlled to meet the operating limits. The axial power distribution can be significantly changed due to core power level changes, control rod motion, cycle lifetime and xenon distribution. However, during normal operation, the control rod motions, such as allowable rod maximum misalignment between control rods of single bank, rod insertion limits and rod bank overlap, are limited by the technical specifications.

The power distribution control procedure, called constant axial offset control (CAOC), is based on controlling the axial offset within the allowable operating band about the target value at all power levels (Reference 4.3-6). The target value is varied during the cycle since the axial offset varies, as shown in Figure 4.3-19. Control to the target axial offset minimizes the transient xenon effect on the power distribution. The operational procedure is detailed in the technical specifications and surveillance is performed using ex-core detectors calibrated with periodically incore power distribution measurements. There are also alarms which indicate the deviation and time of deviation from the permissible band. This operational strategy was developed to define the normal operation conditions and its results are used to construct the F_Q envelope and the precondition for AOOs.

Power distribution calculations are performed for all normal operation conditions including extensive load follow operation. Different power histories and cycle burnups are considered in order to survey a large number of local power densities as a function of axial elevations. Exhaustive studies of load follow maneuvers for PWR cores similar to the US-APWR are reported in Reference 4.3-6. Figure 4.3-20 shows the calculated F_Q values for the initial core employing a (+5 %, -10 %) target band for CAOC procedure.

All of the above core operation effects and allowable operation modes are taken into consideration for power distribution calculations, which are used for determining the upper bound values of F_Q and $F^N_{\Delta H}$. The technical specifications describe in detail how to maintain the hot channel factors within the permissible values during operation.

An $F^N_{\Delta H}$ limit of 1.73, which includes nuclear uncertainty and margin, is adopted in the US-APWR design. This $F^N_{\Delta H}$ limit absorbs changes in the radial power distribution caused by control rod insertion from all-rods-out position to the rod insertion limits. The variation of maximum $F^N_{\Delta H}$ with core power determines the control rod pattern, the bank sequence and the rod insertion limits to establish the design basis criterion. The $F^N_{\Delta H}$ limits which vary as a function of the core power while meeting the DNB limits, are defined in the technical specifications. Since the worst value of $F^N_{\Delta H}$ generally occurs when the rods are at their insertion limits, the thermal margin is usually increased when the rods are above these positions.

The average linear heat rate is 4.65 kW/ft for the thermal output of 4451 MW. The maximum allowable peak linear power density is 12.1 kW/ft, assuming an F_Q equal to 2.6 and including a calorimetric error of 2 %. With regards to the upper bound envelope for F_Q, an axially constant value of 2.6 is adopted. This envelope conservatively bounds all linear power densities for normal operation of the reactor. Since actual linear heat rate values decrease with reduced core power levels, the maximum allowable F_Q peaking factor may increase as shown in the technical specifications.

Finally, uncertainty and engineering factors are applied to the limiting peaking factors determined with the methods described above. The applicable uncertainty factors are described in Reference 4.3-8 and summarized in Subsection 4.3.2.2.3.

AOOs are those conditions that are expected to occur one or more times during the life of a nuclear power plant. The list of the AOOs and the consequences which may result are discussed in Section 15.0. AOOs produce large distortions on power distribution in both positive and negative axial offset directions and/or power level increase. Power

distributions during AOO, which deviate from normal power distributions, are considered for the determination of the reactor protection system setpoints to maintain margin to overpower or departure from nucleate boiling limits.

The objectives of power distribution calculations during AOOs are to evaluate the consequence of specified events to satisfy safety related parameters such as peak linear heat rate and design basis axial shapes for DNBR evaluations and to provide the required information for the core protection system which define the penalty function shapes in the over power and over temperature ΔT setpoint equation.

Then, AOOs such as control rod withdrawal, uncontrolled dilution/boration and cooldown events are considered to determine the penalty function.

$F^N_{\Delta H}$ limits are taken as input to the thermal-hydraulic analyses including most of AOOs in which the radial power distribution does not deviate from normal operation. Additionally, a conservative radial power distribution is used for DNB analysis which bounds all normal operation conditions at all times in cycle life. This distribution localizes core power while assuming a flat rodwise power distribution in the lead-power assembly, and includes a fuel rod with the design value of $F^N_{\Delta H}$. These assumptions are selected for DNB analysis to minimize thermal mixing benefit.

4.3.2.2.3 Power Distribution Monitoring and Experimental Verification

This section describes the instrumentation and methodology used to measure the core power distribution and to derive the associated uncertainties.

The measured power distribution is obtained by processing the data from the incore instrumentation. The incore instrumentation devices are movable detectors (fission chambers) which are inserted into the instrumentation thimbles from the top of the core; the detector current value reading is obtained for each axial position. The output signal of the fission chamber used as an incore instrumentation device is proportional to the U-235 fission reaction rate inside the detector. As described in Reference 4.3-8 the measured signal is converted into a measured power distribution using the following well-known processing algorithm.

$$[P]_{Measured} = \frac{[TRR]_{Measured} \times \left[\frac{FP}{TRR}\right]_{Calculated}}{[Paver]}$$

where P is the relative power, TRR is the thimble reaction rate, FP is the fuel assembly power or the fuel rod power and Paver is all fuel assemblies average power.

The assembly and fuel rod power measurement (relative value) which is obtained by the above formula is compiled to obtained hot channel factors (F_Q and $F^N_{\Delta H}$), radial power tilt and axial offset.

The US-APWR power distribution can be adequately monitored using the ex-core and in-core instrumentations. Perturbations to the core power distribution are controlled by limiting rod insertion and axial flux differences. Details of these limits, alarms and reactor

trip settings are provided in the technical specifications, while the descriptions of the systems are provided in Sections 7.2 and 7.7.

The comparison between 'measured' and predicted power distributions for the same situation includes some measurement error, and it is necessary to account for such error. The accumulated data on power distributions in actual operation are basically data taken during normal operation in steady-state equilibrium conditions, and data from induced xenon transient conditions. Examples of these data are presented in detail in Reference 4.3-5.

As described in Subsection 4.3.2.2.2, uncertainties must be applied to the limiting power distributions. The appropriate uncertainties are discussed in References 4.3-7 and 4.3-8. A summary of the bases, results and conclusions of the referenced reports is given below.

Using measurements of core power distributions with the incore instrumentation system described in Section 7.7 and Subsection 4.4.6, the following uncertainties are considered:

1- Measurement reproducibility.

2 - Errors in the calculated relationship between detector current and local power generation within the fuel assembly.

3 - Errors due to the inference of power some distance from the measurement thimble, i.e. the extrapolation method.

The appropriate allowance for category 1 above has been quantified by multiple measurements made with several inter-calibrated detectors by using the common thimble features of the in-core detector system. This system allows more than one detector to access any thimble. Control of measurement reproducibility is provided by strict adherence to manufacturing specifications. Errors in category 2 above are quantified by comparisons of analytical results and measurements for critical experiment data on arrays of rods with simulated guide thimbles, control rods, burnable poisons, etc. Errors in category 3 are quantified by multiple comparisons of two 'measured' power distributions of actual plants in which extrapolated results were compared to 'reference' results.

The approach for determining the above uncertainties is discussed in Reference 4.3-7, which describes critical experiments performed and plant measurements taken with incore instrumentation systems. In Reference 4.3-7, the uncertainties listed above are evaluated quantitatively. The Reference 4.3-8 report re-evaluates the uncertainties under the conditions of the US-APWR incore instrumentation system. Both reports conclude that the uncertainty associated with peak linear heat rate (F_Q x P) results in an allowance of five percent, at a 95 percent probability at a 95 percent confidence level. For conservatism, an eight percent uncertainty factor in F_Q x P is adopted for US-APWR nuclear design.

A similar analysis for the uncertainty in $F^N_{\Delta H}$ x P (hot rod integral power) results in an allowance of four percent, at a 95 percent probability at a 95 percent confidence level. A conservative six percent uncertainty factor is applied to $F^N_{\Delta H}$ x P for US-APWR nuclear design.

4.3.2.3 Reactivity Coefficients

In operating reactors, the transient changes in the neutron effective multiplication factor due to the change of some plant conditions, such as density, temperature, void and power, can be expressed in terms of reactivity coefficients. In a PWR, important reactivity coefficients to compensate for the rapid reactivity insertion and the associated increases in reactor power are the fuel temperature coefficient and moderator coefficients due to the change of the temperature and density. The combined effect of fuel and moderator temperature changes due to power level changes can be translated into power coefficients. Other moderator coefficients, related to the pressure and the void, are relatively not very significant in PWRs, but void effects are included for shutdown margin considerations.

The reactivity coefficients are calculated using the analytical methods described in Subsection 4.3.3.1. Comparisons of calculated and experimental reactivity coefficients are included in Reference 4.3-5.

Since reactivity coefficients change with core parameters such as cycle burnup and control rod insertion ratio, ranges of coefficients are employed in transient analysis to determine the response of the plant throughout its life. The results of such simulations and the reactivity coefficients used are presented in Chapter 15.

4.3.2.3.1 Fuel Doppler Coefficient

The fuel Doppler coefficient is defined as the change in reactivity per degree change in effective fuel temperature. As a consequence of the Doppler effect, resonance cross sections are broadened and the neutron absorption in the resonance region is increased and, thus, the neutron escape probability decreases by the increase in temperature. U-238 has several narrow resonance peaks, so in PWRs, which are fueled with low enriched uranium, the Doppler temperature coefficients are negative. The Pu-240 has a large neutron absorption resonance peak and its concentration increases with cycle burnup as shown in Figure 4.3-3, so the Doppler coefficient becomes more negative with cycle burnup. The influence of other isotopes is considered, however, they are relatively small compared with U-238 and Pu-240.

The effective fuel temperature and the reactivity change are calculated with the analytical method described in Subsection 4.3.3.1. Reactivity is calculated by slightly varying the effective fuel temperature around the reference value. The moderator temperature is held constant, in order to specifically exclude the moderator temperature effect. The Doppler temperature coefficient is a weak function of the boron concentration. Typical Doppler temperature coefficients for BOC and EOC as a function of the fuel effective temperature are shown in Figure 4.3-21.

The Doppler power coefficient is the change in reactivity due to the change of the core power level, excluding the moderator temperature effect. Figure 4.3-22 shows the typical Doppler power coefficient as a function of the core power level.

The upper and the lower Doppler coefficient limits used in the accident analysis are reported in Subsection 15.0.0.2.4

4.3.2.3.2 Moderator Coefficients

The moderator coefficients measure reactivity change due to a change in specific moderator parameters. The most important moderator coefficient is the moderator temperature (density) coefficient. This coefficient is discussed below, along with the moderator pressure and coolant void coefficients.

4.3.2.3.2.1 Moderator Temperature (Density) Coefficients

The moderator temperature coefficient is defined as the change in reactivity per degree change in the moderator temperature. The effects of the changes in moderator density and temperature are generally considered together. The moderator coefficients presented in this subsection are related to normal conditions, since coefficients during specific events can be affected largely by the entire plant conditions.

The moderator coefficients are calculated using three and two dimensional analytical methods described in Subsection 4.3.3.1. The moderator temperature is varied slightly from its reference value resulting in a consistent change in moderator density.

The moderator temperature coefficient is largely dependent on the soluble boron concentration, since the boron and water density decreases with increasing moderator temperature. A decrease in the soluble boron density introduces a positive component in the moderator density coefficient. If the concentration of soluble boron is large enough, the moderator temperature coefficient becomes positive.

Therefore, at BOC, the soluble boron concentration may be reduced using burnable absorbers in order to achieve a negative moderator temperature coefficient. Since the soluble boron concentration usually decreases with cycle burnup, the moderator temperature coefficient becomes more negative. This effect is enlarged by Plutonium isotope and fission product buildup with burnup. Figure 4.3-23 shows the unrodded, hot full power moderator temperature coefficient changes with burnup for the initial core. The moderator temperature coefficients are shown as a function of the moderator temperature from hot zero power to hot full power at BOC and EOC of the initial core (Figure 4.3-24).

4.3.2.3.2.2 Moderator Pressure Coefficient

The moderator density can be changed due to reactor coolant pressure changes. As shown in the previous subsection, a change in the moderator density results in a change of reactivity. Moderator Pressure Coefficient at BOC is approximately 0.09 pcm/psia and becomes 0.4 pcm/psia at EOC at operating temperature, so it is a minor effect. The moderator pressure coefficient can be determined from the moderator density coefficient by translating pressure differences into density differences.

4.3.2.3.2.3 Moderator Void Coefficient

The moderator void coefficient is defined as the change in core reactivity due to the presence of voids in the moderator. Since the void content in the moderator is very low in a PWR at normal operation, the moderator void coefficient is not very important. The core average void fraction is less than 0.1 % (Subsection 4.4.2.4). The void coefficient at BOC

is approximately - 40 pcm/percent void and becomes -150 pcm/percent void at EOC at operating temperature.

4.3.2.3.3 Power Coefficient

The reactivity change due to the change on the power level, including both the effect of the moderator and Doppler temperature effect, is known as power coefficient. The power defect is defined as integral reactivity changes from one power level to another one. The axial redistribution effect is implicitly included since three dimensional analytical methods are used for the evaluation. Typical power coefficients are shown in Figure 4.3-25 for the BOC and EOC of the initial core. The power coefficient becomes more negative with burnup, reflecting the behavior of the moderator temperature and Doppler temperature coefficients as described above.

4.3.2.3.4 Reactivity Coefficients Used in Transient Analysis

Figures 4.3-21 through 4.3-25 show the best estimate values for the initial core. Limiting values are used as design limits in the transient analysis. Since the most limiting values of the reactivity coefficient vary depending on the transient, whether the most or least negative coefficient, the BOC or EOC and some special aspects such as spatial non-uniformity are considered. As shown in Chapter 15, conservative values of coefficients taking into account uncertainties and possible parameter variations due to different reload cores are considered. In most cases, the most limiting combination of coefficients is used for Chapter 15 transient analysis. The transient reevaluation will be required if the coefficient for a specific cycle falls out of the range of the coefficient selected for that transient.

4.3.2.4 Control Requirements

The primary factors for the core reactivity changes with reactor operation are fuel burnup, burnable poison depletion and control rod insertion, as well as those which depend on the changes to reactor power such as moderator and fuel temperatures, and xenon and samarium concentrations.

These reactivity changes are compensated by two independent systems.

Boron concentration in the primary system is adjusted to compensate the relatively slow reactivity changes mainly due to change of fuel isotopic composition in the fuel, depletion of burnable absorber, and buildup of fission products to maintain the reactor in a critical state.

The RCCAs are moved to control the relatively fast reactivity changes mainly due to reactor thermal power changes and coolant temperature variations. In this way, at any reactor operation state, the RCCAs have the ability to rapidly shutdown the reactor (hot shutdown state), and rod insertion limits are set as a function of the reactor power to fulfill this function.

4.3.2.4.1 Reactivity Control Requirements

4.3.2.4.1.1 Moderator and Fuel Temperature and Void Defects

When the reactor power level changes from full power to zero power, the power reduction is accompanied by the fuel temperature decrease and reactivity is added due to the Doppler effect (Subsection 4.3.2.3.1). In addition, the moderator temperature also decreases, and the positive reactivity due to the moderator temperature effect is added (Subsection 4.3.2.3.2). The temperature distribution changes inside the core and results in a flux redistribution effect, which is the reactivity addition due to the power shift to the top of the core where fuel is less depleted. Additionally, void collapse adds reactivity due to power reduction. Although the reactivity worth of the void content is small in PWRs, it is included in shutdown margin considerations.

Therefore, when the reactor is shutdown from any power level, the control rods must compensate for the reactivity added by these primary factors.

4.3.2.4.1.2 Burnup and Fission Products

The reactivity change due to fuel burnup accompanied by the depletion of fissile isotopes, buildup of fission products and transuranic isotopes, and the depletion of the burnable absorber is compensated for by adjusting the boron concentration in the primary system to keep the reactor critical. The critical boron letdown curve depends on the amount of burnable absorber loaded in the core. The amount of burnable absorber loaded at the beginning of the cycle is sufficient to reduce the critical boron concentration to obtain a negative moderator temperature coefficient.

4.3.2.4.1.3 Xenon and Samarium Poisoning

Among the fission products produced during reactor operation, Xe-135 and Sm-149 have particularly large thermal neutron absorption cross sections.

Xe-135 and Sm-149 isotopes concentration changes, and the associated reactivity changes, occur at a slow rate compared with the power level change. Consequently, the reactivity change is usually controlled by the adjustment of the boron concentration in the moderator.

4.3.2.4.1.4 Permitted Rod Insertion at Power

In order to compensate for the reactivity added by the power reduction following reactor shutdown (moderator temperature effect, Doppler effect, redistribution effect and void effect), RCCAs are inserted. Therefore, it is necessary for reactor operation at any power level that the reactivity provided by the control rods exceeds the power defect requirement with enough margin. In order to fulfill this requirement and to achieve acceptable power peaking factors, control rod insertion is restricted.

In addition, the control rod insertion limits are established to minimize the distortion of the core power distribution during normal operation and the reactivity insertion and local

power peaking in the event of a rod ejection accident. The control rod insertion limit is set as a function of the reactor power level.

Since parameters like reactivity coefficient and redistribution effect differ with the fuel loading pattern and cycle burnup, control rod insertion limits are verified through cycle burnup for each core.

Rod insertion limits are addressed in the technical specifications. Rod positions are monitored and the operator is notified by an alarm if the limit is approached. When the RCCAs reach the insertion limit, a boron concentration change would be required to compensate for additional reactivity changes.

4.3.2.4.2 Reactivity Control Provisions

The core reactivity control is performed by two independent methods: the maneuvering of RCCAs and the boron concentration adjustment in the RCS. In addition to these two methods, and to achieve a negative moderator temperature coefficient at hot conditions, both integral and discrete burnable absorbers are used.

4.3.2.4.2.1 Control Rods

The core is designed so that the RCCAs have the following control capability.

- Even with the most reactive RCCA stuck in the fully withdrawn position, the RCCAs provide enough negative reactivity to rapidly shutdown the reactor from hot full power (with the control rods at their insertion limit position) to hot shutdown state.

- The RCCAs have enough differential reactivity worth to stabilize the reactor to load changes.

- When the reactor power changes from hot full power to hot zero power conditions, the reactivity change due to phenomena like fuel temperature, primary coolant temperature and void variations are controlled by control banks.

- Reactivity changes due to small variations in boron concentration, moderator temperature or xenon concentration are controlled by control banks.

4.3.2.4.2.2 Soluble Boron

The adjustment of boron concentration in the primary coolant by the CVCS controls relatively slow reactivity changes. The CVCS is designed so that the boron concentration adjustment will compensate for the following reactivity changes:

- Reactivity changes due to the primary coolant temperature variation from cold shutdown to hot shutdown conditions.

- Reactivity changes produced by fuel burnup, depletion of burnable absorbers and buildup of fission products and transuranic isotopes.

- Reactivity changes produced by xenon and samarium concentration changes.

The boric acid provided by the CVCS allows achieving sub-criticality at cold condition with sufficient shutdown margin.

The positive reactivity insertion rate produced by boron dilution is limited by the boron dilution rate and the boron worth.

The boron concentration during refueling, with all RCCAs inserted, keeps an effective multiplication factor (k_{eff}) below 0.95, and the core remains subcritical even without the RCCAs inserted.

Boron concentrations for different core conditions are presented in Table 4.3-2.

4.3.2.4.2.3 Burnable Absorbers

Burnable absorbers are used to control the high reactivity excess of the core at the beginning of cycle in order to reduce the boron concentration in the moderator to achieve negative moderator temperature coefficients, and also to flatten the power distribution. Two kinds of burnable absorbers, Gadolinia and borosilicate glass, are used in the US-APWR initial core (Subsection 4.3.2.1).

4.3.2.4.2.4 Normal Operation Control

The approach to hot zero power critical is initiated by the full withdrawal of the shutdown banks and then withdrawal of the control banks above rod insertion limits. The final critical approach is made first by the adjustment of the boron concentration in the primary system and then by the control bank. Allowable rod insertion limits are discussed in Subsection 4.3.2.4.1.4 and in the technical specifications. Successive boron concentration adjustments and control rod movements are performed to achieve full power condition from hot zero power condition.

During normal base load operation, reactivity variations are mainly compensated for by boron concentration adjustment (Figure 4.3-5).

Reactivity changes due to power level changes are controlled by control rod motion. However, control rod motions are limited by the control rod insertion limits, so when the rods reach the insertion limit, boron concentration is adjusted to compensate the reactivity change.

Axial xenon oscillations are damped by control rod movement. Peak xenon startup is accomplished with the combination of boron concentration change and rod motion.

4.3.2.4.3 Shutdown Margin

The shutdown margin is defined as the amount by which the core would be subcritical at hot shutdown conditions following a reactor trip. The shutdown margin is determined considering that the control rods are initially at the insertion limit position and following the trip signal all the rods except for the most reactive one, which is conservatively assumed to remain at the top of the core, are inserted in the core. Shutdown margin is calculated

using the analytical methods described in Subsection 4.3.3.1. This shutdown margin expected value includes an allowance for the reactor average temperature uncertainty and an allowance of 10 % for the rod cluster control assembly worth (Reference 4.3-5). The fulfillment of the required shutdown margin as specified in the technical specifications is demonstrated in Table 4.3-2.

After the trip, when the temperature of the reactor changes from hot zero power to cold shutdown condition, boration is required to keep the shutdown margin as specified in the technical specifications. Boron concentrations required for different core conditions are shown in Table 4.3-2, and are well below the boron solubility limit.

4.3.2.5 Control Rod Patterns and Reactivity Worths

The US-APWR has 69 RCCAs as shown in Figure 4.3-4. Each RCCA is comprised of 24 absorber rods which are inserted in the core through the control rod guide thimbles of each fuel assembly. The absorber rod is composed of Ag-In-Cd alloy in stainless steel cladding. The RCCAs are divided by function into two groups, the shutdown group and the control group.

The control group has the capability to compensate reactivity changes due to phenomena such as fuel temperature, primary coolant temperature and void variations associated with reactor power changes from hot full power to hot zero power conditions. This group has the capability to control reactivity changes due to variations in core power and boron concentration and/or xenon concentration. Even though the boron concentration adjustment in the coolant is the primary means to compensate for reactivity changes due to changes in neutron absorber material and fuel burnup, the control group can also be used for this purpose.

The shutdown group together with the control group provides enough negative reactivity to rapidly shutdown the reactor from hot full power to the hot shutdown state, assuming the highest worth RCCA is stuck out of the core.

Each group is further subdivided into banks to provide for precise reactivity control. The shutdown group is separated into 4 banks, named SA, SB, SC and SD. The control group is separated into 4 banks, named A, B, C and D. Each bank is comprised of four or more RCCAs, but they are controlled and operated as a unit.

RCCAs are withdrawn in a given order as follows: SA, SB, SC, SD, A, B, C and D, while the insertion is done in the reverse order. At full withdrawal the rod position is 265 step while the inserted rod position is 0 step.

During normal operation condition, the shutdown group is kept completely withdrawn and the control group is kept at or above the insertion limit to ensure an acceptable power distribution, maintain minimum shutdown margin, and also to limit the reactivity insertion and power peaking in the case of a rod ejection accident. Bank insertion limits as a function of power are given in the technical specifications.

During normal operation, selected banks are maneuvered automatically or manually to control the reactor power to the load demand. When the reactor is tripped, all RCCAs are inserted by gravity.

Expected positions of shutdown and control banks for cold, hot zero power and full power for both BOC and EOC are summarized in Table 4.3-2. However, the positioning of the control banks for criticality is determined by the boron concentration in the coolant and the bank insertion limitation as a function of the power level.

Allowable rod misalignment is addressed in the technical specifications.

The maximum controlled reactivity insertion rate introduced by the RCCA withdrawal is restricted by the maximum velocity of the control rod drive mechanism and the reactivity worth of the RCCA bank. The maximum velocity of the rod drive mechanism is limited to 45 inch/min.

The RCCA maximum reactivity worth and maximum reactivity insertion rate are limited to maintain the reactor coolant pressure boundary integrity and to ensure the core cooling for the core internal structures. Therefore, the maximum reactivity worth for a control rod ejected from its insertion limit position, the maximum reactivity insertion rate produced by the accidental withdrawal of two control banks at the maximum velocity and the maximum negative reactivity change due to the drop of a RCCA during operation condition are limited by design.

Table 4.3-2 summarizes the maximum allowable reactivity insertion rate for rod withdrawal accident. The maximum allowable worth for a control rod ejection and drop accident are presented in Subsections 15.4.8 and 15.4.3.3.1.2, respectively.

Scram reactivity as a function of time after scram initiation for the initial core is shown in Figure 4.3-26. Rod worth versus rod position is calculated assuming all the rods out as the initial condition, and conservatively, the flux distribution is assumed to be bottom skewed. All feedback is conservatively assumed to be frozen during the rod insertion. At these conditions, the reactivity worth of all rods but the one with the highest worth stuck out of the core is calculated as a function of the insertion position using the analytical method described in Subsection 4.3.3.1. The rod position as a function of time for the 14 ft core is used to translate position into time.

4.3.2.6 Criticality of Reactor During Refueling

The reactor is maintained sub-critical during refueling with a k_{eff} less than 0.95, as explained in Subsection 4.3.1.3.

Table 4.3-3 summarizes k_{eff} values for single assemblies and groups of adjacent fuel assemblies, assuming the assemblies are dry, immersed in unborated water, and of the refueling boron concentration. Verification of sub-criticality is performed with the method presented in Subsection 4.3.3.2. Since the k_{eff} values are for unirradiated uranium fuel assemblies with the maximum allowable U-235 enrichment of 5wt % (Table 4.2-1), the k_{eff} data shown in the table are the upper bound values.

The k_{eff} of a single 17x17 fuel assembly with uranium enrichment less than 5wt % is less than 0.95, independent of the boron concentration and the water density. Therefore, fuel assembly transfer and handling meets criticality limits.

In the fully refueled core, the maximum k_{eff} will not exceed 0.95, with the boron concentration required in the technical specifications and all control rods inserted. Even with the removal of all control rods, the core is sub-critical at the required boron concentration. Table 4.3-2 shows that the boron concentration necessary to fulfill these requirements is lower than the refueling boron concentration. Further, the criticality of the reactor during refueling is always monitored.

4.3.2.7 Stability

Two primary considerations for power stability are total core power and power distribution perturbations due to xenon oscillations.

The US-APWR power reactivity coefficients are negative throughout the whole fuel cycle, as stated in Subsection 4.3.2.3. The core is therefore inherently stable to total power oscillations. Moreover, oscillations or undesirable changes in total power output of the core are reliably detected and the information is available for the operator and the protection system.

However, in a large reactor, xenon induced power distribution oscillations may occur even without a change in the total core power. These oscillations may occur as a result of a sudden power distribution change, which is rapid in comparison with the time constant of the xenon and iodine chain. Xenon and iodine distributions become out of equilibrium with the power distribution and thus an oscillation condition can develop. The core is considered stable if the magnitude of the power distribution oscillation decreases with time.

The US-APWR core is larger than the Mitsubishi 4 loop PWR design, both in the number of fuel assemblies and the active fuel length. However, from the view point of other parameters which are significant in the stability of the core against xenon induced oscillations, moderator temperature and Doppler coefficients are similar to those of the current 4 loop PWR plants, while power density is reduced.

4.3.2.7.1 Stability Analysis

The xenon induced power distribution oscillations for the US-APWR are analyzed using the modal perturbation method, which allows the determination of the degree of stability for a particular oscillation mode. The stability of a reactor can be characterized by the stability index. The power distribution perturbation can be written as a function of time as:

$$\delta P(t) = a \cdot e^{b \cdot t} \cdot \cos\left(\frac{2 \cdot \pi \cdot t}{T}\right) + c$$

where a and c are constants, T is the period of the oscillation and b is the stability index.

At a first approximation, T can be obtained as the time difference between successive maxima flux peaks and the stability index b as

$$b = \frac{2}{T} \ln\left(-\frac{a_2 - a_3}{a_1 - a_2} \right)$$

where a_1, a_2 and a_3 are successive maxima and minima in the perturbed flux at times t, $t + T/2$ and $t + T$. A negative stability index b indicates stability for the oscillatory mode being investigated.

Xenon induced power distribution oscillations can be analyzed by 3 dimensional ANC calculation. The axial offset and the quadrant tilt difference are the quantities that represent the power perturbation for axial and horizontal (X-Y plane) direction, respectively.

In the axial direction, a power distribution change can be produced by control rod motion during a plant load change, which produces a change in the moderator temperature and fuel temperature distributions. Xenon oscillations are generally larger for longer cores. PWR cores become less stable to axial xenon oscillation with cycle burnup due to the flattened power distribution, but if oscillations occur they can be controlled by the RCCAs.

In the horizontal plane, a power distribution change can be produced as the result of an abnormal asymmetric insertion of RCCAs. PWR cores generally become more stable to horizontal oscillations late in the cycle, due to larger negative feedback coefficients.

Uncontrolled xenon oscillations are only allowed during specific physics tests. Induced xenon oscillation tests were performed at conventional Mitsubishi plants. The tests were conducted at the beginning of the first cycle as part of the startup test program. Comparisons of xenon induced power distribution oscillations have been performed between 3 dimensional ANC calculations and measured results, to verify code accuracy. The analyses of the US-APWR horizontal and axial power xenon induced oscillations have been performed with analytical methods described in Subsection 4.3.3.1.

Xenon-induced power oscillation measurement data support the conclusion that the ANC code shows good agreement with the predicted stability index. Detailed test conditions, calculation model assumptions, and results of measurement versus prediction comparisons are reported in Reference 4.3-5.

The US-APWR has larger equivalent diameter compared with the standard 4 loop PWR plants since it has 257 fuel assemblies. However, ANC results show that the US-APWR core is stable to horizontal xenon oscillations throughout the entire cycle. The calculated horizontal stability index is approximately -0.05 hr^{-1} at BOC and the core becomes more stable with fuel burnup, due to an increasingly negative moderator temperature coefficient.

At BOC, the calculated axial xenon oscillation stability index shows that the core is stable, but the axial stability index becomes zero at MOC. However, the axial oscillation periods are long enough to allow the control rod system to easily control the axial xenon transient. An EOC simulation shows that power distribution oscillations can be controlled by control rod movements, even for power distribution oscillations induced by perturbations that

deviate widely from the axial offset target band and could exceed limits if not controlled. Reactivity changes due to control rod movements are compensated with boron dilution/boration and the reactor power is maintained constant.

The axial stability index behavior with core burnup for the US-APWR is the same as other PWRs with an active length of 12 ft or 14 ft. There are several operating PWRs with an active core length of 14 ft, and they have experienced no xenon-induced oscillations incidents that have prevented normal operation. In addition, Mitsubishi PWRs have never had uncontrollable xenon oscillation incidents.

4.3.2.7.2 Oscillation Detection and Suppression

Induced horizontal or axial xenon oscillations are readily detected by ex-core detectors. The ex-core signals are available to the operator and the operator takes actions to suppress power distribution oscillations. The ex-core signals also form part of the protection system.

The US-APWR is stable against horizontal xenon induced oscillations at all times in core life. Tilt in the core horizontal power distribution is continuously monitored by the ex-core detectors and the information is available to the operator, but significant horizontal oscillations are not likely as long as RCCA control is performed as required by the technical specifications.

Core axial offset is continuously monitored by the axially segmented ex-core detectors and the information is available to the operator. If axial xenon oscillations threaten to move the core axial offset outside the allowable operation band, the operator will take corrective actions before the limits are reached in accordance with the technical specifications. Control rod banks are moved or the reactor power is reduced to keep the axial offset within the allowable operation band.

The periods of xenon-induced oscillations are long relative to the times for operator reaction and control mechanism actuation, so these oscillations are easily controllable at all times in life.

4.3.2.8 Vessel Irradiation

Since the reactor vessel is irradiated by neutrons generated by nuclear fission within the reactor core, an evaluation of the neutron flux distribution in the reactor vessel is performed.

The neutron flux generated in the reactor core is decreased by the neutron reflector, core barrel and reactor coolant which exist between core and reactor vessel. In the evaluation of neutron flux distribution in the reactor vessel, the evaluation technique is appropriately selected to consider the attenuation in each region.

The neutron flux evaluation methodology is selected in accordance with regulatory position 1, “neutron fluence calculational methods”, of the Regulatory Guide 1.190, “Calculational and Dosimetry Methods for Determining Pressure Vessel Neutron Fluence” (Reference 4.3-9). The evaluation methodology is described in Reference 4.3-20. The summary of the methodology is as follows.

The DORT code (Reference 4.3-10) is used to evaluate neutron flux distributions. DORT is widely used in the nuclear industry for flux-distribution evaluations of reactor vessels. DORT is a discrete ordinates Sn code, and can perform calculations in (X, Y), (R, θ) and (R, Z) geometry. Each of these geometric capabilities is used as described below.

To determine the reactor vessel neutron flux distribution, (R, θ) geometry is selected, modeling the circular shape of the reactor vessel and core barrel. Likewise, the irregular shapes of the core and the neutron reflector are “smoothed” and are modeled as circular regions. Calculations of the perpendicular neutron flux distribution in the reactor vessel are performed with an (R, Z) geometric model. On the other hand, in the evaluation of the neutron reflector neutron flux distribution, greater local spatial accuracy is desired. Therefore, (X, Y) geometry is selected for this region, and the “polygon” shape of the side facing the reactor core of the neutron-reflector is modeled by straight lines.

For the DORT calculations, the BUGLE-96 (Reference 4.3-11) cross section library is used. This library is generated from ENDF/B-VI data collapsed to 47 neutron energy groups.

Fuel assembly and pinwise power distributions are obtained by standard reactor core calculations and are used as the fission source terms for the neutron flux distribution calculations outside the reactor core. The average power distribution in a representative reactor core operating at full power is used. This distribution is considered to be representative of the core average power distribution during the plant lifetime. This approach is considered appropriate for reactor vessel irradiation calculations, because the integrated flux (neutron fluence) during operation is considered most important. A typical neutron flux inside the reactor vessel obtained by the above evaluation is shown in Table 4.3-4. In addition, fast neutron fluence (time integrated neutron flux) at reactor vessel is shown in Table 4.3-5.

Calculation uncertainty of this flux estimation methodology is within 20 %, which was estimated by uncertainty analysis. The reactor vessel surveillance program is discussed in Subsection 5.3.1.6.

4.3.3 Analytical Methods

4.3.3.1 Nuclear Design Methods

A lattice physics code and a core simulator have been mainly used for US-APWR nuclear design. The lattice physics code is used for generating group constants for core simulation and the core simulator is then used for calculating the main nuclear parameters, such as power distribution, exposure, critical boron concentration, and reactivity coefficients.

The NRC-approved code PARAGON (Reference 4.3-12) is used as a lattice physics code. PARAGON is a heterogeneous two dimensional transport assembly calculation code based on the current coupling collision probability method.

The effective cross sections of each nuclide included in each region of heterogeneous assembly are generated from the multi-group cross section library, based on assembly specification data such as material composition, configuration and temperature. The 70

energy group library is mainly based on ENDF/B-VI files. This library contains resonance integrals which are used for generating effective cross sections considering the self-shielding effect, as a parameter of temperature and background cross section. For nuclides whose resonance cross section gives a large impact on core neutronics, intermediate resonance (IR) approximation and equivalence theory are used to consider resonance self-shielding effect on heterogeneous geometry. As for the delayed neutron data calculation, Keepin nuclear database (Reference 4.3-13) is used.

The fine energy group neutron spectrum of each region of each cell in the heterogeneous assembly is calculated with the current coupling collision probability method. In this calculation, each cell is treated as a node, and each node is coupled with neutron current. The multi-group neutron flux of each region of each cell is calculated using neutron current and flux obtained from collision probability method. Then, the critical spectrum is calculated by a standard B1 calculation. This B1 spectrum is used to normalize the flux distribution from the two dimensional transport calculation, and group constants for core simulator are calculated using the normalized neutron spectrum. In the PARAGON depletion calculation, the differential equations for the composition change by isotopic depletion and buildup of each material in the assembly to evaluate the composition change are solved applying Laplace transformation. The predictor-corrector method is used for accurate evaluation of composition change.

The fuel temperature, which is used for Doppler calculations, is obtained as follows. First, the inner cladding temperature is calculated for a given moderator temperature considering surface crud and cladding thermal conductivity. Then, pellet temperature distribution is calculated by a one dimensional heat conduction equation, considering radial power distribution, pellet-cladding gap conductance (which depends on internal pressure of fill gas) and thermal conductivity of the pellet. The burnup dependent pellet-cladding gap model is an empirical model based on the operating plant measurement data of Doppler coefficient and defect. The effective flat fuel temperature for U-238 and Pu-240, which are the most important nuclides for Doppler calculation, are obtained from the pellet temperature distribution applying the radial weighting factor, which is determined preserving the resonance absorption for the actual pellet temperature distribution.

For neutron economy, the US-APWR employs a steel neutron reflector instead of the conventional baffle reflector. The neutron reflector cross section for the core simulator is generated by a one dimensional PARAGON calculation. In comparison with the conventional baffle reflector, the stainless steel thickness increases while the coolant area in outer core region decreases. To confirm the applicability of PARAGON for the neutron reflector, a critical experiment (Reference 4.3-5) was performed in Tank type Critical Assembly (TCA), Japanese critical facilities, with iron neutron reflector.

The NRC approved code ANC (References 4.3-14 and 4.3-15) is used as a core simulator. ANC is a three dimensional two group diffusion core calculation code based on nodal expansion method. Using few-group constants generated by PARAGON, ANC calculates nuclear parameter discussed in Subsection 4.3.2 such as critical boron concentration, power distribution, exposure, reactivity coefficients and core stability. A discontinuity factor is used for cross section homogenization correction and a pin power reconstruction method is used for calculating pin-by-pin power distribution. Nuclides

which have a large impact on group constants, such as the xenon and samarium, are treated explicitly in group constants. To calculate time-dependent xenon and samarium concentrations, a three dimensional two-group time-dependent neutron diffusion equation is solved. In this calculation, the thermal-hydraulic feedback (fuel temperature and moderator density) is limited to a steady state model. The isotopic depletion and buildup for these nuclides are evaluated and the effect on group constants is considered in the ANC calculation.

The approval of PARAGON/ANC is described in the Reference 4.3-12 topical report. This report describes critical experiments and Post-Irradiation Examination (PIE) analyses that were performed with PARAGON and compared with measurement data. HZP startup tests and HFP normal operation measurement data were also compared with PARAGON/ANC calculation results. These results show good performance and demonstrate the applicability of PARAGON/ANC for PWR core design. MHI qualification of this design methodology is provided in Reference 4.3-5.

The US-APWR core features as described in Section 4.1 are essentially similar to those of conventional U.S. and Japanese PWRs. From the neutronic viewpoint, the main differences are the increase of the assembly number to 257, the increase of the active fuel length to 14 ft and the use of the neutron reflector. However, the use of a core with 257 fuel assemblies is already planned for the Japanese APWR, and there is considerable experience with 14 ft fuel in U.S. and Europe. From the neutronics viewpoint, these differences are essentially included in the applicability of the current methodology. The increase of core size impacts the core stability. However, as described in Subsection 4.3.2.7, the US-APWR core is stable. The applicability of PARAGON for generating neutron reflector cross section is described in Reference 4.3-5. Consideration of such factors leads to the conclusion that the US-APWR core features are within the range of applicability encompassed by the current methodology.

In addition to the calculation results described in Reference 4.3-12, B&W and TCA critical experiment analysis, which includes Gadolinia fuel, have been performed with the PARAGON/ANC code system as described in Reference 4.3-5. In this report, pin-by-pin reaction rate and reactivity are compared with PARAGON calculation results. PIE analyses for the Japanese and the European PWRs with UO_2 fuel have also been performed. The PARAGON calculation results have been compared with measurement data. Comparisons of these critical experimental data and PIE with results from the PARAGON/ANC code system show good agreement.

For the operating plant comparisons, analysis of 10 cycles of 2 Japanese PWR plants has been performed. The plant configuration covers a 3 loop plant with 157 assemblies and a 4 loop plant with 193 assemblies. The lattice configuration covers the 17x17 fuel assembly. The enrichment range covers from 2.0 wt% to 4.8 wt%. As for the burnable absorber, borosilicate glass and Gadolinia burnable absorber are used in the plants. The Gadolinia content ranges from 6.0 wt% to 10.0 wt% and the number of Gadolinia rods per assembly ranges from 16 to 24 rods. Nuclear physics startup tests and HFP normal operation measurement data (critical boron concentration versus burnup, radial and axial power distribution) have been compared with PARAGON/ANC calculation. These operational plant analyses by the PARAGON/ANC code system show good performance, as described in Reference 4.3-5.

4.3.3.2 Nuclear Criticality Safety Calculational Analysis Methods

MCNP version 5 and ENDF/B-V continuous-energy neutron library data (Reference 4.3-16) have been used for modeling 3D geometry systems for criticality safety calculations described in Subsections 4.3.2.6 and 9.1.1. The validation of this methodology, in accordance with "Guide for Validation of Nuclear Criticality Safety Calculational Methodology" (Reference 4.3-18), is detailed in Reference 4.3-17 and summarized below.

A set of 120 critical benchmarks, from "International Handbook of Evaluated Criticality Safety Benchmark Experiments" (Reference 4.3-19), that cover a wide range of enrichment, materials and geometries, have been selected and modeled with MCNP. The objective conditions are sufficiently covered within this range. The 120 critical benchmarks analysis results in a weighted mean k_{eff} of 0.9971, with a bias of 0.0029 and a standard deviation of 0.0030. The bias is the difference between the calculated weighted mean k_{eff} and the critical experiment modeled and the standard deviation is the square root of the sum of the squared variance about the mean and the squared average total uncertainty.

4.3.4 Changes

The US-APWR nuclear design is very similar to those of conventional PWRs currently operating in the U.S and Japan. The main difference between previous core designs and the US-APWR is the use of 257 fuel assemblies. Although an increase in core size could have effect on power distribution stability, it has been concluded that the US-APWR core is stable with respect to horizontal xenon oscillations and therefore meets design requirements.

4.3.5 Combined License Information

No additional information is required to be provided by a COL Applicant in connection with this section.

4.3.6 References

4.3-1 General Design Criteria for Nuclear Power Plants, NRC Regulations Title 10, Code of Federal Regulations, 10 CFR Part 50, Appendix A.

4.3-2 U.S. Nuclear Regulatory Commission, Standard Review Plan for the Review of Safety Analysis Reports for Nuclear Power Plants, NUREG-0800, Section 4.3, March 2007.

4.3-3 Mitsubishi Fuel Design Criteria and Methodology, MUAP-07008-P (Proprietary) and MUAP-07008-NP (Non-Proprietary), Rev. 2, July 2010.

4.3-4 Criticality Accident Requirements, NRC Regulations Title 10, Code of Federal Regulations, 10 CFR 50.68.

4.3-5 Qualification of Nuclear Design Methodology using PARAGON/ANC, MUAP-07019-P (Proprietary) and MUAP-07019-NP (Non-Proprietary), December 2007.

4.3-6 Morita, T., et al., Power Distribution Control and Load Following Procedures, WCAP-8385 (Proprietary), September 1974.

4.3-7 Spier, E. M., Evaluation of Nuclear Hot Channel Factor Uncertainties, WCAP-7308-L-P-A (Proprietary), June 1988.

4.3-8 US-APWR Incore Power Distribution Evaluation Methodology, MUAP-07021-P (Proprietary) and MUAP-07021-NP (Non-Proprietary), December 2007.

4.3-9 Calculational and Dosimetry Methods for Determining Pressure Vessel Neutron Fluence, NRC Regulatory Guide 1.190, March 2001.

4.3-10 Oak Ridge National Laboratory, DOORS3.2: One, Two- and Three Dimensional Discrete Ordinates Neutron/Photon Transport Code System, RSICC Computer Code Collection CCC-650.

4.3-11 Oak Ridge National Laboratory, BUGLE96: Coupled 47 Neutron, 20 Gamma-Ray Group Cross Section Library Derived from ENDF/B-VI for LWR Shielding and Pressure Vessel Dosimetry Application, RSICC Data Library Collection DLC-185.

4.3-12 Ouisloumen, M. et al., Qualification of the Two-Dimensional Transport Code PARAGON, WCAP-16045-P-A (Proprietary) and WCAP-16045-NP-A (Non-Proprietary), August 2004.

4.3-13 G. R. Keepin, et al., Delayed Neutrons from Fissionable Isotopes of Uranium, Plutonium and Thorium, Physical Review 107, 1044, 1957.

4.3-14 Liu, Y.S., et al., ANC - A Westinghouse Advanced Nodal Computer Code, WCAP-10965-P-A (Proprietary), and WCAP-10966-A (Non-Proprietary), September 1986.

4.3-15 Nguyen, T. Q., et al., Qualification of the PHOENIX-P/ANC Nuclear Design System for Pressurized Water Reactor Cores, WCAP-11596-P-A (Proprietary), and WCAP-11597-A (Non-Proprietary), June 1988.

4.3-16 X-5 Monte Carlo Team, MCNP - A General N-Particle Transport Code, Version 5 - Volume I: Overview and Theory, LA-UR-03-1987, Los Alamos National Laboratory, April 2003.

4.3-17 Validation of the MHI Criticality Safety Methodology, MUAP-07020, December 2007.

4.3-18 Guide for Validation of Nuclear Criticality Safety Calculational Methodology, NUREG/CR-6698, January 2001.

4.3-19 International Handbook of Evaluated Criticality Safety Benchmark Experiments, NEA/NCS/DOC(95)03/IV, September 2006 Edition.

4.3-20 Calculation Methodology for Reactor Vessel Neutron Flux and Fluence, MUAP-09018-P Rev.1 (Proprietary) and MUAP-09018-NP Rev.1 (Non-Proprietary), October 2009.

Table 4.3-1 Reactor Core Description (Initial Core) (Sheet 1 of 2)

Active Core		
Active core equivalent diameter		153 in
Active fuel height		165.4 in
H/U atomic ratio (Assembly average, cold)		5.57
Core average linear power density		4.65 kW/ft
Neutron reflector		
Composition	78% SS and 22% water	
Thickness (in)	3.7 to 13.8	
Fuel assemblies		
Total number in the core		257
Rod array		17 x 17
Rods per assembly		264
Rod pitch		0.496 in
Assembly pitch		8.466 in
Material and number of top and bottom grids	Inconel 718	2
Material and number of middle grids	Zircaloy-4	9
Material and number of guide thimbles	Zircaloy-4	24
Material and number of in-core instrumentation guide tube	Zircaloy-4	1
Guide thimble outer/inner diameter (upper part)	0.482 in / 0.450 in	
Guide thimble outer/inner diameter (lower part)	0.429 in / 0.397 in	
Instrumentation guide tube outer/inner diameter	0.482 in / 0.450 in	
Fuel rods		
Cladding outer diameter		0.374 in
Cladding material and thickness	ZIRLO™	0.0224 in
Gap		0.0033 in

Table 4.3-1 Reactor Core Description (Initial Core) (Sheet 2 of 2)

Fuel pellets		
Uranium: material and density	Sintered UO_2	0.384 lb/in^3
Integral burnable absorber: material and density	Sintered (UO_2 + Gd_2O_3)	0.371 lb/in^3(10 wt%) 0.376 lb/in^3(6 wt%)
Diameter		0.322 in
Length		0.453 in
Rod cluster control assemblies		
Neutron absorber material and density	Ag-In-Cd	0.367 lb/in^3
Neutron absorber diameter		0.341 in
Cladding material and thickness	SS-304	0.0185 in
Number of absorber rods per cluster		24
Number of clusters in the core		69
Discrete burnable absorbers rods, initial core		
Absorber material	Borosilicate glass	
B-10 content		3.28 x 10^{-5} lb/in
Inner tube material and inner/outer diameter	SS-304	0.169 in / 0.181 in
Cladding material and inner/outer diameter	SS-304	0.344 in / 0.381 in
Absorber length		159.4 in

Table 4.3-2 Main Nuclear Design Parameters for the Initial Core (Sheet 1 of 3)

Parameter	Design limits	Best estimate
Total heat flux hot channel factor, F_Q	2.60	2.05*1
Nuclear enthalpy rise hot channel factor (full power), $F^N_{\Delta H}$	1.73	1.50
Delayed neutron fraction, β_{eff} (%)	0.44 to 0.75	0.50 to 0.69
Prompt neutron lifetime, ℓ^* (μs)	8 to 20	14.0 to 15.3
Reactivity coefficients		
Doppler power coefficient (pcm/%power) BOC EOC	See Subsection 15.0.0.2	-12.4 to -7.4 -12.1 to -7.6
Moderator temperature coefficient*2 (pcm/°F)	See Subsection 15.0.0.2	-39.5 to -0.8
Moderator density coefficient (pcm/g/cm^3)	< 0.51 x 10^5	< 0.32 x 10^5
Maximum ejected rod worth (pcm)	See Subsection 15.4.8	
Maximum dropped rod worth (pcm)	See Subsection 15.4.3.3.1.2	
Maximum rod withdrawal insertion rate (pcm/s)	75	31.0 to 51.6
Maximum fuel assembly k_∞ (BOC, Cold, NoXe, 0ppm)		1.456
Maximum core reactivity k_{eff} (BOC, Cold, ARO, NoXe, 0ppm)		1.223

Notes:
*1 Normal base load operation
*2 In the power operating range

Table 4.3-2 Main Nuclear Design Parameters for the Initial Core (Sheet 2 of 3)

Boron concentration (ppm)		**Best estimate**
Cold shutdown*1, BOC, no xenon, ARO, k_{eff}=0.99		1796
Hot shutdown*2, BOC, no xenon, ARO, k_{eff}=0.99		1706
Refueling boron concentration*3		4000
Cold shutdown*1, BOC, no xenon, ARI*4, k_{eff}≤0.95		1850
Hot zero power, BOC, no xenon, ARO, k_{eff}=1.00		1579
Hot full power, BOC, no xenon, ARO, k_{eff}=1.00		1444
Hot full power, BOC, equilibrium xenon, ARO,k_{eff}=1.00		1086
Boron coefficient (pcm/ppm)		-9.3 to -8.0
Rod worth (%Δρ)		BOC, HZP, NoXe
Bank D		0.96
Bank C (D in)		0.91
Bank B (D+C in)		0.80
Bank A (D+C+B in)		0.54
Reactivity requirements (%Δρ)	**BOC worths**	**EOC worths**
Power defect including void and Tavg uncertainty (1)	1.31	2.77
Delta RIA*5 (2)	0.19	-
Trip rod worth	4.94	5.47
Trip rod worth (Less 10 %) (3)	4.44	4.92
Shutdown margin		
Calculated margin (3) - (1) - (2)	2.94	2.15
Required shutdown margin	1.6	1.6

Notes:
*1 Temperature of cold shutdown is 68 deg.F
*2 Temperature of hot shutdown is 557 deg.F
*3 Design value
*4 All control rods inserted
*5 Delta RIA : limiting RIA – HFP RIA, RIA : rod insertion allowance

Table 4.3-2 Main Nuclear Design Parameters for the Initial Core (Sheet 3 of 3)

Expected RCCAs positions at different core conditions (step)								
Core Condition	BOC and EOC							
	Shutdown bank				Control bank			
	SA	SB	SC	SD	A	B	C	D
Cold	0	0	0	0	0	0	0	0
Hot zero power	265	265	265	265	265	265	≥130	≥0
Full power	265	265	265	265	265	265	265	≥205

Table 4.3-3 k_{eff} for 5 wt% U-235 Enriched Uranium Fuel Assemblies

(USL:0.9414(1))

Array	Dry	Non borated water	4000 ppm borated water
1x1	0.0962	0.9402	0.5867
2x2	0.1781	1.2350	0.8401
3x3	0.2572	1.3500	0.9348
4x4	0.3323	1.4056	0.9789
5x5	0.3987	1.4364	1.0020

Note: Each value includes uncertainties of material and fabrication, and calculation(2σ)

(1)USL (Upper safety Limit) contains calculational uncertainty and 5% margin.

Table 4.3-4 Typical Neutron Flux inside the Reactor Vessel

(unit: $n/cm^2/s$)

	E>1MeV	1MeV>E>3.35keV	3.35keV>E>0.414eV	E<0.414eV
At the inside surface (peak)	5.2×10^9	1.1×10^{10}	8.0×10^9	1.1×10^{10}
At the 1/4 thickness location (peak)	2.5×10^9	1.0×10^{10}	3.3×10^9	1.9×10^8
Core center (peak)	1.0×10^{14}	1.7×10^{14}	1.2×10^{14}	3.8×10^{13}
Core outer radius at mid height (peak)	4.6×10^{13}	8.0×10^{13}	5.7×10^{13}	1.7×10^{13}
Core top, on axis	2.5×10^{13}	3.9×10^{13}	3.1×10^{13}	2.4×10^{13}
Core bottom, on axis	2.7×10^{13}	4.2×10^{13}	3.3×10^{13}	2.9×10^{13}

Table 4.3-5 Fast Neutron Fluence at the Reactor Vessel

(unit: n/cm^2)

	Fast neutron fluence (E>1MeV, 60EFPY)
At the inside surface (peak)	9.8×10^{18}
At the 1/4 thickness location (peak)	4.7×10^{18}

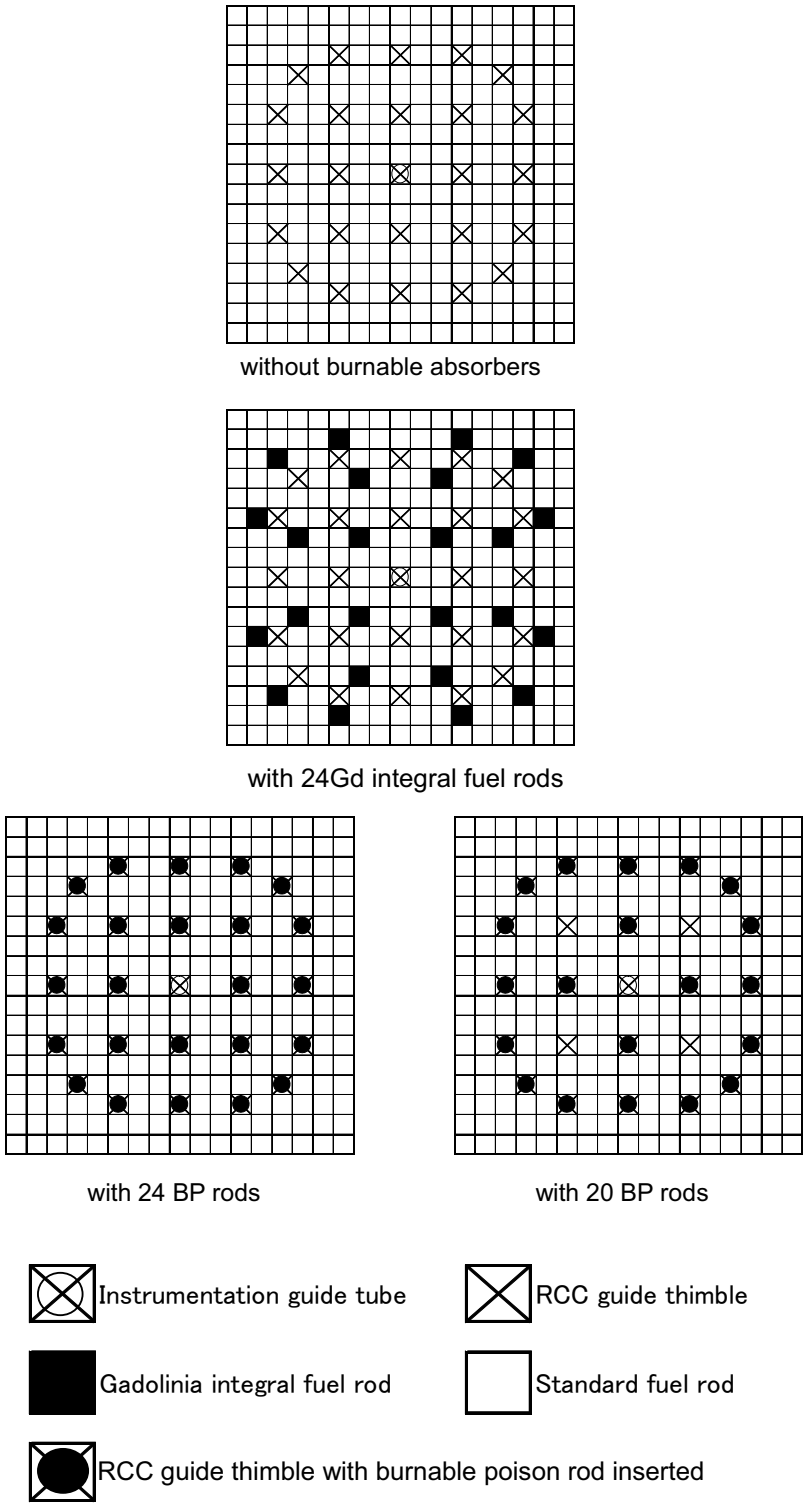

Figure 4.3-1 Arrangement of Fuel and Burnable Poison Rods (Initial Core)

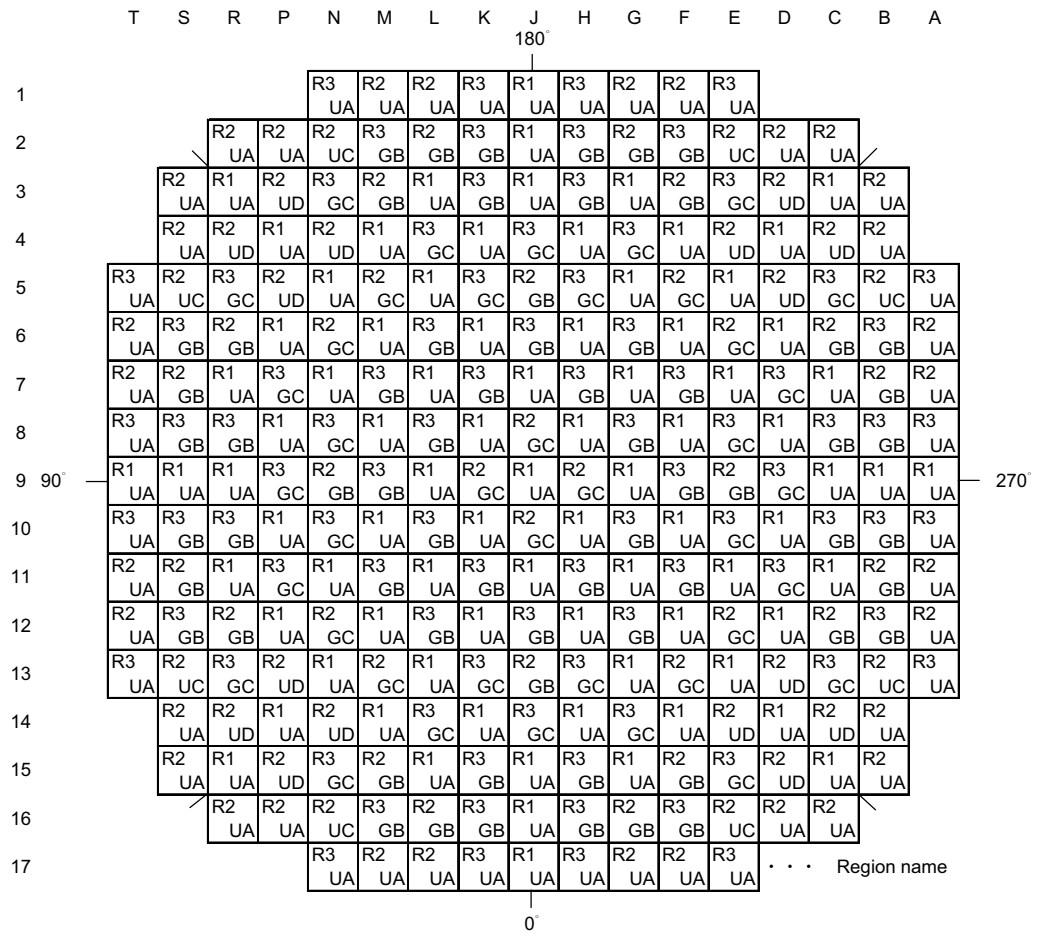

Region	Number	Uranium rods/FA		Gadolinia rods/FA				BP rods/FA	
		Number	U-Enrich.	Number	U-Enrich.	Gd-Content	Abs.Length	Number	Abs.Length
R1UA	81	264	2.05 wt%	-	-	-	-	-	-
R2UA	32	264	3.55 wt%	-	-	-	-	-	-
R2UC	8	264	3.55 wt%	-	-	-	-	20	159.4in
R2UD	16	264	3.55 wt%	-	-	-	-	24	159.4in
R2GB	20	240	3.55 wt%	24	1.95 wt%	10 wt%	159.4in	-	-
R2GC	12	240	3.55 wt%	24	1.95 wt%	6 wt%	159.4in	-	-
R3UA	16	264	4.15 wt%	-	-	-	-	-	-
R3GB	44	240	4.15 wt%	24	2.55 wt%	10 wt%	159.4in	-	-
R3GC	28	240	4.15 wt%	24	2.55wt%	6 wt%	159.4in	-	-

Abs. length: the upper approximately 5.9in of the absorber rod does not contain absorber material

Figure 4.3-2 Initial Core Fuel Loading Pattern

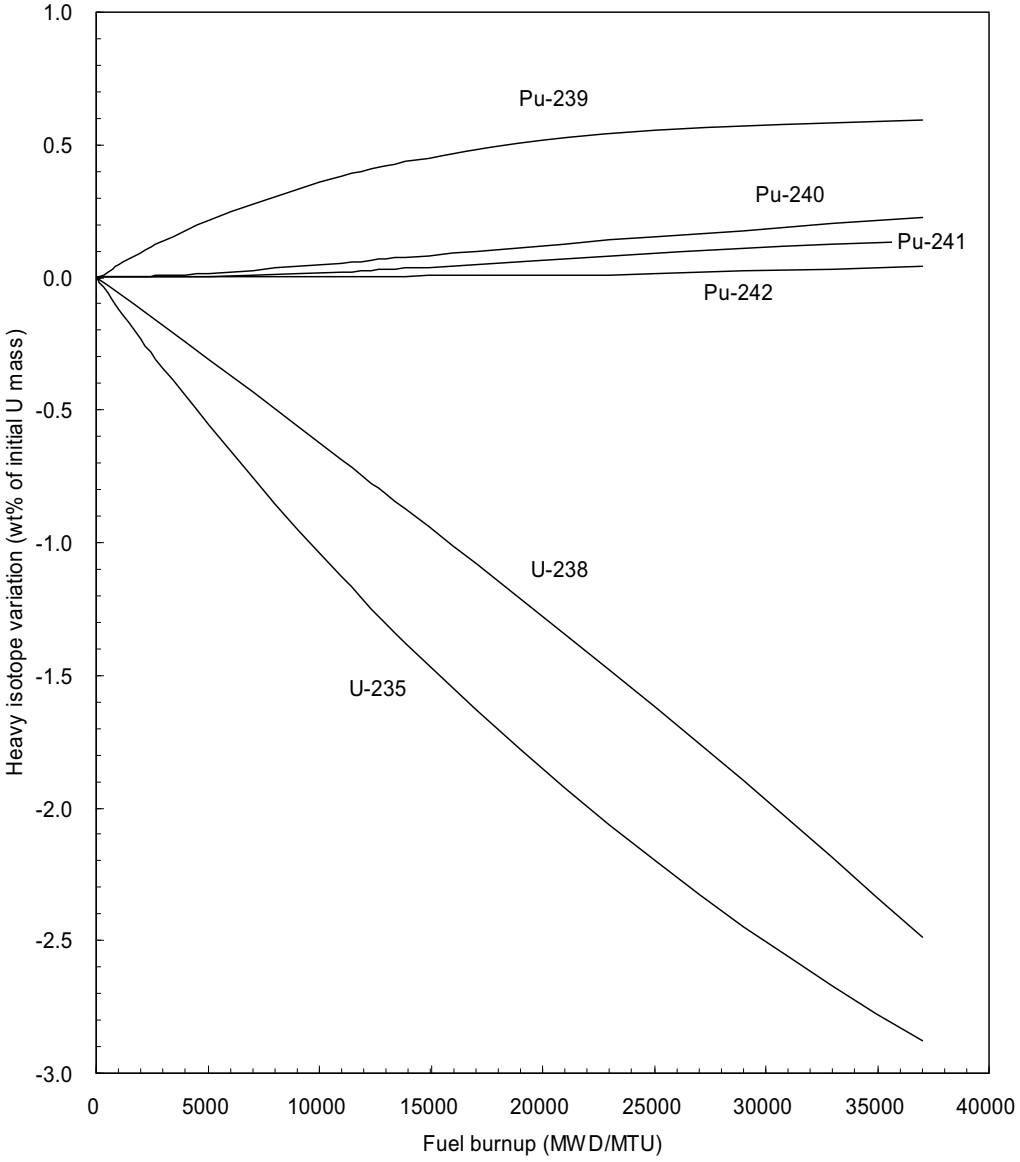

Figure 4.3-3 Heavy Isotopes Depletion and Buildup (Typical Fuel)

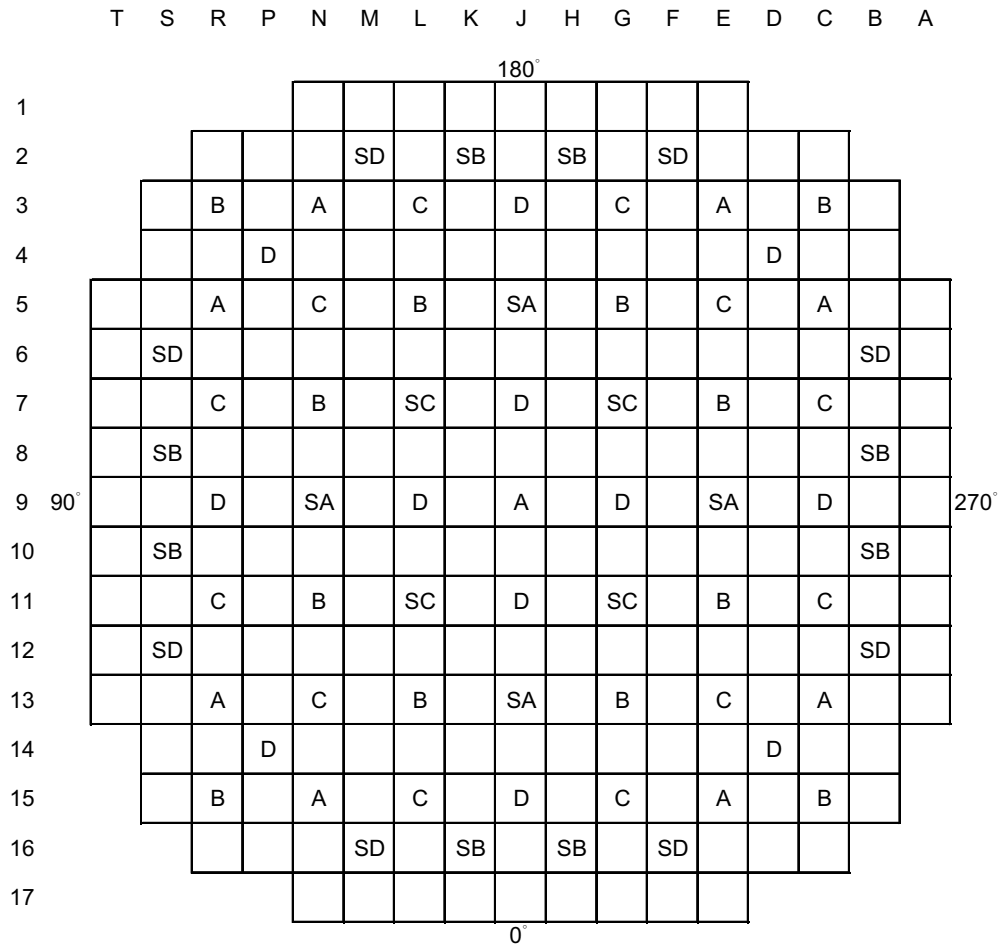

		Number of RCCAs
A:	Control group, Bank A	9
B:	Control group, Bank B	12
C:	Control group, Bank C	12
D:	Control group, Bank D	12
SA:	Shutdown group, Bank A	4
SB:	Shutdown group, Bank B	8
SC:	Shutdown group, Bank C	4
SD:	Shutdown group, Bank D	8

Figure 4.3-4 Fuel and Rod Cluster Control Assemblies Core Configuration

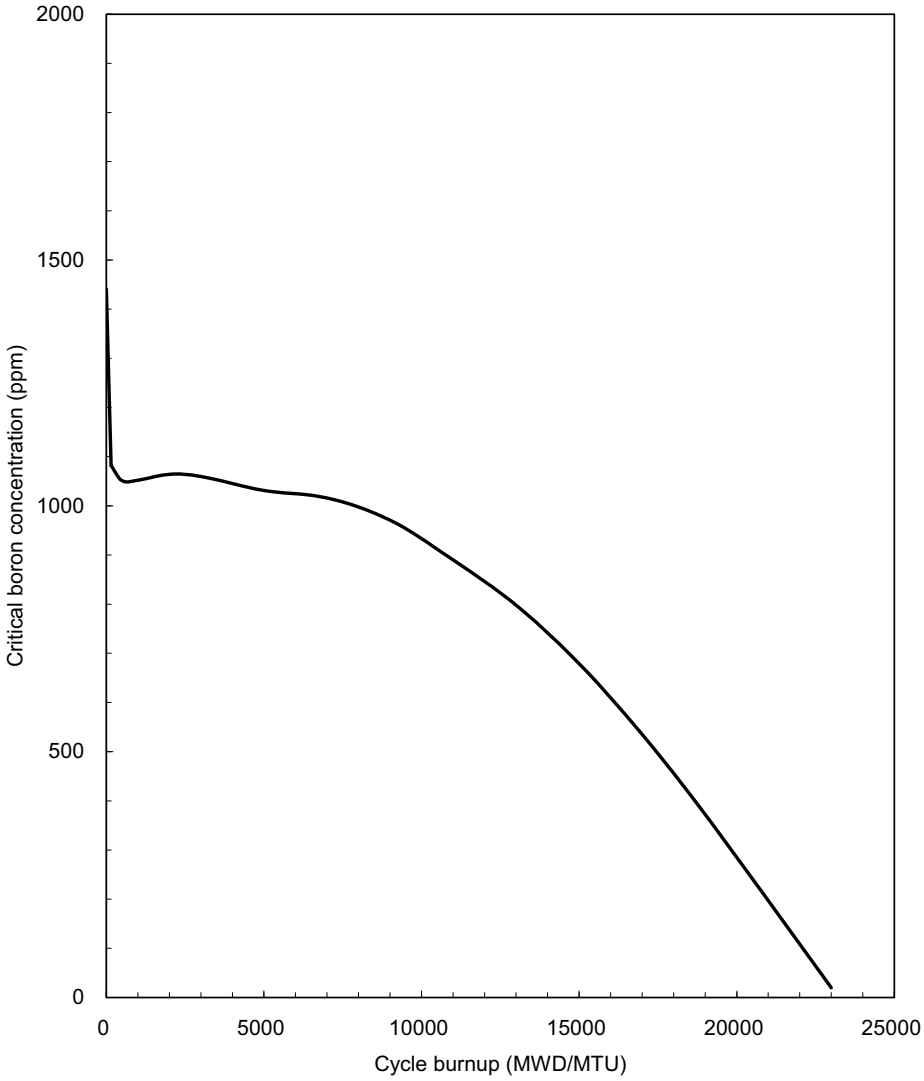

(HFP, ARO[1])

Note: (1) Control Bank D withdrawn to 'bite' position

Figure 4.3-5 Initial Core Soluble Boron Concentration versus Core Depletion

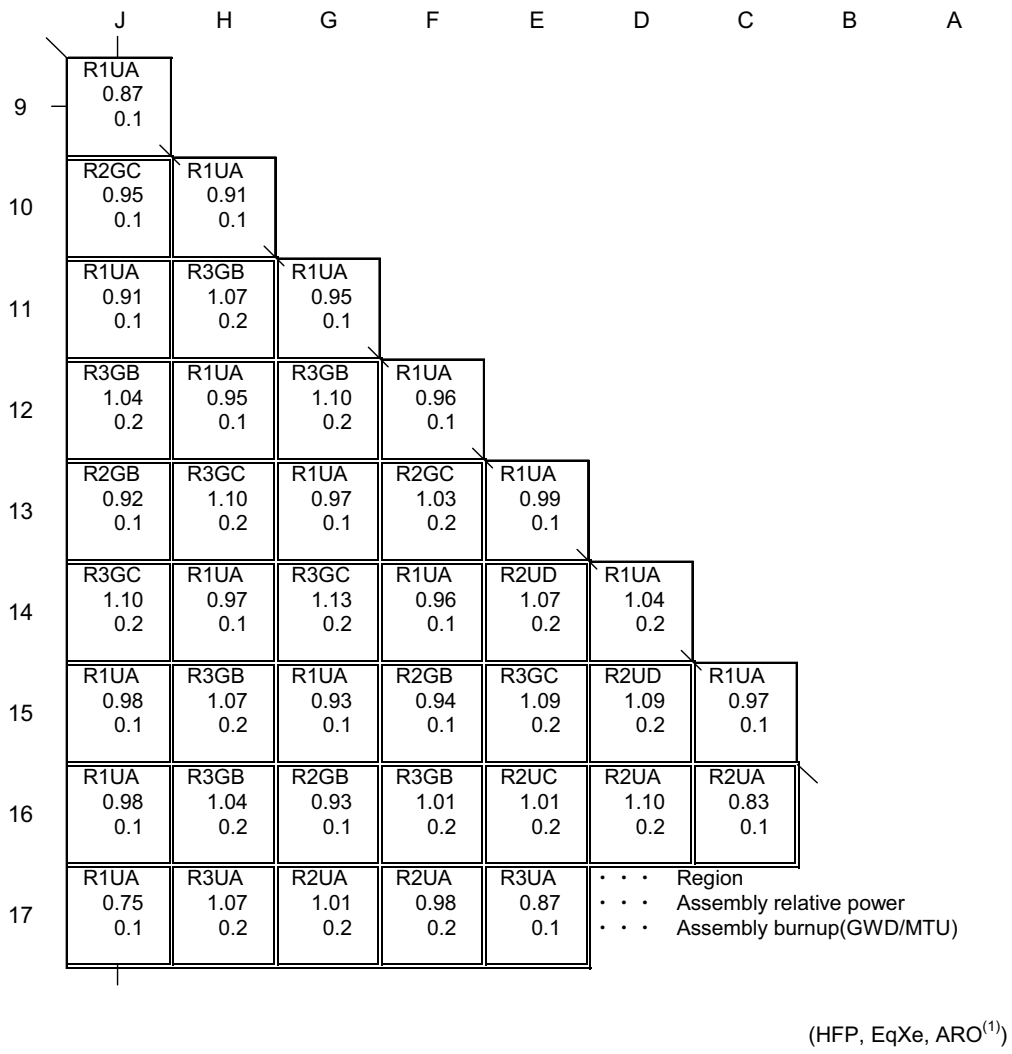

Note: (1) Control Bank D withdrawn to 'bite' position

Figure 4.3-6 Normalized Radial Power and Burnup Distributions at 0.15 GWD/MTU

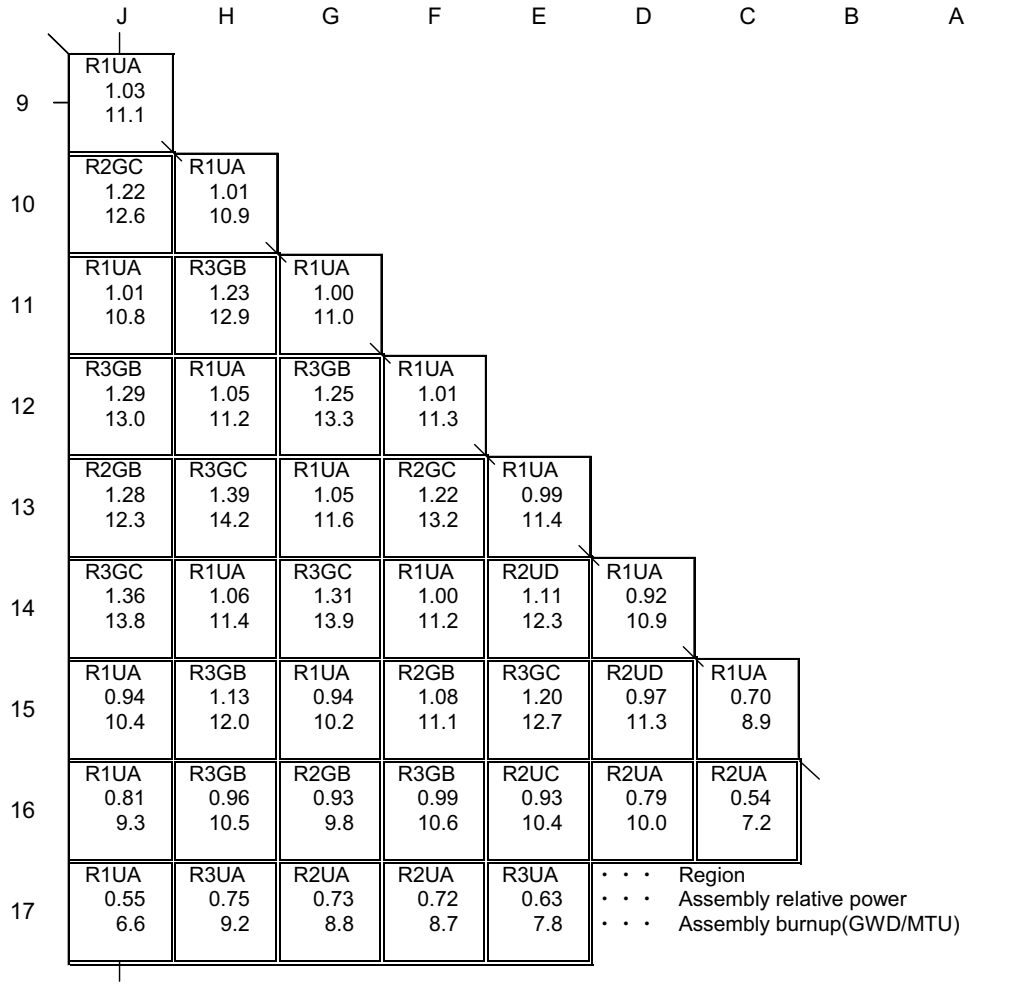

Note: (1) Control Bank D withdrawn to 'bite' position

Figure 4.3-7 Normalized Radial Power and Burnup Distributions at 11 GWD/MTU

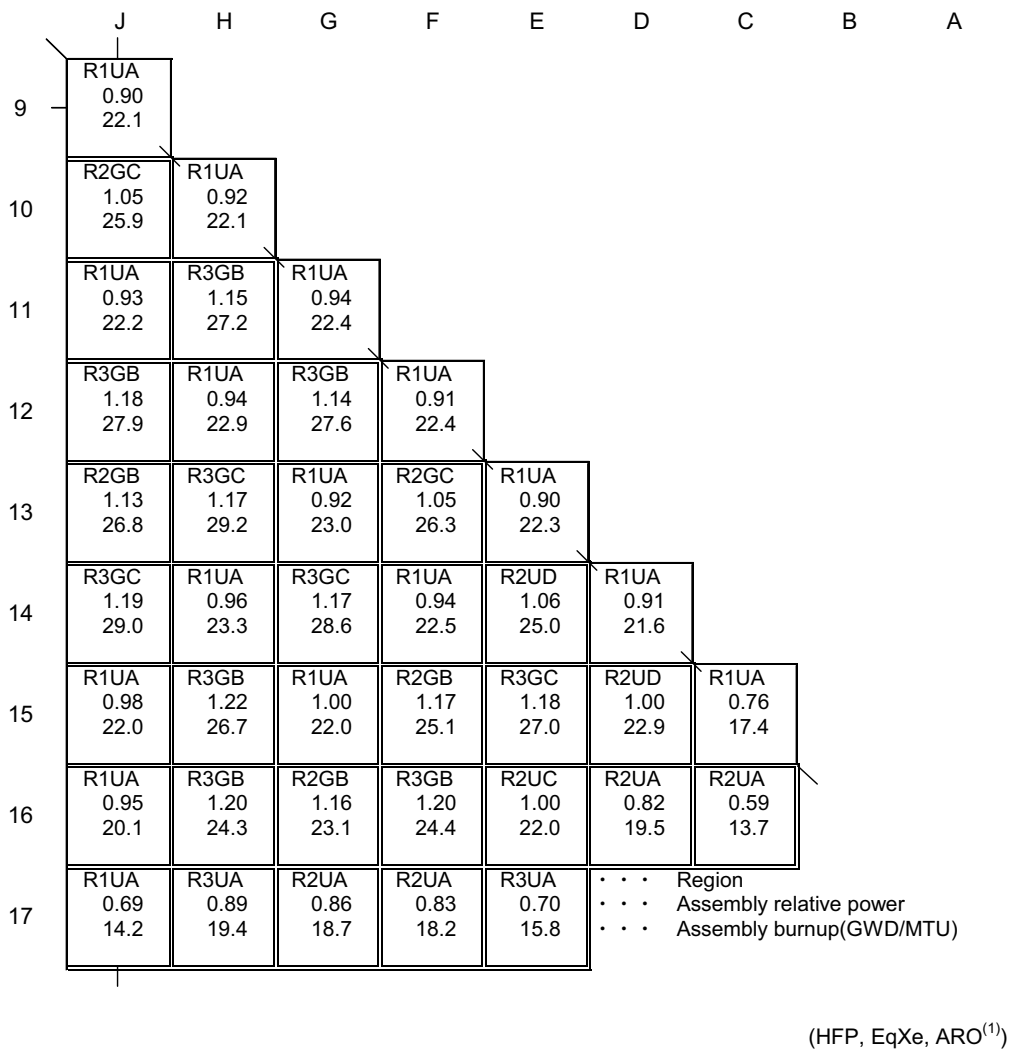

Note: (1) Control Bank D withdrawn to 'bite' position

Figure 4.3-8 Normalized Radial Power and Burnup Distributions at 23 GWD/MTU

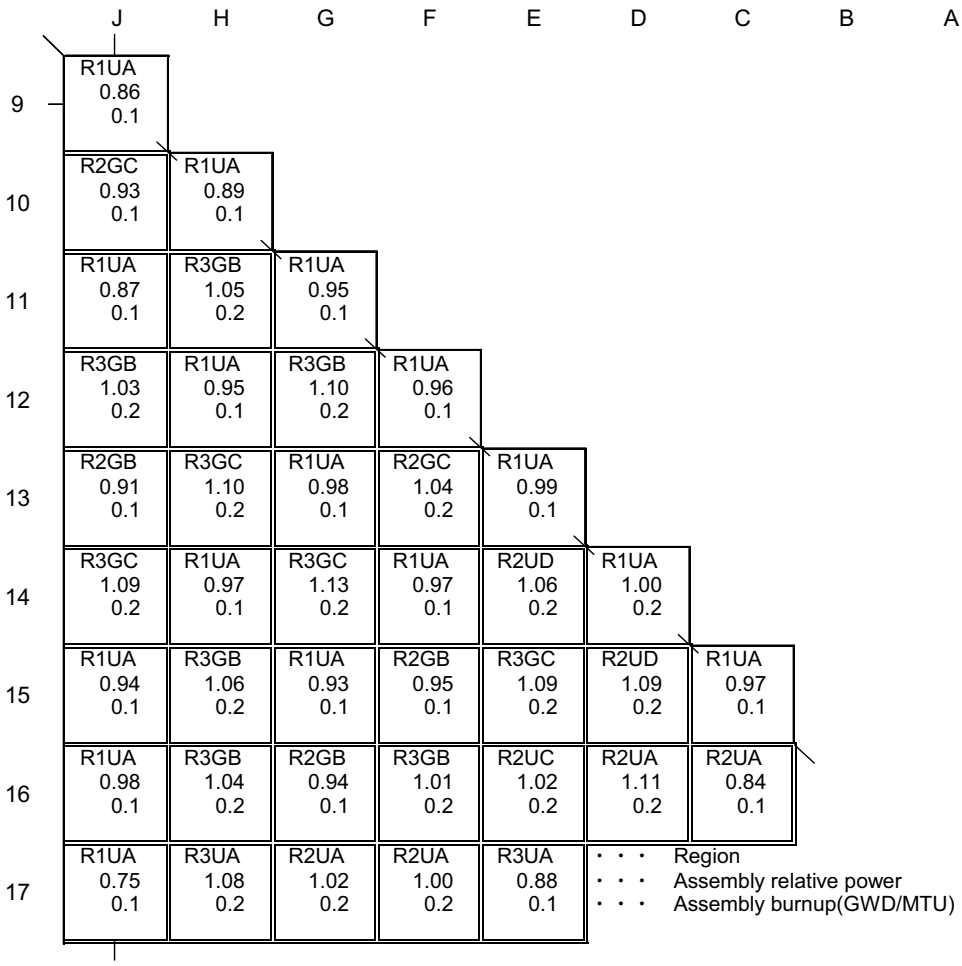

Figure 4.3-9 Normalized Radial Power and Burnup Distributions at 0.15 GWD/MTU

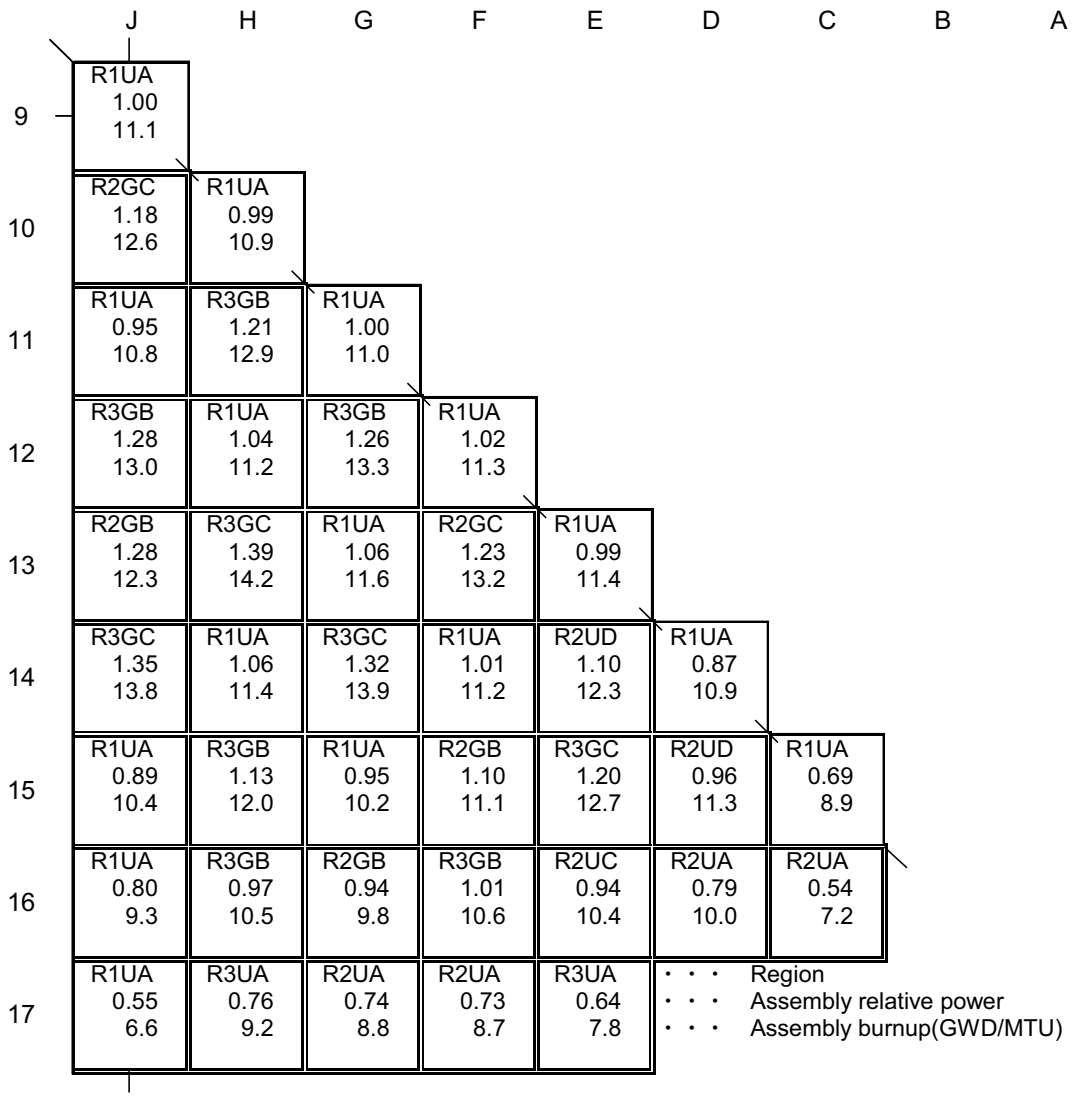

Figure 4.3-10 Normalized Radial Power and Burnup Distributions at 11 GWD/MTU

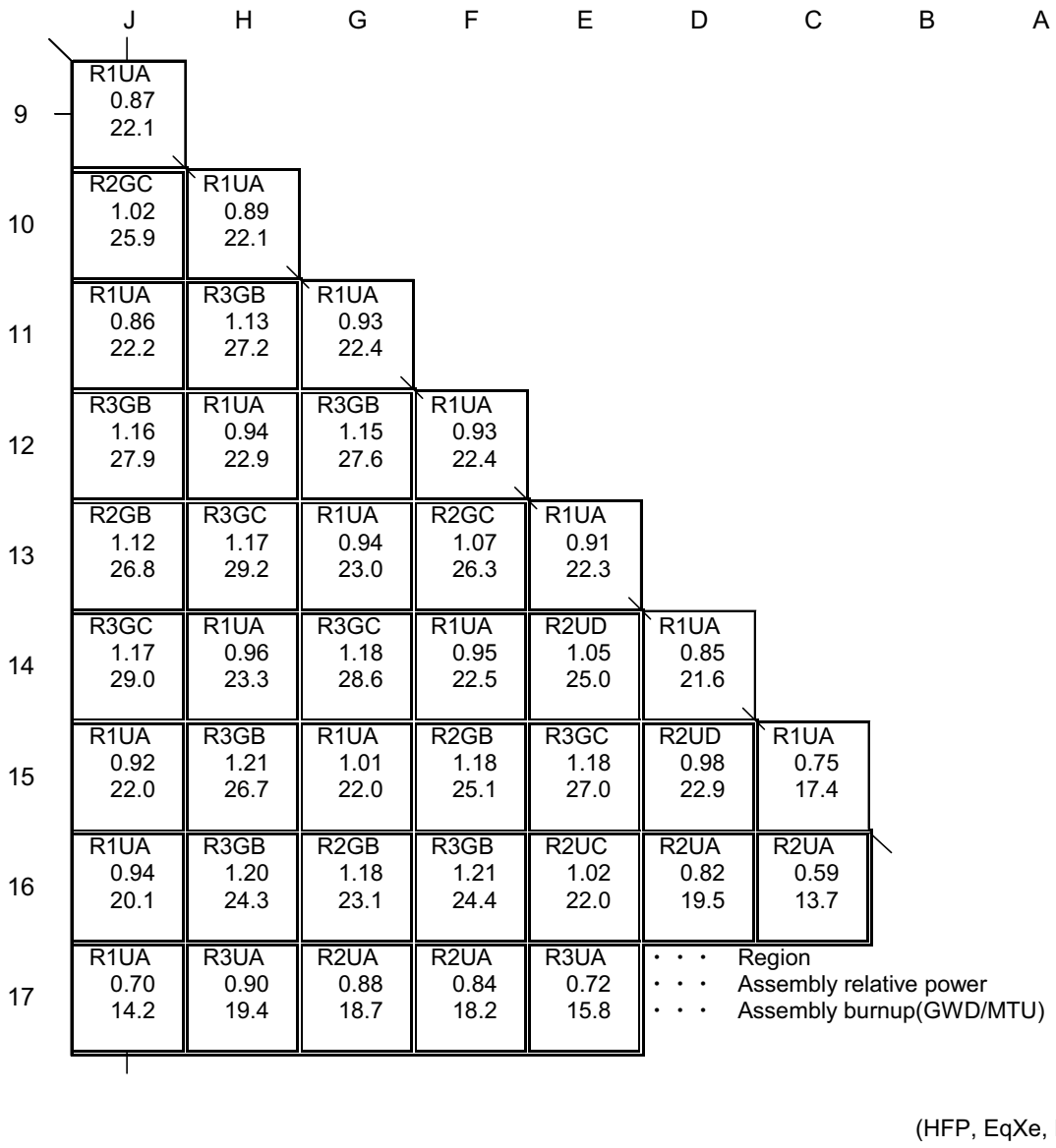

Figure 4.3-11 Normalized Radial Power and Burnup Distributions at 23 GWD/MTU

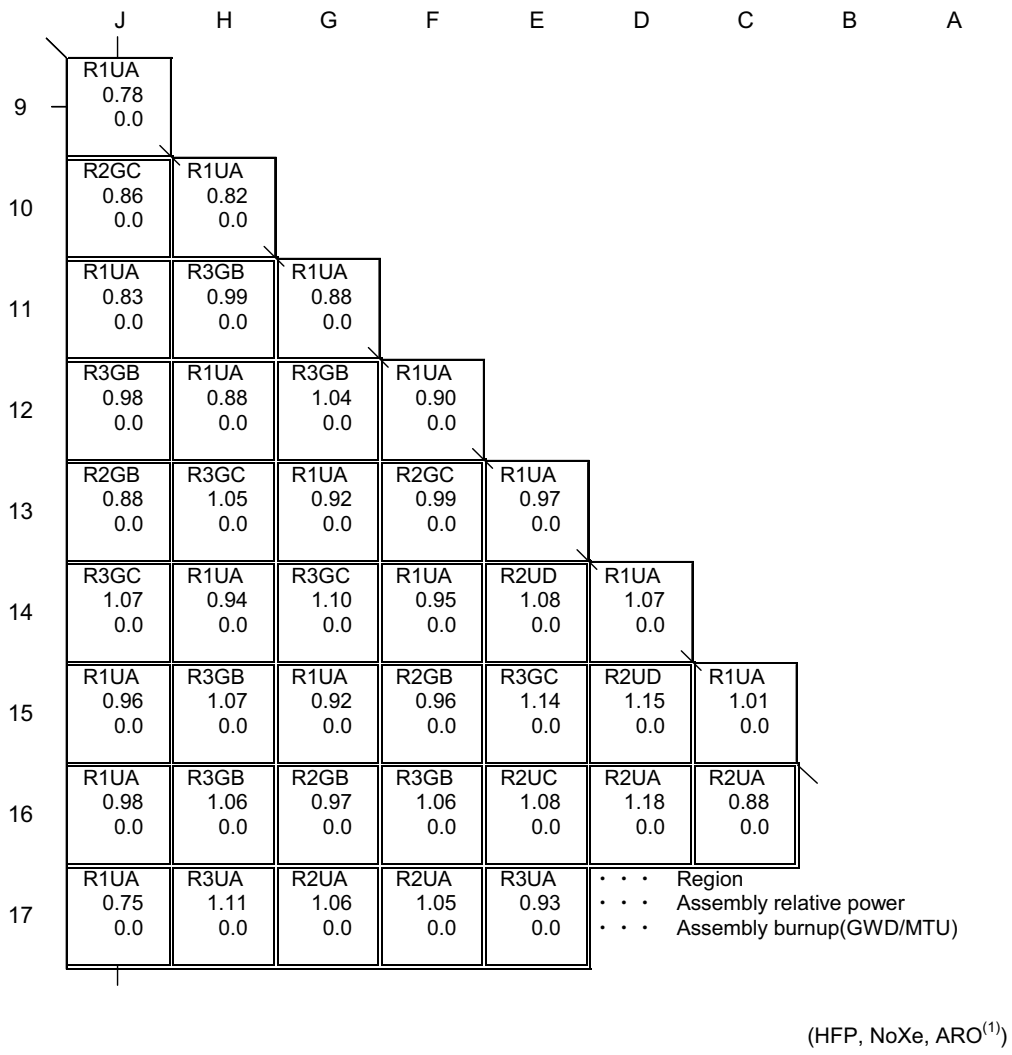

Note: (1) Control Bank D withdrawn to 'bite' position

Figure 4.3-12 Normalized Radial Power and Burnup Distributions at 0 GWD/MTU

Assembly (G-14)

	1	2	3	4	5	6	7	8	9	10	11	12	13	14	15	16	17
1	1.400	1.350	1.327	1.329	1.305	1.248	1.321	1.366	1.376	1.363	1.315	1.239	1.293	1.313	1.308	1.328	1.373
2	1.350	1.244	1.164	1.204	1.166	0.307	1.166	1.252	1.306	1.249	1.160	0.304	1.155	1.190	1.147	1.223	1.323
3	1.326	1.164	0.303	1.184	1.224		1.149	1.231		1.228	1.143		1.212	1.169	0.298	1.144	1.300
4	1.328	1.204	1.183		1.241	1.161	0.298	1.122	1.219	1.119	0.296	1.152	1.228		1.166	1.182	1.301
5	1.305	1.166	1.223	1.240	1.207	1.201	1.103	1.159	1.220	1.155	1.096	1.191	1.194	1.224	1.204	1.145	1.278
6	1.247	0.307		1.161	1.200		1.136	1.195		1.190	1.130		1.187	1.145		0.301	1.221
7	1.320	1.165	1.148	0.298	1.102	1.136	0.295	1.114	1.207	1.109	0.293	1.126	1.090	0.294	1.130	1.143	1.292
8	1.365	1.251	1.230	1.121	1.158	1.194	1.114	1.166	1.223	1.161	1.106	1.184	1.145	1.106	1.210	1.227	1.335
9	1.373	1.304		1.217	1.219		1.206	1.223		1.219	1.199		1.205	1.200		1.278	1.342
10	1.359	1.246	1.226	1.118	1.155	1.190	1.110	1.163	1.220	1.159	1.103	1.180	1.141	1.101	1.205	1.221	1.328
11	1.311	1.157	1.142	0.296	1.096	1.130	0.293	1.108	1.200	1.104	0.291	1.120	1.083	0.291	1.121	1.133	1.280
12	1.236	0.304		1.151	1.191		1.128	1.186		1.181	1.121		1.177	1.134		0.297	1.206
13	1.291	1.154	1.211	1.228	1.195	1.189	1.092	1.148	1.208	1.143	1.085	1.178	1.180	1.209	1.189	1.129	1.259
14	1.313	1.189	1.169		1.226	1.147	0.294	1.109	1.204	1.105	0.292	1.136	1.210		1.147	1.163	1.280
15	1.310	1.148	0.298	1.167	1.206		1.133	1.214		1.209	1.125		1.191	1.149	0.292	1.123	1.276
16	1.334	1.227	1.146	1.185	1.147	0.302	1.147	1.232	1.285	1.228	1.139	0.299	1.133	1.166	1.124	1.199	1.299
17	1.387	1.332	1.306	1.306	1.282	1.225	1.297	1.342	1.351	1.337	1.288	1.213	1.265	1.285	1.280	1.301	1.349

(HFP, EqXe, ARO[(1)])

Note: (1) Control Bank D withdrawn to 'bite' position

Figure 4.3-13 Rodwise Power Distribution at 0.15 GWD/MTU

Assembly (H-13)

	1	2	3	4	5	6	7	8	9	10	11	12	13	14	15	16	17
1	1.399	1.391	1.402	1.419	1.436	1.456	1.445	1.438	1.438	1.435	1.436	1.440	1.413	1.389	1.369	1.363	1.390
2	1.361	1.348	1.362	1.381	1.409	1.078	1.412	1.400	1.437	1.395	1.401	1.070	1.384	1.351	1.332	1.326	1.362
3	1.356	1.348	1.010	1.439	1.457		1.449	1.436		1.431	1.437		1.429	1.408	0.993	1.331	1.367
4	1.371	1.364	1.437		1.465	1.463	1.037	1.398	1.434	1.393	1.033	1.442	1.435		1.406	1.348	1.386
5	1.391	1.394	1.457	1.468	1.429	1.457	1.409	1.398	1.438	1.392	1.395	1.434	1.400	1.434	1.426	1.379	1.408
6	1.415	1.073		1.472	1.463		1.456	1.445		1.438	1.441		1.432	1.438		1.065	1.433
7	1.410	1.409	1.462	1.049	1.421	1.463	1.044	1.410	1.445	1.404	1.040	1.439	1.392	1.029	1.430	1.393	1.427
8	1.409	1.403	1.454	1.419	1.415	1.457	1.415	1.406	1.445	1.399	1.401	1.434	1.386	1.385	1.422	1.386	1.425
9	1.412	1.443		1.458	1.459		1.455	1.449		1.442	1.441		1.430	1.425		1.426	1.427
10	1.411	1.405	1.456	1.421	1.417	1.459	1.417	1.408	1.446	1.401	1.403	1.435	1.388	1.387	1.424	1.388	1.427
11	1.415	1.415	1.467	1.054	1.425	1.467	1.049	1.413	1.449	1.407	1.044	1.443	1.395	1.034	1.434	1.398	1.432
12	1.424	1.081		1.480	1.469		1.462	1.451		1.443	1.447		1.439	1.445		1.072	1.441
13	1.403	1.406	1.468	1.478	1.438	1.465	1.417	1.405	1.445	1.399	1.403	1.442	1.408	1.443	1.435	1.389	1.418
14	1.386	1.378	1.450		1.476	1.474	1.045	1.407	1.443	1.402	1.042	1.451	1.446		1.418	1.361	1.399
15	1.375	1.365	1.023	1.454	1.470		1.461	1.447		1.441	1.448		1.441	1.421	1.005	1.346	1.383
16	1.383	1.367	1.380	1.397	1.424	1.090	1.425	1.412	1.449	1.407	1.413	1.081	1.397	1.365	1.348	1.344	1.382
17	1.426	1.415	1.422	1.438	1.453	1.471	1.459	1.452	1.451	1.448	1.449	1.454	1.428	1.406	1.387	1.384	1.414

(HFP, EqXe, ARO[1])

Note: (1) Control Bank D withdrawn to 'bite' position

Figure 4.3-14 Rodwise Power Distribution at 11 GWD/MTU

Assembly (F-16)

	1	2	3	4	5	6	7	8	9	10	11	12	13	14	15	16	17
1	1.259	1.236	1.229	1.233	1.246	1.266	1.253	1.248	1.250	1.248	1.252	1.263	1.240	1.221	1.208	1.200	1.208
2	1.236	1.214	1.223	1.230	1.255	1.015	1.260	1.245	1.274	1.243	1.256	1.010	1.244	1.215	1.200	1.180	1.185
3	1.228	1.223	0.967	1.291	1.300		1.305	1.287		1.283	1.298		1.286	1.272	0.949	1.188	1.181
4	1.232	1.229	1.290		1.306	1.314	0.992	1.263	1.284	1.259	0.987	1.302	1.290		1.261	1.193	1.185
5	1.243	1.252	1.298	1.305	1.274	1.301	1.270	1.255	1.282	1.250	1.261	1.287	1.256	1.280	1.266	1.212	1.194
6	1.260	1.011		1.310	1.299		1.300	1.286		1.280	1.290		1.278	1.283		0.977	1.207
7	1.245	1.253	1.297	0.987	1.265	1.297	0.984	1.255	1.275	1.250	0.977	1.281	1.243	0.966	1.259	1.206	1.188
8	1.236	1.234	1.276	1.254	1.247	1.280	1.252	1.239	1.266	1.234	1.241	1.262	1.223	1.223	1.236	1.185	1.176
9	1.234	1.258		1.271	1.270		1.269	1.263	⊗	1.258	1.258		1.246	1.238		1.206	1.169
10	1.227	1.223	1.264	1.241	1.234	1.267	1.239	1.226	1.254	1.220	1.227	1.249	1.209	1.208	1.222	1.170	1.160
11	1.225	1.229	1.273	0.962	1.239	1.271	0.958	1.228	1.248	1.221	0.948	1.251	1.212	0.935	1.227	1.174	1.155
12	1.228	0.978		1.272	1.259		1.258	1.244		1.237	1.245		1.231	1.234		0.931	1.155
13	1.197	1.203	1.247	1.252	1.221	1.245	1.213	1.197	1.224	1.191	1.200	1.224	1.192	1.213	1.197	1.143	1.123
14	1.171	1.166	1.224		1.237	1.242	0.930	1.190	1.209	1.183	0.920	1.220	1.207		1.173	1.106	1.095
15	1.149	1.144	0.900	1.208	1.215		1.215	1.196		1.190	1.201		1.184	1.167	0.861	1.082	1.072
16	1.136	1.118	1.128	1.135	1.157	0.929	1.157	1.141	1.165	1.135	1.144	0.912	1.126	1.096	1.078	1.056	1.056
17	1.137	1.118	1.116	1.122	1.134	1.150	1.135	1.127	1.126	1.122	1.122	1.128	1.103	1.082	1.065	1.053	1.055

(HFP, EqXe, ARO[(1)])

Note: (1) Control Bank D withdrawn to 'bite' position

Figure 4.3-15 Rodwise Power Distribution at 23 GWD/MTU

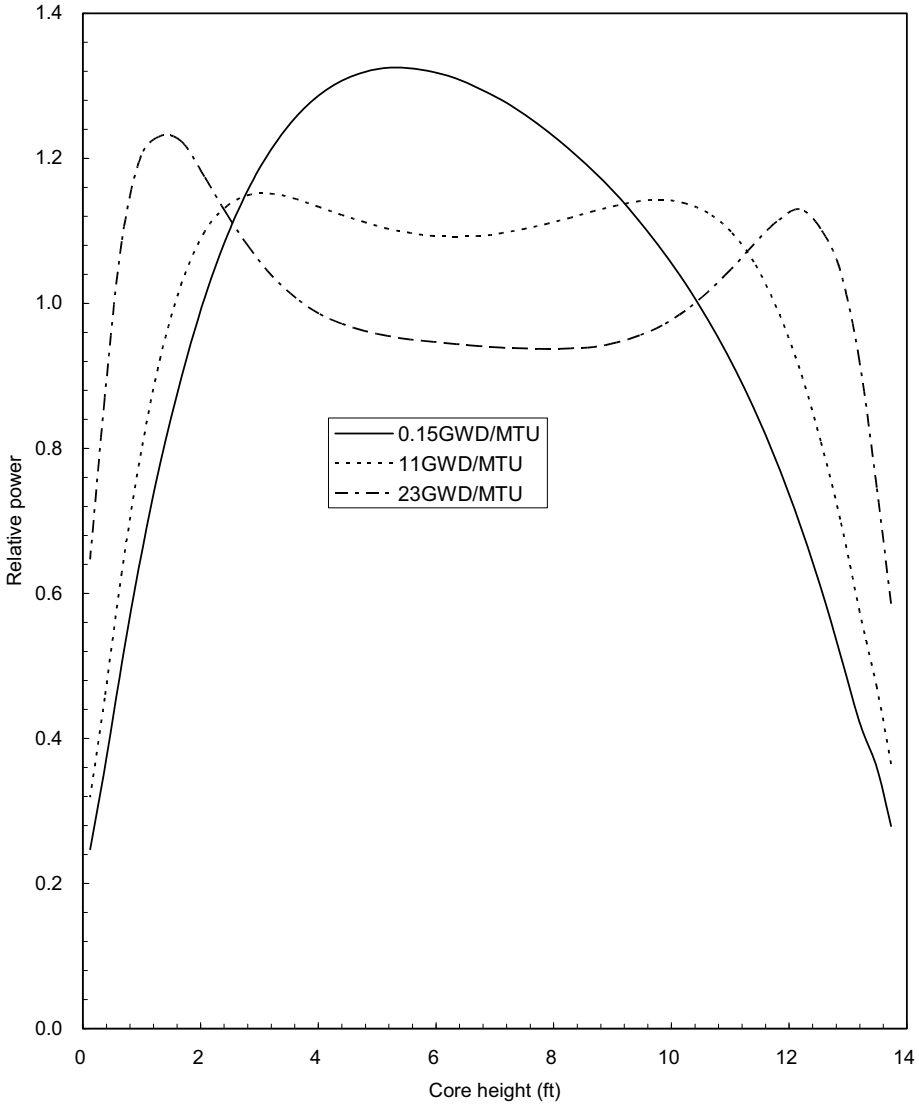

(HFP, EqXe, ARO[1])

Note: (1) Control Bank D withdrawn to 'bite' position

Figure 4.3-16 Normalized Axial Power Distribution for the Initial Core

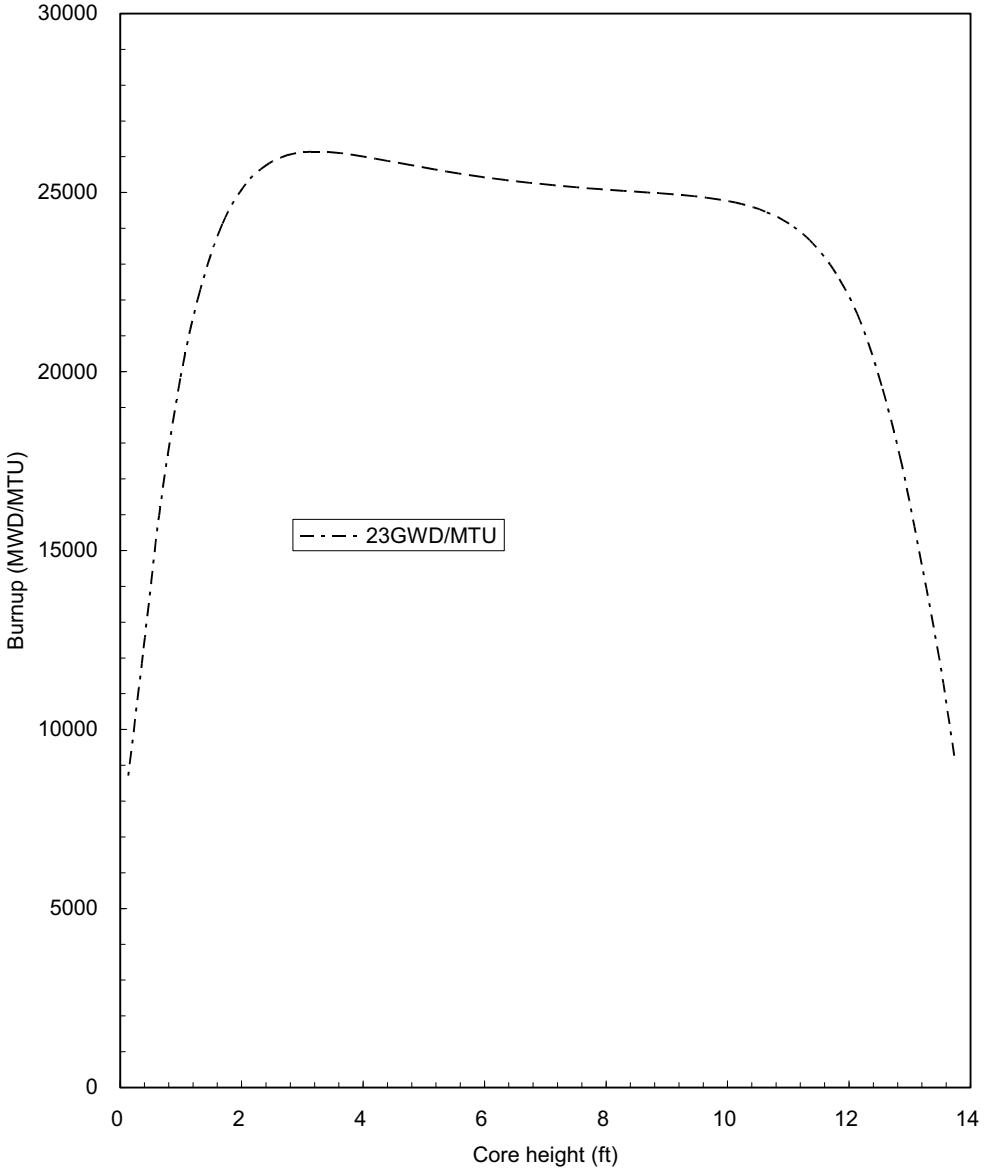

Figure 4.3-17 Axial Burnup Distribution for the Initial Core

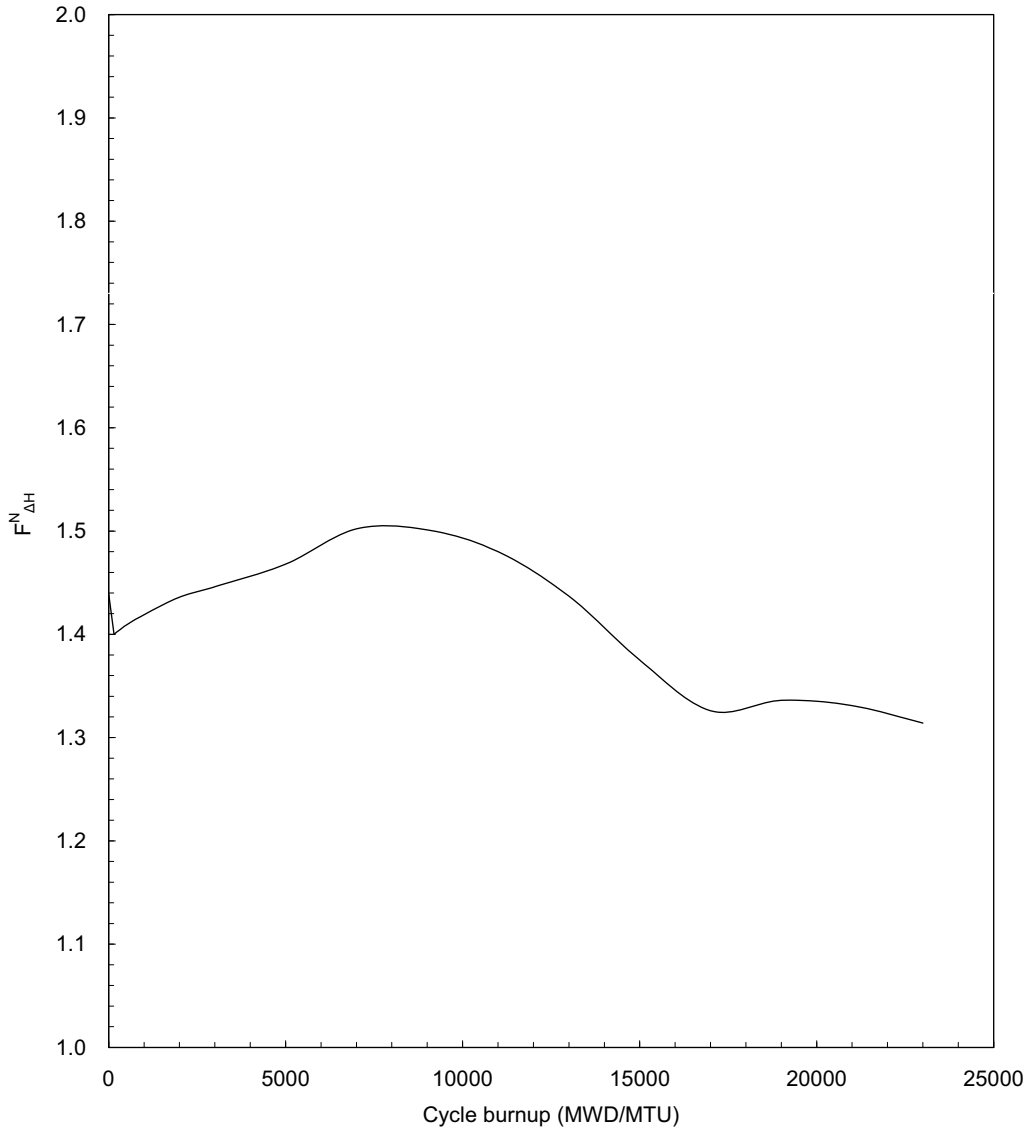

Note: (1) Control Bank D withdrawn to 'bite' position

Figure 4.3-18 Calculated $F^N_{\Delta H}$ versus Core Depletion for the Initial Core

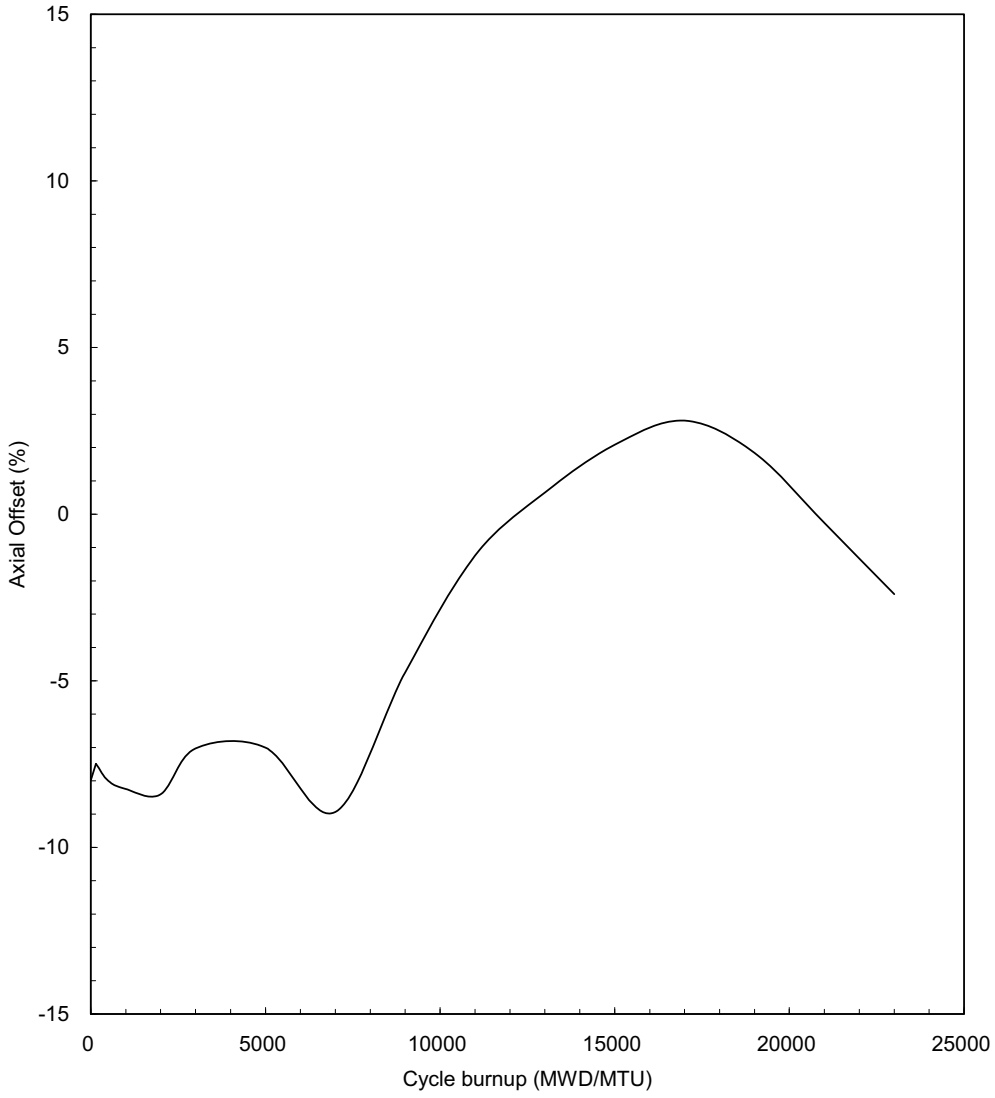

(HFP, ARO[1])

Note: (1) Control Bank D withdrawn to 'bite' position

Figure 4.3-19 Axial Offset versus Core Depletion for the Initial Core

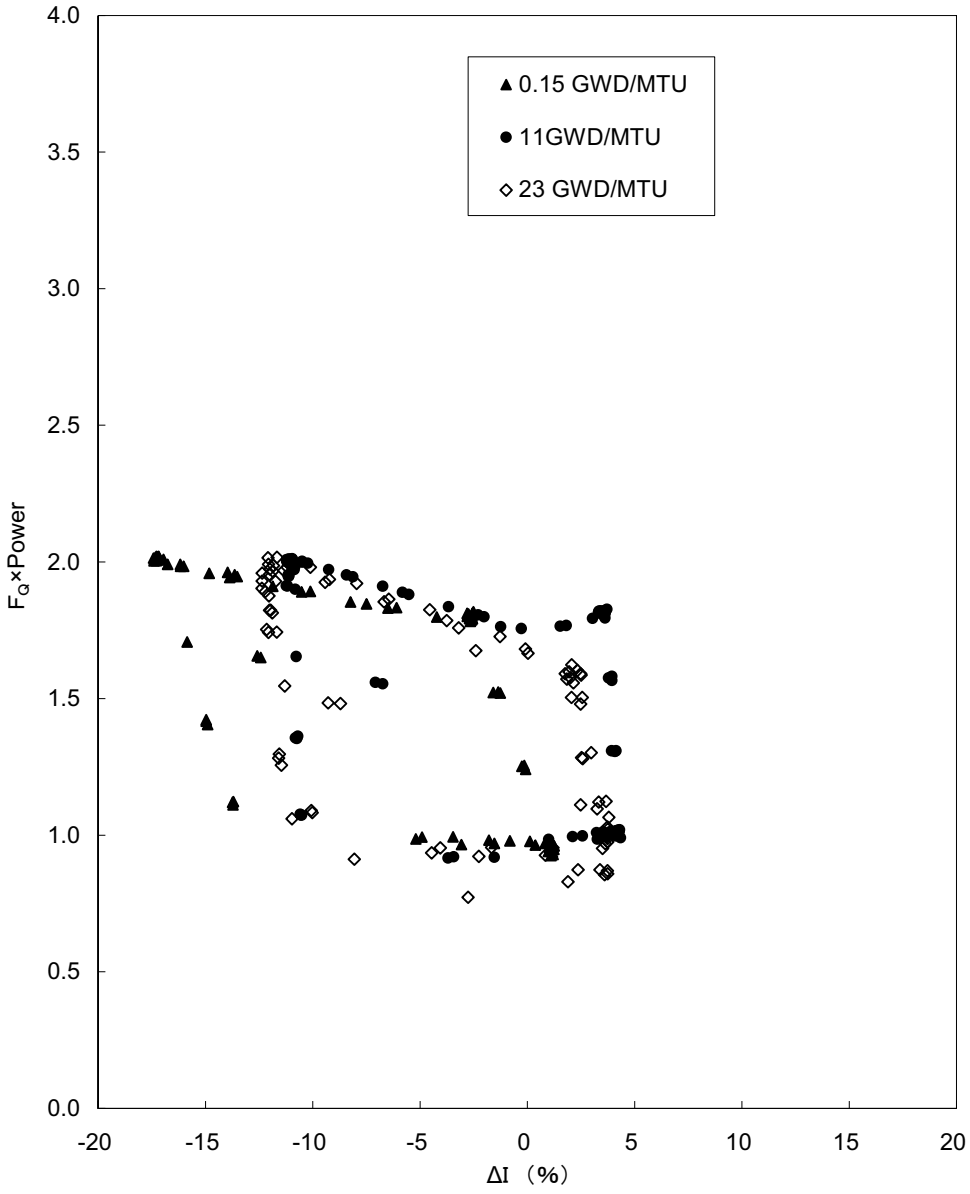

Figure 4.3-20 Calculated F_Q Values versus Flux Difference for the Initial Core

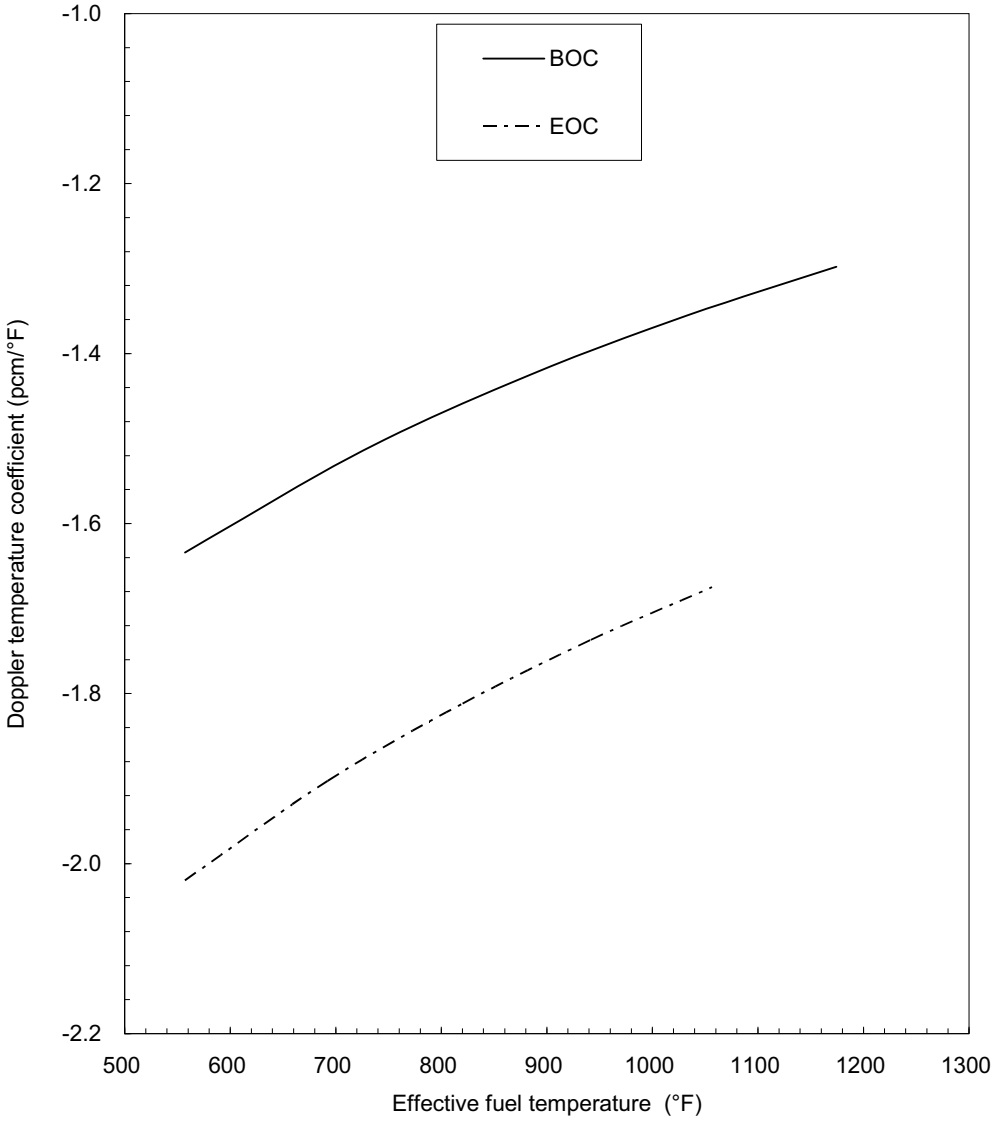

Figure 4.3-21 Typical Doppler Temperature Coefficient versus Effective Fuel Temperature for the initial core

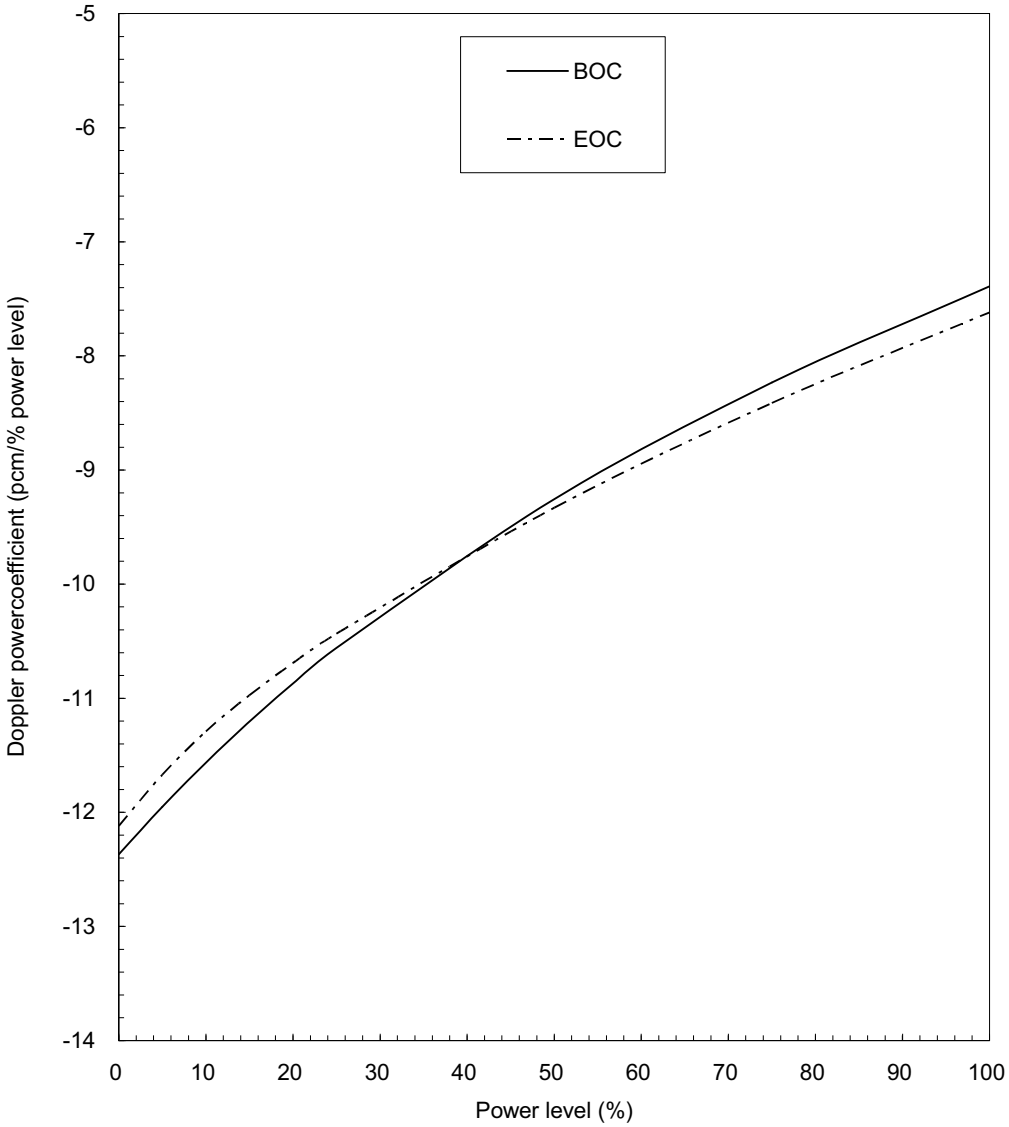

Figure 4.3-22 Typical Doppler Power Coefficient versus Core Power Level for the initial core

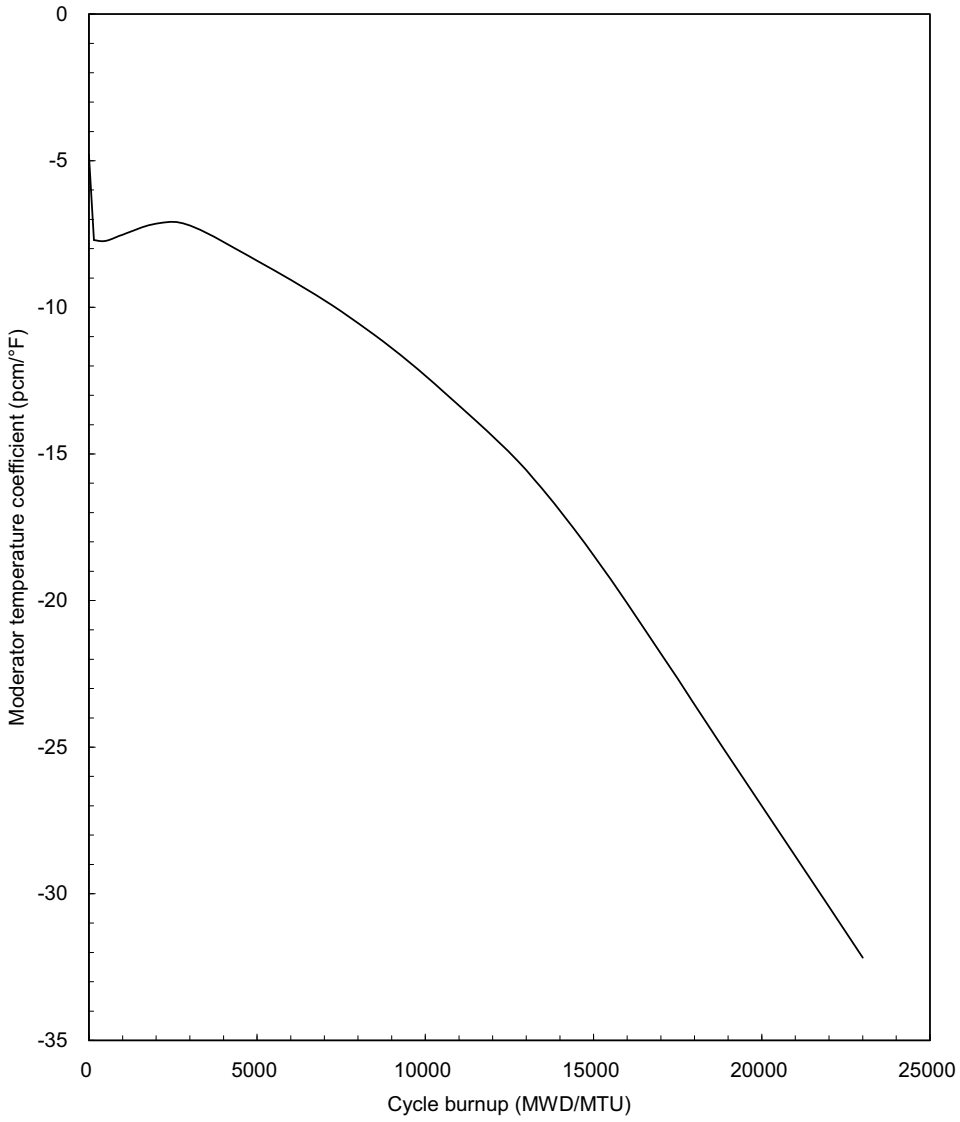

(Initial Core, HFP, ARO(1))

Note: (1) Control Bank D withdrawn to 'bite' position

Figure 4.3-23 Moderator Temperature Coefficient versus Core Depletion

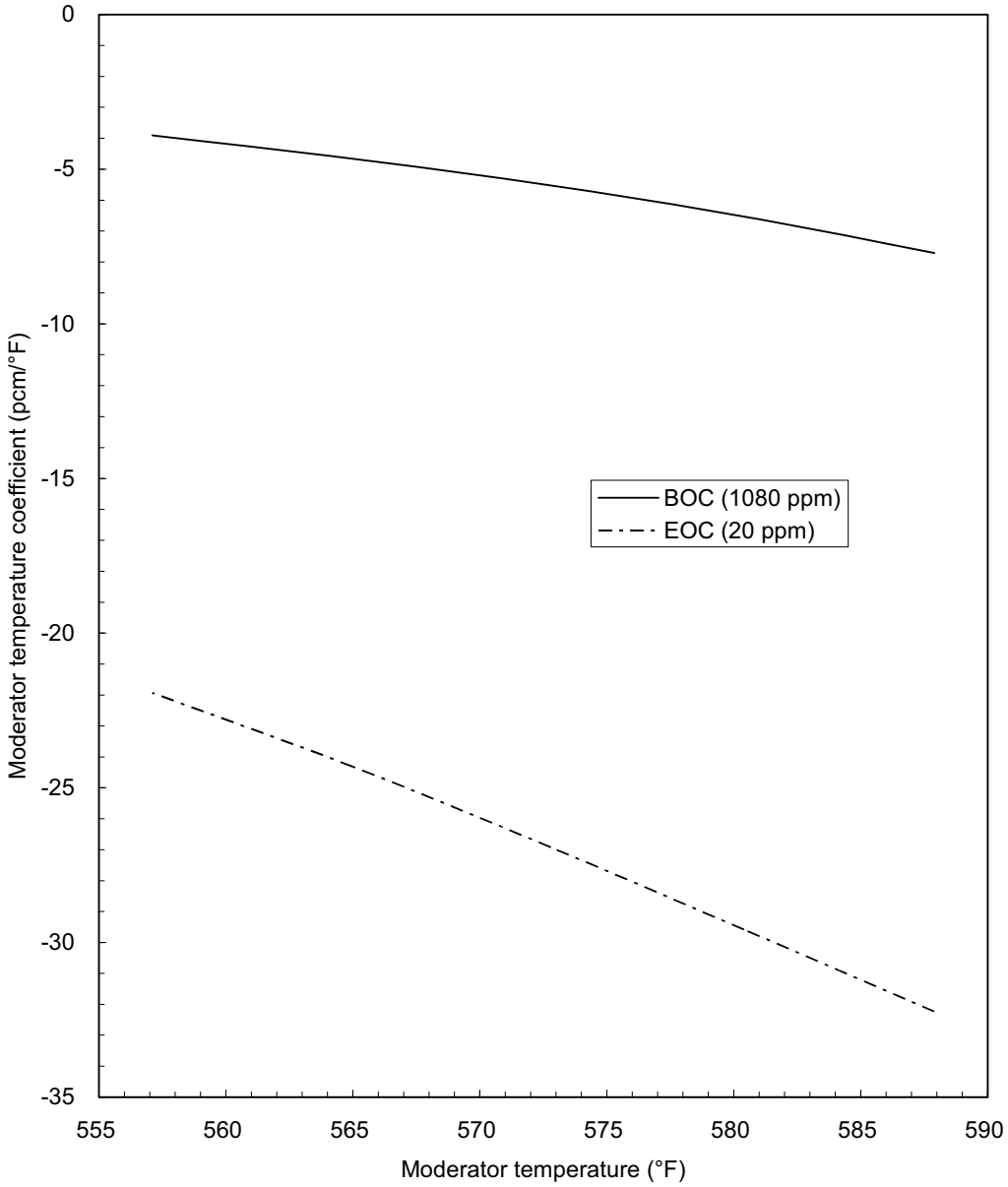

Figure 4.3-24 Typical Moderator Temperature Coefficient versus Moderator Temperature

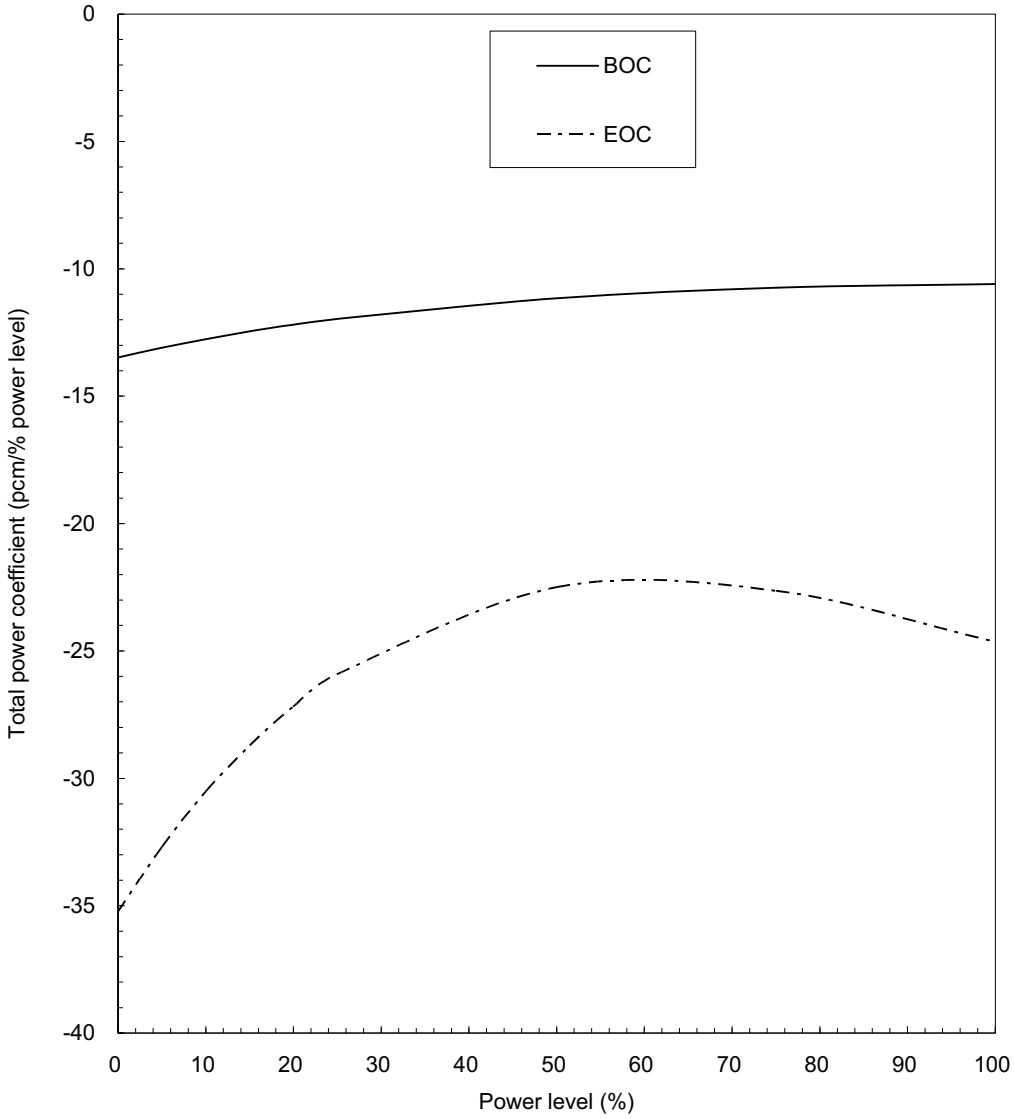

Figure 4.3-25 Typical Power Coefficient versus Core Power Level

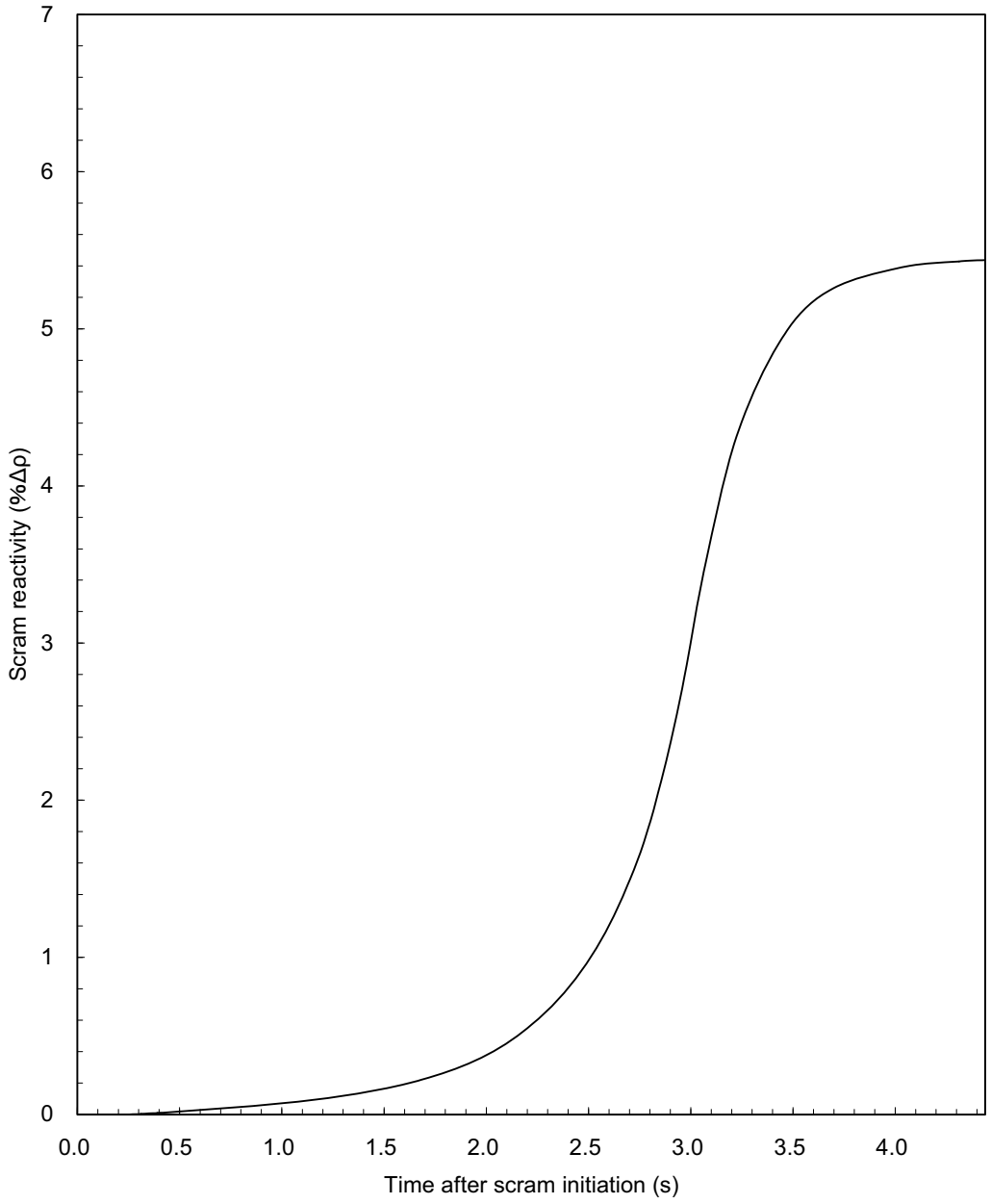

Figure 4.3-26 Scram Reactivity as a Function of Time after Scram Initiation

4.4 Thermal-Hydraulic Design

The US-APWR core thermal-hydraulic design ensures adequate cooling for the reactor core during normal operation and anticipated operational occurrence (AOO) conditions and keeps fuel integrity in compliance with the design requirements under various conditions.

This section describes the thermal-hydraulic design of the US-APWR. The description includes design bases, details of the thermal-hydraulic design of the reactor core and reactor coolant system (RCS), evaluations of the thermal-hydraulic design, testing and verification techniques related to thermal-hydraulic performance and instrumentation to be used in measuring and monitoring thermal-hydraulic parameters important to safety.

4.4.1 Design Bases

General Design Criterion (GDC) 10 of the Appendix A to 10 CFR Part 50 (Reference 4.4-1) requires that the reactor core and associated coolant, control, and protection systems shall be designed with appropriate margin to assure that specified acceptable fuel design limits are not exceeded during any condition of normal operation, including the effects of AOOs. Since fuel cladding is one of the three fission product barriers, its integrity has to be maintained during normal plant operation and AOOs to contain the fission products.

In addition, GDC 12 (Reference 4.4-1) requires that the reactor core and associated coolant, control, and protection systems shall be designed to assure that power oscillations which can result in conditions exceeding specified acceptable fuel design limits are not possible or can be reliably and readily detected and suppressed.

The following design bases are essential to achieve the above objectives.

4.4.1.1 Departure from Nucleate Boiling

4.4.1.1.1 Design Basis

There is at least a 95-percent probability at a 95-percent confidence level that the hot fuel rod in the core does not experience a departure from nucleate boiling (DNB) phenomenon during normal operation and AOOs.

4.4.1.1.2 Discussion

DNB is the onset of the transition from nucleate boiling to film boiling. Beyond DNB, steam vapor generated on a heated surface tends to form a steam layer between the heated surface and the surrounding liquid flow, and it may lead to a remarkable decrease in heat transfer.

By preventing DNB, no heat transfer mode beyond nucleate boiling is allowed and adequate heat transfer between the fuel rod surface and the core coolant is assured. Since the temperature difference between the fuel cladding surface and the coolant flow surrounding it is only a few degrees, additional design bases for the maximum fuel cladding temperature are not needed.

The critical condition for DNB occurrence can be characterized by surface heat flux. The departure from nucleate boiling ratio (DNBR), the ratio of predicted DNB heat flux to actual local heat flux as defined in Subsection 4.4.2.2.1, is used to express the margin to the point of DNB occurrence.

To predict DNB heat flux for the US-APWR fuel design, the WRB-2 DNB correlation as described in Subsection 4.4.2.2.1 is adopted. The local coolant conditions utilized by the WRB-2 correlation are provided by the VIPRE-01M code as described in Subsection 4.4.2.2.1. The compatibility of WRB-2 with VIPRE-01M for the Mitsubishi fuel design has been verified, as described in Reference 4.4-2.

The uncertainties of several parameters that affect DNBR, such as those associated with plant operating parameters, nuclear and thermal parameters, fuel fabrication parameters, computer codes, and DNB correlation predictions, are considered statistically in the revised thermal design procedure (RTDP, Referece.4.4-3) to obtain design limits of the minimum DNBR value in the core (Min. DNBR) described in Subsection 4.4.2.2.1. With the uncertainties, the design limits of Min. DNBR are determined such that there is at least a 95-percent probability at a 95-percent confidence level that the hot fuel rod in the core does not experience a DNB.

The input parameters to the VIPRE-01M code are adopted at their nominal values. The Min. DNBR is maintained above the design limit during normal operation and AOOs.

The design limits of Min. DNBR for the US-APWR that are obtained by the VIPRE-01M code and the WRB-2 DNB correlation are 1.35 for a typical channel and 1.33 for a thimble channel, respectively. Those values were determined based on sensitivity analyses for US-APWR core conditions and uncertainties with VIPRE-01M and WRB-2.

The safety analysis limit of Min. DNBR is determined as 1.45 for both the channel types, accommodating the DNBR penalties incurred due to rod bows described in Subsection 4.4.2.2.4 and transition core geometry, and/or reserving more core operational flexibilities.

For the analyses where the RTDP is not applicable, all the uncertainties except DNB correlation uncertainty are deterministically taken into account. The input parameters to VIPRE-01M are applied in a conservative way. The DNBR limit covers the DNB correlation uncertainty, and also provides necessary margin to offset the DNBR penalties, if needed.

4.4.1.2 Fuel Temperature

4.4.1.2.1 Design Basis

There is at least a 95-percent probability at a 95-percent confidence level that the fuel rod with the most limiting linear heat rate (kW/ft) does not cause the fuel pellet to melt during normal operation and AOOs.

4.4.1.2.2 Discussion

By precluding fuel pellet melting, the fuel pellet geometry is preserved and any possible adverse effects of molten fuel pellet on the cladding are eliminated. It can thus prevent the fuel cladding from mechanical and chemical damages.

The melting temperature of uranium dioxide pellets is 5072°F (2800°C) for un-irradiated fuel and decreases by 58°F (32°C) per 10,000 MWD/MTU (Reference 4.4-4). The melting temperature of the gadolinia fuel is 4892°F (2700°C) at maximum content of 10 wt% and decreases by 58°F (32°C) per 10,000 MWD/MTU, the same as for uranium dioxide pellets (Reference 4.4-4).

Thermal performance analyses of fuel rods are conducted by using the fuel rod design code (FINE code; Reference 4.4-4). Considering the uncertainties in the analysis model and the fuel fabrication, fuel temperature analyses for various burnup and linear heat rate show that the fuel temperature design basis is met.

The peak linear heat rates during normal operation and AOOs are confirmed to be covered by the limit of linear heat rate for the first and reload cores. This ensures that the fuel center-line temperatures remain below the melting temperature for the fuel rods. Due to the lower melting temperature and the lower thermal conductivity of gadolinia fuel rods, fuel temperature analysis will provide more severe result than that of uranium dioxide fuel on the same linear heat rate condition. However, the evaluation shows that the temperature of gadolinia fuel rods is not critical because the peak linear heat rate for gadolinia fuel rods is decreased by their reduced UO_2 enrichment content.

4.4.1.3 Core Flow

4.4.1.3.1 Design Basis

Sufficient coolant flow is provided for the reactor core. Conservatively assumed RCS flow and effective core flow are applied in thermal-hydraulic designs.

4.4.1.3.2 Discussion

The core thermal-hydraulic design based on the assumption of conservative core RCS flow and core bypass flow provides sufficient core cooling and ensures core safety.

Thermal design flow (TDF), which is the allowable minimum value of RCS flow is 112,000 gpm per a RCS loop as described in Section 5.1. The estimated minimum value of the effective core cooling flow is 91.0 percent of the RCS flow rate, which is the total RCS flow minus the design core bypass flow.

The TDF is estimated with reserved margin for the steam generator tube plugging and the uncertainties on pressure loss, pump performance and flow measurement. The TDF is evaluated assuming 10 percent of steam generator tube plugging and RCS flow is measured to confirm that it is maintained above TDF. When RTDP is adopted for the thermal-hydraulic design, the minimum measured flow (MMF), which is the minimum flow without accounting for flow measurement uncertainty, and the core bypass flow without uncertainty are used for estimating the Min. DNBR in a core. The measurement

uncertainty for RCS flow and the uncertainty of core bypass flow are statistically treated in the design limits of Min. DNBR.

The core bypass flows are not considered effective for the reactor core heat removal. As described in Subsection 4.4.4.2, the core bypass flow consists of the flow through control rod guide thimbles and in-core instrumentation guide tubes in the fuel assemblies, the neutron reflector cooling flow, the leakage to the core cavity, reactor vessel (RV) head cooling flow, and leakage to the RV outlet nozzles, and a maximum core bypass flow of 9.0 percent is estimated considering the uncertainties of pressure loss and fabrication. The RTDP considers those uncertainties statistically in the design limits of Min. DNBR and therefore the Min. DNBR is evaluated using the core bypass flow which does not include the uncertainties.

4.4.1.4 Hydraulic Stability

4.4.1.4.1 Design Basis

Hydraulic instability does not occur at any operational modes during normal operation and AOOs.

4.4.1.4.2 Discussion

If boiling flow in a reactor system is susceptible to thermal-hydraulic instabilities, it is undesirable due to the following reasons:

- Flow oscillations tend to affect the local heat transfer characteristics and may induce boiling crisis,
- Sustained flow oscillations may cause detrimental mechanical vibration of components, and
- Flow oscillations may cause problems in system control for core power or core power distribution.

However, thermal-hydraulic instability has not been identified in PWRs since pressure and flow rate conditions are large enough to suppress the change of flow characteristics resulting from the void generation, and serve to stabilize the system. A detailed discussion is given in Subsection 4.4.4.6.

4.4.1.5 Other Considerations

Fuel cladding integrity is maintained by complying with the above mentioned design criteria and the fuel design bases described in Subsection 4.2.1. No additional criteria are required.

Other parameters, such as fuel rod cladding-to-pellet gap characteristics, coolant flow velocity and distribution, and coolant void, may be important parameters in thermal-hydraulic design to a certain extent, but are not limiting factors in themselves. Each of these parameters plays its part in the thermal-hydraulic models and analyses following the design bases.

4.4.2 Description of Thermal-Hydraulic Design of the Reactor Core

4.4.2.1 Summary Comparison

Table 4.4-1 provides a comparison of the design parameters for the US-APWR with those of typical U.S. 4-loop plants (12-ft and 14-ft cores).

4.4.2.2 Critical Heat Flux Ratios

The Min. DNBRs in the hot typical channel and the hot thimble channel for normal operation and AOOs are provided in Table 4.4-1. The typical channel is a unit flow channel which is bounded by four quarter-regular fuel rods and the thimble channel is a unit flow channel which is bounded by three quarter-regular fuel rods and one quarter-thimble. The hot channel involves a peak power rod (hot rod). The Min. DNBRs are defined as the minimum values of DNBR in each type of hot channel, i.e., the hot typical channel and the hot thimble channel.

The Min. DNBRs are evaluated by the following methodology.

4.4.2.2.1 DNB Correlations and Analysis

The DNBR is defined as:

$$\mathrm{DNBR} = \frac{q''_{\mathrm{DNB}}}{q''_{\mathrm{local}}}$$

where

q''_{DNB}: DNB heat flux predicted by DNB correlation

q''_{local}: actual local heat flux

The US-APWR fuel design conditions for DNB heat flux prediction are predominantly covered by the applicable parameter range of WRB-2 DNB correlation (Reference 4.4-5). Analyses for relatively low system pressure conditions, W-3 DNB correlation (References 4.4-6 and 4.4-7) may be used as a supplementary tool. Its details are described in Subsection 4.4.4.1.

q''_{DNB} is predicted by WRB-2 DNB correlation as follows:

$$q''_{\mathrm{DNB}} = \frac{q''_{\mathrm{DNB\_EU}}}{F}$$

where

$q''_{\mathrm{DNB\_EU}}$: DNB heat flux predicted by WRB-2 DNB correlation assuming uniform axial heat flux distribution

F : shape factor that accounts for non-uniform axial heat flux distribution effect (Reference 4.4-6)

W-3 DNB correlation takes the following form:

$$q''_{DNB} = \frac{q''_{DNB\_EU\_W3} \times CWF}{F}$$

where

$q''_{DNB\_EU\_W3}$: DNB heat flux predicted by W-3 DNB correlation assuming uniform axial heat flux distribution and replacing hydraulic equivalent diameter by equivalent diameter based on heated perimeter

CWF : cold wall factor that accounts for the unheated wall effect (Reference 4.4-8)

The local thermal-hydraulic conditions needed by DNB correlations are provided by VIPRE-01M code as described in Subsection 4.4.4.5.2. VIPRE-01M with the above DNB correlations is able to determine the Min. DNBR for the US-APWR core design at various conditions during normal operation and AOOs.

The VIPRE-01M analysis provides detailed flow and energy distribution in the core at the prescribed plant operating conditions, such as reactor power, total coolant flow rate, coolant inlet temperature and RV pressure. The analysis takes into consideration power profiles, core bypass flow, inlet flow mal-distributions and mixing effect in the core as described in Subsection 4.4.2.2.2.

The uncertainties in DNB correlation prediction and in some typical input parameters for VIPRE-01M analysis are treated statistically and are included in the design limits of Min. DNBR for RTDP (Reference 4.4-3). These uncertainties are discussed in Subsection 4.4.2.9.1.

4.4.2.2.2 Hot Channel Factors

The hot channel factors are defined as the ratios of the maximum to the core average of quantities relevant to the core thermal-hydraulic design. Two types of hot channel factors are considered.

- Heat flux hot channel factor, F_Q

- Enthalpy rise hot channel factor, $F_{\Delta H}$

F_Q represents the ratio of the local linear heat rate at the hotspot to the core-averaged linear heat rate. $F_{\Delta H}$ represents the ratio of the integrated enthalpy rise along the hot channel to the core-averaged enthalpy rise.

Each hot channel factor consists of a nuclear and an engineering hot channel factor component, which describe neutron power distributions and variations in flow conditions and fabrication, respectively. The nuclear hot channel factors are described in Subsection 4.4.4.3.1 and the engineering hot channel factors are described as follows:

- Heat Flux Engineering Hot Channel Factor, F_Q^E

F_Q^E is determined by statistically combining the fabrication variations for fuel pellet diameter, density, and enrichment. F_Q^E represents the possibility of a local heat flux spike caused by the local variance of the above mentioned factors as well as fuel pellet eccentricity and fuel rod diameter variation. However, as shown in Reference 4.4-9, no DNB penalty is required due to such a small heat flux spike.

- Enthalpy Rise Engineering Hot Channel Factor, $F_{\Delta H}^E$

$F_{\Delta H}^E$ accounts for the following contributors, whose effects are directly considered in the VIPRE-01M subchannel analysis, described in Subsection 4.4.4.5.2, under all reactor operating conditions.

- Pellet diameter, density, and enrichment

The effects of these parameters on the overall hot rod power are grouped as one of the engineering hot channel factor, $F_{\Delta H}^{E}{}_{,1}$, which is included in the hot channel heat generation in the VIPRE-01M analysis. This engineering hot channel factor is one of the statistically treated input parameters in RTDP. $F_{\Delta H}^{E}{}_{,1}$ is determined from manufacturing data.

- Inlet flow mal-distribution

The core inlet flow mal-distribution is directly considered in core thermal-hydraulic analysis using VIPRE-01M. As described in Subsection 4.4.4.2, a 10 percent reduction in the hot assembly inlet flow is used in design analyses.

- Flow redistribution

The flow redistribution phenomenon due to the non-uniformity of flow resistance and non-uniform fuel rod heat generation is accounted for in the VIPRE-01M analyses. Local and/or bulk boiling that tends to create such flow redistribution described above is considered by the physical models incorporated.

- Flow mixing

The flow mixing caused by cross flow and turbulence is accounted for in the VIPRE-01M analysis. The VIPRE-01M turbulent mixing model is discussed in Reference 4.4-2. The mixing parameter, thermal diffusion coefficient (TDC), used in the design analysis is based on experimental data, and is discussed in Subsections 4.4.2.2.3 and 4.4.4.1.

The flow mixing tends to reduce the enthalpy rise in the hot channel and thus provides additional thermal performance to the limiting hot channel. The mixing vanes on top of each intermediate grid spacer effectively enhance flow mixing.

4.4.2.2.3 Thermal Mixing

The thermal energy exchange rate between neighboring flow channels due to turbulent mixing is proportional to the difference in the local volume-averaged fluid enthalpy of the respective channels and the local axial mass flow rate.

The proportionality constant TDC is defined by the following equation.

$$TDC = \frac{w'}{Ga}$$

where

w': : effective flow exchange rate per unit length (lbm/ft-s)

G : : fluid axial mass velocity (lbm/ft^2-s)

a : : lateral flow area between channels per unit length (ft^2/ft)

The TDC value for the design analysis is 0.026, which was selected conservatively in comparison with the empirically determined value based on the mixing tests, as described in Subsection 4.4.4.1.

4.4.2.2.4 Effects of Rod Bow on DNBR

The DNBR penalty incurred by rod bow is accounted for in the core DNB analysis (Reference 4.4-10). This penalty should be offset by applicable design margin that is reserved explicitly or resulting from conservatism in the evaluation models.

The maximum DNBR rod bow penalty for the US-APWR core is less than 1 percent. The safety analysis limit of Min. DNBR, as described in Subsection 4.4.1.1.2, is determined with a sufficient reserve margin to offset the rod bow penalty in DNBR.

4.4.2.3 Linear Heat Generation Rate

The maximum and core-averaged linear heat rates are provided in Table 4.4-1. These values are based on heat generated in fuel and densified active heated length. The definition of the maximum linear heat rate is given in Subsection 4.1.3.

4.4.2.4 Void Fraction Distribution

Void fraction is very small and localized in PWR cores. The core-averaged void fraction in US-APWR is less than 0.1 percent. With the prevailing design condition and hot channel factors in the RTDP analysis, the maximum and average void fractions in the hot channel at full power level are 12 percent and 2 percent, respectively. The void models used in the VIPRE-01M code are described in Subsection 4.4.2.7.3.

4.4.2.5 Core Coolant Flow Distribution

In thermal-hydraulic design and safety analysis, VIPRE-01M calculates flow and enthalpy distributions in the core. Extensive experimental verification of VIPRE-01M enthalpy and flow predictions are presented in References 4.4-2 and 4.4-11.

4.4.2.6 Core Pressure Drops and Hydraulic Loads

The pressure drops across the core and across the RV are show in Table 4.4-1. The core pressure drop includes the unrecoverable pressure drops across the fuel assembly, lower core support plate and upper core plate. The RV pressure drop includes RV inlet and outlet nozzle, and lower and upper plenums in addition to the core pressure drop. They are determined based on the classical fluid mechanistic relationship described in Subsection 4.4.2.7.2.

The pressure drops in Table 4.4-1 are the values at the hot full power condition assuming best estimate flow (BEF) for the RCS flow and their uncertainties are also shown in the table. They are used to determine a set of RCS flow conditions which includes TDF and mechanical design flow (MDF) described in Section 5.1.

The pressure drop causes upward hydraulic load on components in the core and the RV. As described in Subsection 4.2.3.5, the fuel assemblies do not cause liftoff during normal operation and AOOs except pump over speed condition, and no extra plastic deformation is provided for the holddown spring in case of liftoff at the pump over speed. The pump over speed is defined as the flow condition which is 20 percent greater than MDF.

The hydraulic loads for those fuel design evaluations are conservatively determined using MDF. For the analysis of cold start up conditions, the MDF is re-evaluated for the cold coolant density.

4.4.2.7 Correlations and Physical Data

4.4.2.7.1 Heat Transfer Coefficients

Fuel surface heat transfer coefficients are used for the analyses of fuel temperature and thermal response, and coolant subcool boiling. As the heat transfer mode at the fuel surface is limited prior to DNB during normal operation and AOOs, forced convection and nucleate boiling correlation are used in those analyses.

Classical Dittus-Boelter correlation (Reference 4.4-12) and Thom's correlation (Reference 4.4-13) are used for the forced convection and nucleate boiling heat transfer coefficients, respectively. These correlations provide adequate or conservative predictions for wall temperature in the PWR core conditions (Reference 4.4-14).

$$\frac{hD_e}{k} = 0.023\left(\frac{D_e G}{\mu}\right)^{0.8}\left(\frac{C_p \mu}{k}\right)^{0.4} \qquad \text{(Dittus-Boelter; for forced convection)}$$

where

h : : heat transfer coefficient (Btu/hr-ft^2-°F)

D_e : : hydraulic equivalent diameter (ft)

k : : fluid thermal conductivity (Btu/hr-ft-°F)

G : : mass velocity (lbm/hr-ft^2)

μ : : fluid viscosity (lbm/ft-hr)

C_P : : fluid heat capacity (Btu/lb-°F)

$$\Delta T_{sat} = 0.072 \exp\left(-\frac{P}{1260}\right) q''^{0.5}$$ (Thom; for nucleate boiling)

where

ΔT_{sat} : : wall superheat, $T_W - T_{sat}$ (°F)

q'' : : wall heat flux (Btu/hr-ft^2)

P : : pressure (psia)

T_W : : wall temperature (°F)

T_{sat} : : saturation temperature (°F)

Local boiling is assumed to occur at the point where the wall super heat predicted by Dittus-Boelter correlation is in excess of that predicted by Thom's correlation.

4.4.2.7.2 Pressure Drops

In a PWR, core coolant is assumed to be of single-phase and incompressible. Two-phase flow effects are neglected in the RV pressure drop evaluation because the core average void is negligibly small, as shown in Subsection 4.4.2.4. Regarding the core thermal-hydraulic subchannel analysis, two-phase flow effects are considered and the models are described in Subsection 4.4.2.7.3.

Unrecoverable pressure losses consist of form loss and frictional loss in the flow path. The core and RV pressure losses are calculated by the following equation:

$$\Delta P = \left(K + f\frac{L}{D_e}\right)\frac{\rho V^2}{2g_c(144)}$$

where

ΔP :unrecoverable pressure drop (psi)

ρ :fluid density (lbm/ft^3)

L :length (ft)

D_e :hydraulic equivalent diameter (ft)

V :fluid velocity (ft/s)

g_c :Constant, 32.174 ($lbm\text{-}ft/lbf\text{-}s^2$)

K :form loss factor (-)

f :friction loss factor (-)

Constant fluid density is assigned for each component in the core and RV. Because of the complex core and RV flow geometry, it is practically impossible to obtain precise analytical values for the form and friction loss factors. Therefore, empirical values or correlations for these coefficients are adopted from geometrically similar models.

Values for unrecoverable pressure loss across the RV, including the inlet and outlet nozzles, and across the core are provided in Table 4.4-1. These results are used for the RCS flow estimation. Tests of the RCS flow rate are conducted prior to initial criticality and during start-up as described in Subsection 4.4.5.1, to verify that the flow rates used in the design are conservative.

4.4.2.7.3 Void Fractions

The model used to predict void fractions in VIPRE-01M analysis consists of non-equilibrium steam flow quality model and relationship between void fraction and steam quality.

Non equilibrium steam quality model provides true steam flow quality, which is defined as a fraction of steam mass flow rate to the total mixture flow rate. Considering the non-equilibrium effect between saturated steam and subcooled bulk liquid water, the model provides true steam quality, which includes the effect of subcooled void, at each location from the void detach point through the core exit.

Void fraction is determined by entering the true steam quality above into the relationship between void fraction and steam quality, which complies with mass balance of steam and liquid water. The estimated void fraction is used in the VIPRE-01M analysis of flow distribution in core.

Further description of the model is provided in References 4.4-2 and 4.4-11.

4.4.2.8 Thermal Effects of Operational Transients

Two major thermal design bases described in Subsections 4.4.1.1 and 4.4.1.2 are actualized primarily by over temperature and over power ΔT reactor trips. The over temperature ΔT trip keeps core thermal power below the core thermal (DNB) limit, which is determined as a function of RCS pressure and RV average temperature. The over

power ΔT trip keeps core thermal power below the specific overpower condition, and prevents excess peak linear heat rate and fuel centerline melting. These reactor trip functions ensure the thermal-hydraulic design bases are met during normal operation and AOOs, in cooperation with other specific reactor protection functions for such plant parameters as core neutron flux level, RCS pressure and RCS coolant flow, as shown in the safety analyses in Chapter 15. Descriptions of the reactor protection systems are provided in Chapter 7.

4.4.2.9 Uncertainties in Estimates

4.4.2.9.1 Uncertainties in DNB analyses

For the key parameters related to DNBR analyses, uncertainties are conservatively considered. Some of them are treated as statistical uncertainties in RTDP.

- DNB correlation

The uncertainty in DNB correlation is determined from the result of the analyses for DNB test data, as described in Subsection 4.4.4.1. This uncertainty is involved in the design limits of Min. DNBR. In case of RTDP, it is combined statistically with other uncertainties described below.

- Plant operation parameters

Uncertainties of relevant plant operating parameters for DNBR analyses, such as reactor power, pressure, reactor coolant temperature and core flow rate, are taken into account to cover measurement error allowances. The uncertainty of core bypass flow is determined conservatively as described in Subsection 4.4.4.2. These uncertainties are included in the statistical evaluation of the design limits of Min. DNBR for RTDP, as described in Subsection 4.4.1.1.

- Heat flux distributions

The core heat flux distribution including its uncertainty is covered, by a conservatively determined enthalpy rise nuclear hot channel factor and axial power distribution as described in Subsection 4.4.4.3. In addition, a conservative engineering hot channel factor is considered as described in Subsection 4.4.2.2.2. Measurement uncertainties associated with the nuclear hot channel factor and fabrication variances represented by the engineering hot channel factor are statistically convoluted in the design limits of Min. DNBR in RTDP.

- Analytical models

The VIPRE-01M code’s capability to accurately predict flow and enthalpy distributions in hot fuel assemblies is discussed in Subsection 4.4.4.5.2 and in References 4.4-2 and 4.4-11. The core modeling options were confirmed to be insensitive to Min. DNBR results and/or selected to provide conservative results. Sensitivity studies in Reference 4.4-2 show that the effect of core inlet flow distribution is negligible small and two-phase flow model is conservatively selected in comparison with other reliable models. A conservative value is used for mixing coefficient as described in Subsection 4.4.4.1. Furthermore, the

DNB correlation is compatible with the VIPRE-01M code and its adopted turbulent mixing, cross flow, and two-phase models (Reference 4.4-2).

4.4.2.9.2 Uncertainties in Fuel and Cladding Temperatures

Uncertainties must be considered in the calculation of fuel pellet temperature. Since the cladding surface temperature is close to the coolant temperature as long as the DNB design basis described in Subsection 4.4.1.1.2 is met, the discussion for the uncertainties is focused on the effect on the fuel pellet temperature calculation.

The fuel pellet temperature uncertainty consists of factors involving pellet-cladding gap and fuel pellet thermal conductivity, which influence the fuel temperature. These uncertainties are evaluated individually and then lumped into a total uncertainty.

Uncertainties involved in the fuel temperature calculation are categorized as follows: (1) fabrication uncertainties, such as variations in the pellet and cladding dimensions and in the pellet density; or (2) analytical model uncertainties, such as variations in the pellet thermal conductivity prediction and the gap conductance models. These uncertainties are quantified based on the fabrication data and by comparison of the models to the measurements (measured vs. predicted) at a 95-percent probability at a 95-percent confidence level (Reference 4.4-4).

The design limit of fuel centerline temperature is determined conservatively below fuel melting temperature to account for the total uncertainty described above.

Other factors which may affect the fuel temperature are considered as follows:

An assumed crud thickness (Reference 4.4-4) is considered in the evaluation of fuel temperature. The temperature rise at fuel rod surface is small even if the crud effect is involved.

The effect of densification on fuel temperature is included in linear heat rate calculation as described in Subsection 4.4.2.11.5 and the resulting rise of linear heat rate is considered in the calculation of fuel temperature.

The uncertainty in local linear heat rate, which consists of the nuclear uncertainty and the fuel fabrication, is considered in the heat flux hot channel factor determination. This uncertainty is described in Subsection 4.3.2.2.

4.4.2.9.3 Uncertainties in Core Hydraulics

The uncertainties of pressure drops for core and RV are shown in Table 4.4-1. These values conservatively cover the uncertainties of test results and correlations.

These pressure drops are used in determining the RCS flow rate described in Section 5.1. The pressure drop uncertainty is considered in the determination of minimum and maximum flow rate, namely TDF (or MMF) and MDF. Thermal-hydraulic evaluations generally use TDF. In the RTDP analysis, MMF is used, because the flow measurement uncertainty included in TDF and core bypass uncertainty is statistically convoluted in the design limits of Min. DNBR. MDF is used for mechanical performance analyses for the

fuel and reactor internal components. These RCS flow rates are justified in reactor coolant flow test prior to initial plant criticality, as described in Subsection 4.4.5.1.

The maximum hydraulic loads on the fuel assembly are evaluated at a pump over speed condition, as a flow rate of 20 percent greater than MDF.

4.4.2.10 Flux Tilt Considerations

Through the use of conventional fuel management and loading patterns, asymmetry of power distribution in the core is expected to be minor and is accommodated within the power distribution margin during normal operation. Minor asymmetries may be experienced due to slight variations in assembly enrichment and burnup, burnable absorber loading and depletion. For reload cores, fairly uniform shuffling of irradiated assemblies and/or burnable absorbers to other quadrants ensures that flux tilts due to previous-cycle asymmetries are minimized.

Flux tilts may also be introduced in the design when the loading pattern requires that the fuel assembly and burnable absorber rods not be loaded in exact quarter-core symmetry. However, these asymmetries are explicitly accounted for in the predicted power distributions and peaking factors.

During operation, control rod insertion or movement could cause asymmetric changes in quadrant power, due to rods that are slightly misaligned but still within technical specification limits. Horizontal (X-Y) xenon oscillations may also cause quadrant power tilts, but these are typically short-lived and self-damping.

From an accident analysis standpoint, a misaligned or dropped rod may cause a significant quadrant power tilt and/or increase peaking factors; these events are analyzed separately in Subsection 15.4.3.

Both ex-core and in-core instrumentations are used to measure the power distribution and quadrant power tilts, and the incore instrumentation system (ICIS) measurements are compared to predictions. Once acceptability is established by review of the in-core maps, in accordance with the technical specifications, the quadrant power tilt alarms and related instrumentation are adjusted to indicate zero quadrant power tilt ratio - a final step in the calibration process. This action confirms that the instrumentation is correctly calibrated to alarm in the event in which an unexplained or unanticipated change in the quadrant-to-quadrant relationships occurs between calibration intervals.

In the event that unexpected quadrant power tilts do occur, the technical specifications provide appropriate corrective actions to continue safe operation of the reactor, such as reducing core power level depending on the magnitude of the unexpected tilt.

4.4.2.11 Fuel and Cladding Temperatures

The discussion of this subsection focuses on the fuel pellet temperature evaluation. Description of fuel cladding integrity is presented in Subsection 4.2.3.1. To be consistent with the fuel temperature design basis, the maximum fuel temperature is maintained below the melting temperature for the fuel pellets as discussed in Subsection 4.4.1.2. For achieving this objective, the design limit for fuel temperature is provided by subtracting

the fuel temperature uncertainty from the melting temperature as discussed in Subsection 4.4.2.9.2. Also, the linear heat rate which corresponds to the design limit for fuel temperature is calculated at various burnups using the relationship between fuel centerline temperature and linear heat rate. Finally, the limit of the local linear heat rate as a function of burnup is set forth with adequate margin below the linear heat rate which corresponds to the design limit for fuel temperature. The linear heat rate is verified to meet its design limit for the first and each reload core. To avoid fuel centerline melting, the limit of linear heat rate is determined at the overpower condition and serves as a basis for overpower protection system setpoints. This approach provides sufficient margin to cover uncertainties in the thermal evaluations.

The dominant factors affecting fuel temperature distributions are the linear heat rate, the fuel thermal conductivity and the pellet-cladding gap conductance. Fuel crud and oxides are also considered in the calculation of the radial fuel temperature distributions.

The factors which influence fuel thermal conductance, such as gap size (or contact pressure), internal gas pressure, gas composition, pellet density, and radial power distribution within the pellet, have been reflected in a semi-empirical model, which also accounts for time-dependent fuel densifications, as given in Reference 4.4-4. This model enables the determination of these factors and their net effects on temperature profiles. This thermal model of FINE code is verified by comparing the predicted fuel centerline temperatures with measured data (Reference 4.4-4).

Fuel rod temperature profiles, including fuel centerline, average, and surface temperatures, are calculated along with the fuel rod lifetime, taking the time-dependent densification into consideration. Maximum fuel temperature can be determined from this calculation.

The factors employed in the determination of the fuel temperatures are as follows, and are further described in Reference 4.4-4.

4.4.2.11.1 Thermal Conductivity of Fuel Pellet

The thermal conductivity for UO_2 fuel of 95 percent theoretical density (k_{95}) degrades with burnup and is affected by Gadolinium contents. The FINE code takes these effects into consideration. The equation of k_{95} is given by the following equation:

$$k_{95} = \frac{1}{11.8 + \alpha \cdot Gd + \beta \cdot Bu + 0.0238 \cdot T} + 8.775 \times 10^{-13} \cdot T^3$$

where

k_{95} : thermal conductivity of 95%TD pellet (W/cm-°C)

T : fuel pellet temperature(°C)

Gd : Gadolinium content (mol%)

Bu : burnup (MWD/kgUO_2)

α, β : constant (Reference 4.4-4)

For other densities, the thermal conductivity is corrected by the following:

$$\frac{k}{k_{100}} = (1 - P)^{1.7}$$

where

P : porosity of fuel pellet, P=(100-%TD)/100

k : thermal conductivity at the porosity of P

k_{100} : thermal conductivity at theoretical density (no porosity)

4.4.2.11.2 Radial Power Distribution in Fuel Pellet

The FINE calculation of the pellet temperatures takes into consideration for the radial variation of the pellet thermal conductivity and the heat generation within the pellet as described in Reference 4.4-4. FINE uses nuclear calculation result of radial power distributions in a tabular format, which is given as a function of rod enrichment and burnup.

4.4.2.11.3 Gap Conductance

Pellet surface temperature is greatly dependent on pellet-cladding gap conductance, which is a function of the gap size and the thermal conductivity of the gas in the gap.

This is modeled in the FINE code combined with the fuel thermal conductivity model and verified by comparing the calculated fuel center-line temperature and measured data. Description of the gap conductance model is presented in Reference 4.4-4.

4.4.2.11.4 Fuel Cladding Temperature

Cladding surface temperature is affected by cladding surface heat transfer coefficients. The model of the heat transfer coefficients at fuel rod surface accounts for heat transfer regimes such as nucleate boiling and forced convection. Surface heat transfer coefficients for those heat transfer regimes are presented in Subsection 4.4.2.7.1. The buildup of oxides and crud on the fuel rod surface causes the cladding surface temperature to increase. The evaluation for fuel cladding temperature considers this temperature rise.

4.4.2.11.5 Peak Linear Heat Rate

The fuel centerline temperature is below the melting temperature during normal operation and AOOs for the fuel life, considering allowances for uncertainties.

For normal operation, the maximum peak linear heat rate is 12.1 kW/ft, considering the total heat flux hot channel factor, F_Q. The effect of densification is considered in core average linear heat rate. The adopted design value of F_Q, as presented in Table 4.3-2 and described in Subsection 4.3.2.2, is 2.6.

The fuel temperature design basis for normal operation and AOOs is described in Subsection 4.4.1.2. The maximum allowable centerline temperature, which is provided by subtracting the fuel temperature uncertainty from the fuel pellet melting temperature, is 4620°F (2550°C) for beginning of life and decreases with burnup. The allowable peak linear heat rate for prevention of centerline melt, which corresponds to above maximum allowable centerline temperature, is 21.9 kW/ft (72.0 kW/m) for beginning of life and decreases with burnup. Peak linear heat rates resulting from overpower transients or operator errors are to be equal or below the linear heat rate for prevention of centerline melt, as presented in Table 4.4-1.

4.4.3 Description of the Thermal and Hydraulic Design of the Reactor Coolant System

4.4.3.1 Plant Configuration Data

An isometric drawing of the RCS is provided in Figure 4.4-1. Approximate dimensions are shown in Figures 5.1-3 and 5.1-4.

The valves in the RCS are shown in Figure 5.1-2. The pipe fittings in the RCS are shown in Table4.4-2.

The total coolant flow through each flow path such as core flow and bypass flow is shown in Table 4.4-3.

Table 4.4-4 shows the volume, flow area, flow path length, height and liquid level of each volume, and bottom elevation for each component in RCS.

Lengths and sizes for the safety injection lines are provided so that the fluid supply rates assumed in the safety analysis described in Chapter 15 are met.

The steady-state pressure, temperature and flow distributions through the RCS are shown in Table 5.1-2.

4.4.3.2 Operating Restrictions on Pumps

The minimum net positive suction head (NPSH) needs to be established before operating the reactor coolant pumps. The operator has to verify that the system pressure satisfies the NPSH requirements prior to operating the pumps.

4.4.3.3 Power-Flow Operating Map (BWR)

This subsection is not applicable to US-APWR.

4.4.3.4 Temperature-Power Operating Map (PWR)

The RV average temperature is controlled by maintaining the specified temperature-power operating map as shown in Figure 4.4-2. The map connects the no load temperature and the full power operating temperature specified for the cycle by a linear relationship.

The US-APWR does not consider power operation with partial or total isolation of a loop. The natural circulation capability of the RCS is described in Section 5.4.

4.4.3.5 Load-Following Characteristics

Reactivity control system can moderately control reactor power level by maneuvering of rod cluster control assemblies (RCCAs) and boron concentration adjustment in the RCS. RCS temperature is controlled by maintaining the temperature-operating map as described in Subsection 4.4.3.4.

4.4.3.6 Thermal and Hydraulic Characteristics Summary Table

The thermal-hydraulic characteristics of the RCS are summarized in Table 4.4-1.

4.4.4 Evaluation

4.4.4.1 Critical Heat Flux

The primary DNB correlation used for the thermal-hydraulic analyses for the US-APWR core is the WRB-2 DNB correlation (Reference 4.4-5). The WRB-2 DNB correlation is confirmed to be applicable for intermediate grid spacers (Z3 type) of the US-APWR fuel as described in Reference 4.4-2.

The range of parameters for the WRB-2 DNB correlation, which was derived based on rod bundle test data obtained at the Heat Transfer Research Facility of Columbia University, is as follows (Reference 4.4-5):

Pressure:	$1440 < P < 2490$	(psia)
Local mass flux:	$0.9 < G_{LOC} < 3.7$	(Mlbm/hr-ft^2)
Local quality:	$-0.1 < X_{LOC} < 0.3$	(fraction)
Heated length:	$L_h < 14$	(ft)
Grid spacing:	$10 < gsp < 26$	(in)
Equivalent hydraulic diameter:	$0.37 < d_e < 0.51$	(in)
Equivalent heated hydraulic diameter:	$0.46 < d_h < 0.59$	(in)

This correlation can be applied to most of the US-APWR core conditions and the correlation limit of 1.17 is conservatively applicable for the WRB-2 DNB correlation in conjunction with VIPRE-01M code (Reference 4.4-2).

The W-3 DNB correlation (References 4.4-6 and 4.4-7), which was developed based on single channel DNB test data and does not take into account mixing vane effects, is used when the WRB-2 DNB correlation is not applicable due to parameters being out of the above ranges or mixing vane effect is not expected. Typically, W-3 DNB correlation is applied in the analyses of accident conditions where the system pressure is below the pressure range of the WRB-2 DNB correlation. For system pressures in the range of 500 to 1000 psia, the W-3 DNB correlation limit is 1.45, while the correlation limit is 1.30 for system pressures greater than 1000 psia (Reference 4.4-15).

A cold wall factor, described in Reference 4.4-8, is applied to the W-3 DNB correlation to conservatively account for the presence of the unheated thimble surfaces.

The design value of TDC used for US-APWR is 0.026. The TDC is conservatively determined from the result of mixing test which was conducted at the Heat Transfer Research Facility of Columbia University. Figure 4.4-3 shows the TDC plotted against Reynolds number for the Mitsubishi designed Z3 grid spacer. The TDC is found to be insensitive to the Reynolds number. The test results show that the design value of TDC is acceptable. An equivalent value of the mixing coefficient is used in the VIPRE-01M evaluations (Reference 4.4-2).

4.4.4.2 Core Hydraulics

RCS flow enters the RV through the inlet nozzles goes down in the annulus between the RV and core barrel (downcomer), and enters upwards into the core after changing direction in the lower plenum. Then, the coolant flows out of the RV through the upper plenum and outlet nozzles.

Generally, flow distribution was observed at the core inlet in the existing flow model tests. However, it is known that the effect of such core inlet flow distribution is insignificant for DNBR analysis, because the flow distribution is immediately dispersed after entering into the core, where a relatively large pressure drop exists in the axial direction. In VIPRE-01M analysis model for DNBR, core inlet flow is reduced 10 percent at the hot assembly location and it is re-distributed to core peripheral fuel assemblies. A sensitivity study has been performed in Reference 4.4-2, and it shows that even an excess higher inlet flow reduction to the hot assembly has a negligibly small effect on the DNBR result.

In addition to the above mentioned major flow path, there are some minor bypass flow paths. Flows going through these paths are not effective for removing heat generated in the core, while some of them are needed to cool the non-fuel components in the core or RV.

Following flows are considered as core bypass flows which are not available for the core cooling.

A. Flow through the head-cooling spray nozzles into the RV upper head,

B. Flow directly going out the outlet nozzle through the gap between the RV and the core barrel,

C. Flow through the neutron reflector,

D. Flow through the control guide thimbles and in-core instrumentation guide tubes and

E. Flow in the extra gap region between the peripheral fuel assemblies and the neutron reflector.

Each bypass flow rate is estimated to balance the pressure drop with that of the main coolant flow path through the core. Its uncertainty is estimated as the effect of the drawing tolerances of the bypass flow path and the pressure loss uncertainty of the main flow path.

The total bypass flow is confirmed to be bounded by the design value of 9.0 percent, which includes the above uncertainty. It is assumed in the core bypass flow estimation that the plugging devices are inserted in the control rod guide thimbles that do not contain any other components.

Pressure drops across each of the flow paths are estimated by the empirical correlation described in Subsection 4.4.2.7.2. The friction and form loss factors are based on widely used empirical correlations or experimental data for similar design reactors.

The local pressure drops in the core calculated in VIPRE-01M analyses are derived from the momentum equations with empirical friction factor correlation, form loss factors for the fuel components such as grid spacers and empirical cross flow pressure loss factor (Reference 4.4-2).

Operation with partial or total isolation of a loop is not taken into account in the US-APWR design.

4.4.4.3 Influence of Power Distribution

The power distribution, which is affected by fuel enrichment, loading pattern, and core power level, is also a function of variables including control rod worth, control rod position, and fuel depletion through core lifetime. In the DNBR analysis, the core power distribution can be characterized by the nuclear enthalpy rise hot channel factor $F_{\Delta H}^{N}$ described in Subsection 4.3.2.2, and the axial heat flux profiles as discussed in Subsection 4.4.4.3.2.

4.4.4.3.1 Nuclear Enthalpy Rise Hot Channel Factor, $F_{\Delta H}^{N}$

The nuclear enthalpy rise hot channel factor, $F_{\Delta H}^{N}$, represents the ratio of the hot channel enthalpy rise to core-average enthalpy rise. The “channel enthalpy rise” is actually the integrated power in each individual fuel rod channel, in which the axial power distribution effect is implicitly reflected. The value of DNBR reflects the enthalpy rise to the point where the DNBR is calculated. In general, the maximum value of the rod integral power is used to identify the most likely rod for Min. DNBR. $F_{\Delta H}^{N}$ is determined to cover the ratio of the maximum value of rod integral power to core averaged integral rod power.

For partial power (i.e., less than full power) operation, a deeper control rod insertion limit than that at rated thermal power (RTP) operation requires relaxation of the $F_{\Delta H}^N$ limit:

$$F_{\Delta H}^{N} = F_{\Delta H}^{RTP}\left[1 + 0.3(1 - P)\right]$$

where

$F_{\Delta H}^{N}$: the limit at partial power

P : the fraction of RTP

$F_{\Delta H}^{RTP}$: the limit at RTP (1.73)

The permitted relaxation of $F_{\Delta H}^N$ is embedded in the DNB protection setpoints and allows for radial power distribution changes with control rod insertion up to the insertion limits, as discussed in Reference 4.4-16.

4.4.4.3.2 Axial Heat Flux Distributions

The axial heat flux (power) distribution changes with burnup and is affected by power level, control rod movement, and transition of xenon distribution in the axial direction. The shift of axial power distribution during normal operation can be contained by controlling the change in axial power imbalance, which is monitored by the ex-core nuclear detectors.

The design axial power distribution shown in Figure 4.4-4 is used in most of DNBR analyses that include determination of the core thermal limit and safety analyses in which the axial power distribution does not change significantly. While this design axial power distribution is selected to practically envelop all axial power distributions from normal operations for the DNBR calculations, the conservatism of this design power shape is to be confirmed in the first and reload core designs.

When the axial power distribution is skewed towards either the upper half or the lower half of the core during AOOs, the over temperature ΔT core protection setpoint will be activated at a lower core power level than that is corresponding to the more axially symmetric power distributions. For this purpose, the setpoint of the over temperature ΔT core protection is also a function of the axial power imbalance.

Other adequate power distributions may be used in specific cases of thermal-hydraulic analysis using VIPRE-01M.

For certain limiting DNB events described in Chapter 15, for which the design axial power distribution shown in Figure 4.4-4 is not bounding, event-specific power distributions are used in DNBR analyses.

In the fuel rod hot spot analyses such as the peak cladding temperature (PCT) determinations for the postulated non-LOCA accidents, the chopped cosine power

distribution with peak-to-average ratio of 1.46 (shown in Figure 4.4-4) is used. The F_Q factor is generated by multiplying the axial peaking factor by radial peaking ($=F_{\Delta H}^N$ x $F_{\Delta H}^{E}{}_{,1}$).

4.4.4.4 Core Thermal Response

As stated in Subsection 4.4.1, the design bases are adopted to prevent DNB from occurring and to prevent fuel melting during normal operation and AOOs. The protection systems described in Chapter 7 are designed to accommodate those requirements.

A summary of the steady-state thermal-hydraulic design parameters is presented in Table 4.4-1. The thermal responses of the core to transients are described in Chapter 15. Anticipated transient without scram (ATWS) is addressed in Subsection 15.8.

The low power and shutdown operation is described in Subsection 19.1.6, in which shutdown procedures including mid-loop operation and thermal-hydraulic characteristics of each operation mode are discussed, and the probabilistic risk assessment for the operation is addressed. Anticipated transients initiated at this operation, such as inadvertent boron dilution during Modes 4 and 5 and Mode 6, are discussed in Chapter 15.

4.4.4.5 Analytical Methods

4.4.4.5.1 RCS Flow Rate

The pressure drop across the RV which is used in determining RCS flow rates is estimated in the way described in Subsection 4.4.4.2. A set of RCS flows described in Section 5.1 is determined considering the uncertainties of pressure loss and pump characteristics.

4.4.4.5.2 Core Analysis

VIPRE-01M is used for the subchannel analyses to obtain the local thermal-hydraulic conditions and DNBRs in the core. It solves the set of conservation equations of mass, momentum and energy in the core for steady-state/transient, coupling with the constitutive models for the physical phenomena such as pressure drop, turbulent mixing and boiling which are described in Subsection 4.4.2.

VIPRE-01M is an extension of the VIPRE-01 code that has been developed and verified by Electric Power Research Institute (EPRI). The following functions for the design application has been added in VIPRE-01M as described in Reference 4.4-2.

- Design DNB correlations, WRB-1 and WRB-2, which are used to predict DNBR for Mitsubishi fuel design
- Fuel properties consistent with Mitsubishi fuel design code (Reference 4.4-4)
- Hot spot PCT analysis option
- Improvements on user interfaces

The second and third functions has been added for transient analysis in Chapter 15. Since the fundamental equations and constitutive models has been left as is in VIPRE-01, VIPRE-01M is capable to provide same local coolant conditions as VIPRE-01. VIPRE-01 is well verified by the extensive experimental verifications as described in Reference 4.4-11, and the results are also valid for VIPRE-01M.

The modeling options for predicting local conditions, which were included in original VIPRE-01, has been selected to provide conservative results as described in Subsection 4.4.2.9.1 and Reference 4.4-2. The applicability and uncertainty of the added design DNB correlation has been validated in Reference 4.4-2.

In the typical design analysis using VIPRE-01M, the fuel assembly with limiting power (hot assembly) is located at the center of the one-eighth symmetric core. The hot subchannels, which are faced with the limiting power rod (hot rod), and their immediate surrounding channels are modeled in detail, while the rest of the core is lumped into a relatively coarse mesh channels.

The hot rod has a limiting power corresponding to the design $F_{\Delta H}^{N}$ value described in Subsection 4.4.4.3.1. For RTDP analyses, the nominal value of $F_{\Delta H}^{N}$ which excludes uncertainty, $F_{\Delta H}^{U}$, is used. To minimize the flow mixing effect, the fuel assemblies surrounding the hot assembly are assumed to have the same power as the hot assembly, and mixing between fuel assemblies is conservatively neglected. Axial power distribution is described in Subsection 4.4.4.3.2.

The deposit of crud on the fuel cladding surface may cause a slightly higher fuel cladding surface temperature and consequently advance the onset of local boiling. VIPRE-01M does not account for such effect of crud directly. However, conservative treatment by the VIPRE-01M modeling method has been demonstrated to bound this effect in DNBR calculations (Reference 4.4-2).

4.4.4.6 Thermal-Hydraulic Instability

Thermal-hydraulic instability may lead the core to undesirable conditions such as reduction of DNB heat flux and/or vibration of the core components. Therefore such instability does not occur during normal operation and AOOs.

Generally, thermal-hydraulic instability is unlikely to occur at PWR operating conditions, where pressure and flow rate are high enough to suppress the change of flow characteristics resulting from the void generation. However, there are two types of potential flow instabilities for PWR operation, Ledinegg type static instability and the density-wave type dynamic instability.

The Ledinegg instability occurs when the slope of the RCS pressure drop versus flow rate curve becomes smaller than that of the pump head versus flow rate curve (Reference 4.4-17), and results in a sudden reduction in flow rate. However the reactor coolant pump head versus flow rate curve for the US-APWR has a negative slope, and the RCS pressure drop versus flow rate curve has a positive slope during normal operations and AOOs. As a result, the Ledinegg instability does not occur in the US-APWR RCS flow.

The physical mechanism which induces density-wave instabilities is well understood. The inlet flow fluctuations create enthalpy and void fraction perturbations in a boiling channel. The combined effect of flow and void fraction perturbations causes perturbations in two-phase pressure drop. Since the total pressure drop across the boiling channel that connects with common headers of parallel channels in the reactor core is nearly constant, the perturbation involved in the two-phase pressure drop feeds back to the system at the inlet flow via acoustic or pressure wave propagation. Under certain operating and boundary conditions with certain geometrical arrangements, the perturbations can be self-sustained or enforced. The period of this oscillation is approximately the time to travel through the channel.

In the US-APWR core, as in the core of typical light-water PWRs, RCS pressure is high and flow rate is large. The increase in system pressure or core flow rate at a given operational power level reduces the void fraction, and thus stabilizes the system.

In addition, US-APWR design adopts open-lattice fuel assemblies in the core. For such cores, flow resistance to lateral flow is insignificant. The two-phase pressure drop perturbation in any fuel assembly is quickly “dissolved” into the surrounding field, via the cross flow between fuel assemblies, and would not generate any real impacts on the inlet flow. Flow stability tests conducted using four parallel channels (Reference 4.4-18) indicate that a boiling flow system with cross-connections is more stable than a boiling flow system without cross-connections or a system having smaller number of channels. The cross-flow resistances simulated in the tests are greater than those in the US-APWR core. Therefore, cross-flow in the open-lattice fuel assemblies serves the function of subduing flow instabilities.

Consequently, density-wave instability will not occur in the US-APWR core under normal operation and AOOs because the void fraction will be small and an open-lattice fuel assembly is in-use.

In summary, significant oscillations induced by coolant flow perturbations will not cause instabilities in the US-APWR core.

4.4.5 Testing and Verification

4.4.5.1 RCS Flow Measurement

As described in Chapter 14.2.12.2, RCS flow measurement tests are performed prior to initial criticality and during start-up process. RCS elbow difference pressure and/or calorimetric data are used to estimate the coolant flow rates in the operating plant. The test verifies that coolant flow rates that have been used in the core thermal-hydraulic analysis are valid and agreeable.

4.4.5.2 Power Distribution Measurement

Power distributions are measured at several core power levels as described in Chapter 14. It is confirmed that the measured peaking factors are conservatively bounded by that adopted in the core thermal-hydraulic analyses.

4.4.5.3 Component and Fuel Inspections

The manufactured components and fuel are inspected and its details are described in Subsection 4.2.4. Fuel rod fabrication data related to thermal-hydraulic analyses, such as pellet and cladding dimensions and density are measured, and it is verified that all deviations and/or uncertainties are enveloped by the engineering hot channel factors described in Subsection 4.4.2.2.2.

4.4.6 Instrumentation Requirements

4.4.6.1 Thermal Power

The DNBR-related core condition and linear heat rate is limited by the over temperature and over power ΔT reactor trips, respectively. These protective functions are described in Section 7.2 and the necessary instrumentation for them is the following:

The temperature rise throughout the RV (ΔT) is used as an instrumentation parameter, which reflects the reactor core thermal power.

The over temperature and over power ΔT reactor trip setpoint is a function of Pressurizer pressure, average coolant temperature for RV, and axial power imbalance. The axial power imbalance is obtained from ex-core neutron detectors.

Further descriptions of the reactor trip systems and their associated instrumentations are contained in Section 7.2.

4.4.6.2 Power Distributions

The power distribution in the reactor core is an important parameter for DNB and fuel rod temperature calculations and must be controlled within allowable design ranges. Power distribution monitoring is provided by a combination of in-core and ex-core instrumentation.

Source-range, intermediate-range, and power-range ex-core neutron flux detectors are used to limit the maximum power output of the reactor within their respective power ranges. The three power ranges of detectors are used to monitor neutron flux from a completely shutdown condition to the overpower condition at 120 percent. The power range channels are intended to protect the core against the consequences of rod ejection accidents, to protect the core against the consequences of adverse power distributions resulting from dropped control rods, to provide the control function of rod movements, and to alert the operator to excessive quadrant power tilt.

The ex-core neutron detectors are used to provide continuous monitoring of axial flux difference ΔI. The axial power distribution variation, which is caused by control rod motion as well as power and xenon transients, can be controlled by limiting ΔI.

The ex-core nuclear instrumentation system is described in Section 7.2.

ICIS is used to measure flux distributions and temperatures.

The incore instrumentation consists of movable neutron detectors (MDs) and core exit thermocouples (TCs). For flux distribution measurements, MDs are inserted into the core through the detector guide thimbles. The detector guide thimbles are inserted into the active core through the RV upper head and reactor internals, which lead the detector guide thimbles to the fuel assemblies, and cover the effective axial fuel length. The detector guide thimbles are fairly uniformly distributed over the core.

The signal processing equipment integrated into the ICIS allows signals to be used to construct an accurate three-dimensional core power distribution suitable for calibrating the ex-core nuclear detector input to the over temperature and over power ΔT reactor trip setpoints.

Core exit temperatures are continuously measured with TCs. TCs provide additional information for radial core power distributions.

Details of the nuclear instrumentation and the control and trip logic are given in Section 7.2. The limits on neutron flux operation and trip setpoints are specified in the technical specifications.

4.4.6.3 Other Monitoring

Other non-safety-related monitoring systems are installed for diagnostics of RV and RCS operating condition.

The loose parts monitoring system provides early detection of loose metallic parts in the RCS. The system is designed to have following characteristics in compliance with Regulatory Guide 1.133 (Reference4.4-19).

The system is an automatic detection system and contains multiple redundant instrumentation channels. Each channel includes a field mounted sensor (piezoelectric accelerometer), preamplifier, signal processing equipment and signal recorder.

The system is designed, as a minimum, to detect a metallic loose part that weighs from 0.25 to 30 lb and impacts with a kinetic energy of 0.5 ft-lb on the inside surface of the RCS pressure boundary within 3 ft of a sensor.

False impact detection, attributable to normal hydraulic, mechanical, and electrical noise, is minimized through the impact detection algorithm:

- Acoustic transients due to known plant operations, such as pump transients, are correlated by time and type of impact and are not alerted as a loose part detection.

- Recurring transients, such as those caused twice within a minute, are more likely to be considered a loose part detection than those that occur at random intervals longer than one minute.

- A floating signal, which is generally attributed to background noise, is used as the approach for setting a reference noise level.

The sensors are strategically located at fixed positions on the RCS to maximize positive impact detection. These positions include the upper and lower plenums of RV and the

inlet plenum of each steam generator, which provide broad coverage. At least two redundant sensors are mounted at each location and physically separated from each other. Sensors are carefully mounted to minimize the effect of mechanical force and thermal expansion.

Calibration is performed prior to plant startup. The system is capable of periodic online channel checks, such as real-time audio monitoring and channel functional tests, and offline channel calibrations during refueling outages.

Components within containment are designed and installed to perform their function through and following an earthquake of half the magnitude of a safe-shutdown earthquake (SSE), as well as normal operating radiation, vibration, temperature and humidity environment.

Other operational concerns are described in following chapters:

- Operating and diagnostic procedures, including maintenance and testing: Chapter 16.
- The training program for plant personnel: Chapter 13.
- Procedures for minimizing radiation exposure to station personnel during maintenance, calibration and diagnostic procedures: Chapter 12.

The core internal monitoring systems (ex-core neutron detectors) can be used to provide continuous monitoring of core vibration. The detected signals are recorded and analyzed based on a spectrum analyzer. Since the vibration frequencies and amplitudes are measured in a preoperational test, the correlation between the detected signals and the core vibration characteristics can be established.

4.4.6.4 Inadequate Core Cooling

For the monitoring of the post-accident inadequate core cooling, degree of subcooling, RV water level and core exit temperature will be measured as described in Section 7.5. Monitoring the degree of subcooling indicates loss of subcooling, occurrence of saturation and recovering to subcooled condition. The RV water level provides information on the decreasing liquid inventory in the reactor. The core exit temperature indicates the increasing steam temperatures associated with inadequate core cooling and the decreasing steam temperatures associated with recovery from inadequate core cooling.

4.4.7 Combined License Information

COL 4.4(1) Deleted

4.4.8 References

4.4-1 General Design Criteria for Nuclear Power Plants, NRC Regulations Title 10, Code of Federal Regulations, 10 CFR Part 50, Appendix A.

4.4-2 Thermal Design Methodology, MUAP-07009-P (Proprietary) and MUAP-07009-NP (Non-Proprietary), May 2007.

4.4-3 Friedland, A. J. and Ray, S., Revised Thermal Design Procedure, WCAP-11397-P-A (Proprietary) and WCAP-11397-A (Non-Proprietary), April 1989.

4.4-4 Mitsubishi Fuel Design Criteria and Methodology, MUAP-07008-P, Revision 2 (Proprietary) and MUAP-07008-NP, Revision 2 (Non-Proprietary), July 2010.

4.4-5 Davidson, S. L. and Kramer, W. R. (Ed.), Reference Core Report VANTAGE 5 Fuel Assembly, WCAP-10444-P-A (Proprietary) and WCAP-10445-NP-A (Non-Proprietary), September 1985.

4.4-6 Tong, L. S., Boiling Crisis and Critical Heat Flux, AEC Critical Review Series, TID-25887, 1972.

4.4-7 Tong, L. S., Critical Heat Fluxes in Rod Bundles, Two Phase Flow and Heat Transfer in Rod Bundles, Annual Winter Meeting ASME, p. 31-46, November 1968.

4.4-8 Motley, F. E., Cadek, F. F., DNB Test Results for R-Grid Thimble Cold Wall Cells, WCAP-7695, Addendum 1-P-A (Proprietary) and WCAP-7958 Add 1-A (Non-Proprietary), January 1975.

4.4-9 Hill, K. W., Motley, F. E., and Cadek, F. F., Effect of Local Heat Flux Spikes on DNB in Non-Uniformly Heated Rod Bundles, WCAP-8174-P-A (Proprietary) and WCAP-8202-A (Non-Proprietary), February 1975.

4.4-10 Skaritka, J., Ed, Fuel Rod Bow Evaluation, WCAP-8691, Revision 1 (Proprietary) and WCAP-8692, Revision 1 (Non-Proprietary), July 1979.

4.4-11 Stewart, C. W., et al., VIPRE-01: A Thermal-Hydraulic Code for Reactor Core, Volume 1-4 (Revision 4, February 2001), Volume 5 (March 1988), NP-2511-CCM-A.

4.4-12 Dittus, F. W., and Boelter, L. M. K., Heat Transfer in Automobile Radiators of the Tubular Type, California University Publication in Engineering 2, No. 13, 443461, 1930.

4.4-13 Weisman, J., Heat Transfer to Water Flowing Parallel to Tube Bundles, Nuclear Science Engineering 6, pp 78-79, 1959.

4.4-14 Tong, L.S. and Weisman, J., Thermal Analysis of Pressurized Water Reactors, Second Edition, American Nuclear Society, 1979.

4.4-15 Letter from A. C. Thadani (NRC) to W. J. Johnson (Westinghouse), Subject: Acceptance for Referencing of Licensing Topical Report, WCAP-9226-P/9227-NP, Reactor Core Response to Excessive Secondary Steam Releases, January 31, 1989.

4.4-16 McFarlane, A. F., Power Peaking Factors, WCAP-7912-P-A (Proprietary) and WCAP-7912-A (Non-Proprietary), January 1975.

4.4-17 Boure, J. A., Bergles, A. E., and Tong, L. S., Review of Two-Phase Flow Instability, Nuclear Engineering Design 25, pp 165-192, 1973.

4.4-18 Kakac, S., et al., Sustained and Transient Boiling Flow Instabilities in a Cross-Connected Four-Parallel-Channel Upflow System, Proceeding of 5th International Heat Transfer Conference, Tokyo, September 1974.

4.4-19 Loose-Part Detection Program for the Primary System of Light-Water-Cooled Reactors, NRC Regulatory Guide 1.133, May 1981.

4.4-20 Vogtle Electric Generating Plant, Updated Final Safety Analysis Report Revision 12, November 5, 2004.

4.4-21 South Texas Project Electric Generating Station (STPEGS) Units 1 and 2, Updated Final Safety Analysis Report (UFSAR), Revision 12, September, 2004.

Table 4.4-1 Thermal-Hydraulic Comparison between US-APWR and Other Designs (Sheet 1 of 2)

Design Parameters	US-APWR	Typical 12-ft 4-loop PWR (Ref. 4.4-20)	Typical 14-ft 4-loop PWR (Ref. 4.4-21)
Core thermal output (MWt)	4,451	3,565	3,853
System pressure (psia)	2,250	2,250	2,250
Coolant conditions			
Minimum measured flow rate, MMF			
(10^6lbm/hr)	172.5	142.9	-
(gpm)	460,000	384,000	-
Thermal design flow rate, TDF			
(10^6lbm/hr)	168.2	139.4	145.0
(gpm)	448,000	374,400	-
Effective flow rate for core cooling			
(10^6lbm/hr)	153.1 (a)	130.5	132.7
(gpm)	407,680 (a)	350,440	-
Effective flow area for core cooling (ft^2)	68.0	54.1	51.3
Core average coolant velocity (ft/s)	14.1 (a)	15.4	15.6
Core average coolant mass velocity (10^6lbm/hr-ft^2)	2.25 (a)	2.41	2.59
Coolant Temperature			
RV/core inlet (°F)	550.6	556.8	549.8 to 561.2
Average rise in RV (°F)	66.4 (a)	63.2	63.6 to 65.0
Average rise in core (°F)	72.1 (a)	66.9	68.7 to 70.3
Average in RV (°F)	583.8 (a)	588.4	582.3 to 593.8
Average in core (°F)(b)	588.8 (a)	592.2	586.9 to 597.8
Heat transfer at normal condition			
Fraction of heat generated in fuel (%)	97.4	97.4	97.4
Effective heat transfer area on fuel surface (c) (ft^2)	91,360	57,505	69,700
Heat flux (c) (10^6Btu/hr-ft^2)			
Core average	0.162	0.206	0.181
Local peak	0.421 (d)	0.515	0.489
Linear heat rate (c) (kW/ft)			
Core average	4.65	5.69	5.20

Table 4.4-1 Thermal-Hydraulic Comparison between US-APWR and Other Designs (Sheet 2 of 2)

Design Parameters	US-APWR	Typical 12-ft 4-loop PWR (Ref. 4.4-20)	Typical 14-ft 4-loop PWR (Ref. 4.4-21)
Local peak	12.1 (d)	14.2	14.0
Power density (e) (kW/l)	89.2	109.2	98.8
Specific power (kW/kg uranium)	32.0 (f)	42.5	36.4
Minimum DNBR at nominal condition			
Typical hot channel	2.05	2.47	2.19
Thimble hot channel	1.98	2.33	2.11
Minimum DNBR during AOOs			
Typical hot channel	$\geq$1.35	$\geq$1.24	$\geq$1.26
Thimble hot channel	$\geq$1.33	$\geq$1.23	$\geq$1.24
Correlation used for above DNBR values	WRB-2	WRB-2	WRB-1
Maximum peak linear heat rate during AOOs (c) (g) (kW/ft)	$\leq$ 21.9 (assuming overpower of 120%)	$\leq$ 22.4 (assuming overpower of 120%)	$\leq$22.0 (assuming overpower of 118%)
Maximum fuel centerline temperature during AOOs (°F)	$\leq$ 4,620	$\leq$ 4,700	$\leq$ 4,700
Pressure drop (h) (psi)			
Across core	32.1$\pm$3.2	25.8$\pm$2.6	39.78$\pm$4.0
Across RV	48.2$\pm$4.8	48.5$\pm$4.9	62.68$\pm$8.9

Notes:

(a) Based on thermal design flow and design core bypass flow (9.0%)

(b) Based on average enthalpy

(c) Based on densified active heated length

(d) Based on heat flux hot channel factor, F_Q = 2.60

(e) Based on cold dimensions

(f) Based on 97% of theoretical density fuel

(g) See Subsection 4.4.2.11.5

(h) Based on best estimate flow rate

Table 4.4-2 RCS Pipe Fittings

Elbows (°)	Size (in)	Radius (in)	Quantity
50	31	54	4
40	31	54	4
90	31	54	8
22. 59’	31	54	4

Table 4.4-3 RCS Thermal Design Flow

Flow	Flow Rate (TDF)
RCS Flow	448,000 gpm
Core Bypass Flow	9 %
Core Flow	91 %

Table 4.4-4 Geometries of Reactor Coolant System Components

Component	Flow Path Length (ft)	Height (ft)	Bottom Elevation[a] (Liquid Level[a]) (ft)	Flow Area (ft^2)	Volume (ft^3)
Hot Leg	17.9	2.6[b]	0[c]	5.2	94
Crossover Leg	28.5	2.6[b]	-10.4[c]	5.2	149
Cold Leg	23.1	2.6[b]	0[c]	5.2	121
Pressurizer	-	62.8	18.9 (48.7)	50.7	2900
Surge Line	72.3	1.1[b]	1.3	0.9	65
Steam Generator					
- Plenum	-	7.9	2.2	5.2	468
- Tubes	-	36.2	10.1	16.2	1120
RV					
- Inlet Nozzle	5.0	2.6[b]	0[c]	5.2	124
- Downcomer	-	28.7	-22.3	43.6	1120
- Lower Plenum	-	9.8	-29.4	68.0[d]	1130
- Active Core	-	13.8	-19.6	68.0[d]	925
- Upper Plenum	-	9.3	-5.8	68.0[d]	1390
- Neutron Reflector	-	13.8	-19.6	5.3	297
- Upper Head	-	10.4	3.5	0.5	1300
- Outlet Nozzle	5.3	2.6[b]	0[c]	5.2	113

Notes:

(a) Based on RV nozzle center = 0.0

(b) Represented by inner pipe diameter

(c) For pipe center line

(d) Represented by core flow area

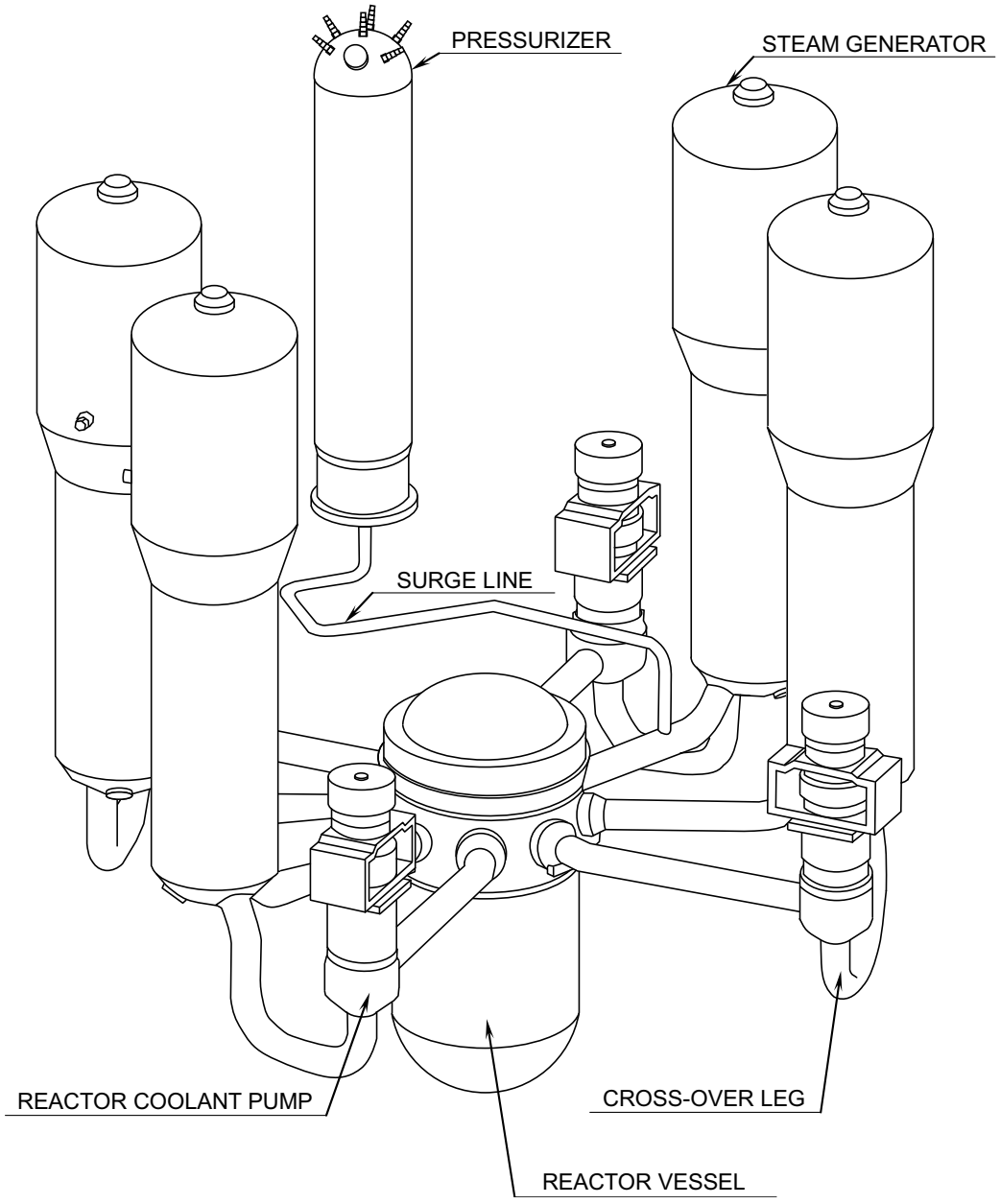

Figure 4.4-1 Isometric View of the Reactor Coolant System

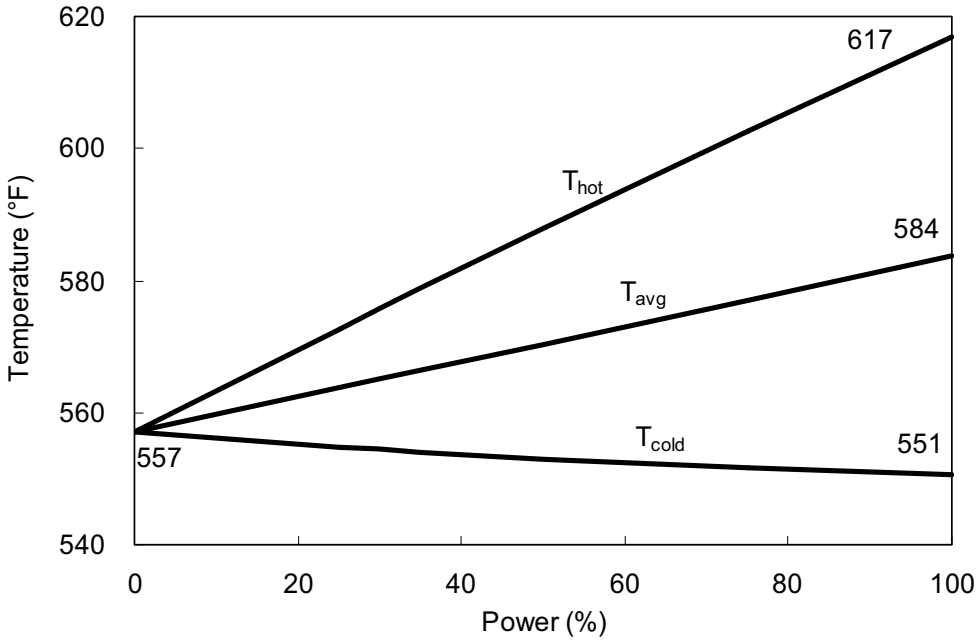

Figure 4.4-2 Typical Temperature-Power Operating Map

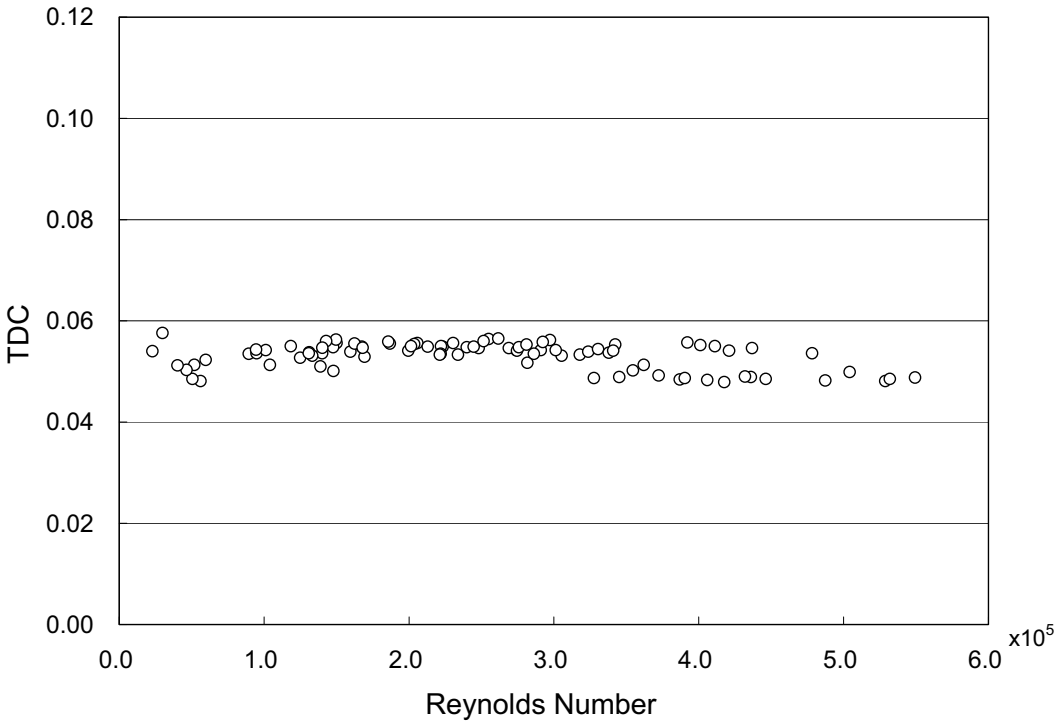

Figure 4.4-3 Thermal Diffusion Coefficient for Intermediate Grid Spacer (Z3 Type) of the US-APWR Fuel

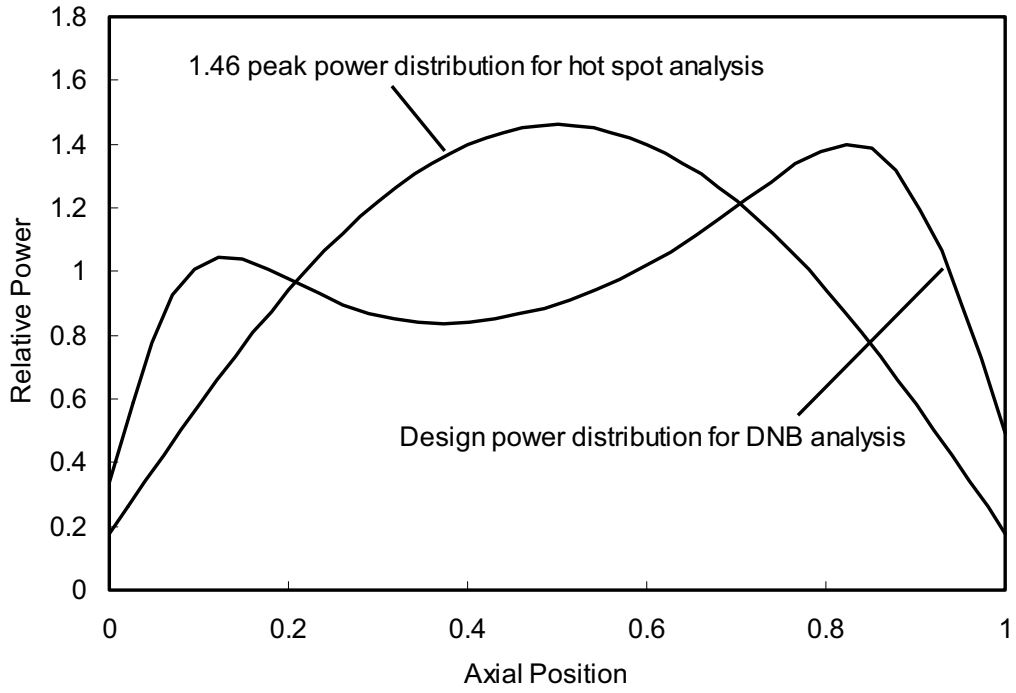

Figure 4.4-4 Axial Power Distributions

4.5 Reactor Materials

This section demonstrates the adequacy of the materials selected for the US-APWR control rod drive system (CRDS) and the reactor Internals and core support structures. All such materials used in the US-APWR have been used successfully for these applications in the United Sates and Japanese PWR.

Subsection 4.5.1 describes the structural materials used in the CRDS. Subsection 4.5.2 describes the materials used in the reactor internals and the core support structure.

To avoid duplication, Section 4.5 refers to Subsection 5.2.3 for additional information on materials specifications and details on matters such as compatibility of the materials with the reactor coolant and control of welding processes.

4.5.1 Control Rod Drive System Structural Materials

This subsection begins with a description of the material specifications. It then addresses austenitic stainless steel components, other materials, and cleaning and cleanliness control. Table 4.5-1 lists the materials of interest.

Information in this subsection addresses relevant requirements of the following General Design Criteria (GDC) of 10 CFR 50, Appendix A (Reference 4.5-1):

- GDC 1, as it relates to quality standards for structures, systems, and components important to safety
- GDC 14, as it relates to low probability of abnormal leakage, rapidly propagating failure, or gross rupture
- GDC26, as it relates to reactivity control system redundancy and capability

This subsection also demonstrates that CRDS structural materials are designed, fabricated, tested, and inspected to quality standards commensurate with the importance of their safety function consistent with 10 CFR 50.55a (Reference 4.5-2).

The CRDS, for purposes of this subsection, is considered to be comprised of the control rod drive mechanisms (CRDMs). It does not include the electrical and hydraulic systems necessary to actuate the CRDMs.

The rod control cluster assembly (RCCA) is described in Section 4.2. Type 403 martensitic stainless steel used for the coupling of the drive rod assembly undergoes a proprietary heat treatment process that achieves the desired coupling stiffness and toughness.

4.5.1.1 Material Specifications

Austenitic stainless steel, nickel based alloys, and cobalt based alloys are selected for CRDM components that are in contact with the reactor coolant water because of their corrosion resistance. The material specifications are listed in Table 4.5-1. The dissolved oxygen level of primary coolant water is controlled to less than 0.1%. This low dissolved

oxygen content water flows into the CRDM housing by thermal siphoning flow and drive rod movement with CRDM stepping and rod drop testing. Thus, the dissolved oxygen level at the inside of CRDM pressure housing is the same as the primary coolant water shortly after startup. In summary, a stagnant primary coolant environment that could result in dissolved oxygen content greater than 0.10 ppm during the plant operation does not exist in any portion of the CRDM.

The properties of the materials selected for the CRDM are found in Section III, Appendix I, Division 1 of the ASME Boiler and Pressure Vessel Code (ASME Code) (Reference 4.5-3) or Section II, Parts D of the ASME Code. Strain hardened and/or cold worked austenitic stainless steels are not used in CRDM components.

All other materials for use in this system are selected for their compatibility with the reactor coolant water, as described in NB-2160 and NB-3120 of the ASME Code. The tempering temperature of martensitic stainless steels are specified to avoid temper britteness. In the case of Type 410 stainless steel; it is tempered above 1050°F.

The metallic and nonmetallic materials used in the CRDMs are the same as those used in operating plants in the United States and Japan.

4.5.1.1.1 Pressure Housing

The pressure housing material in contact with the reactor coolant water is type 316 austenitic stainless steel, which meets the requirements of ASME code Section III. Detailed description of the austenitic stainless steel for pressure housing material is given in Subsection 5.2.3. The material of the CRDM pressure housing is identified in Tables 4.5-1.

Flux rings made from ferrite material are attached around the latch housing to provide a magnetic flux route.

4.5.1.1.2 Latch Assembly

The material for the latch assembly, magnetic poles, plungers and keys is type 410 martensitic stainless steel. Where strength is not an issue, annealed type 410 stainless steel is used because of its superior magnetic properties. Springs are made of Alloy X-750. Link pins are made of cobalt alloy. Tip and pin holes of the latch arms are clad with the cobalt alloy, Stellite. Cobalt cladding is used to improve resistance for wear. Other parts are made of type 304 austenitic stainless steel. Hard chrome plating is applied for sliding surfaces. Chrome carbide coating is applied on the tips of the latch arms to improve resistance to wear.

4.5.1.1.3 Drive Rod Assembly

The material for the drive rod assembly, drive rod, unlatch button and protection sleeve is type 410 martensitic stainless steel. The coupling is fabricated from type 403 martensitic stainless steel. Springs are made of Alloy X-750 and the locking button is fabricated from cobalt alloy. Other drive rod assembly parts are made from type 304 austenitic stainless steel.

4.5.1.1.4 Coil Assembly

The coil housings in the coil assembly are ductile iron castings, selected for their suitable magnetic properties. Coils are wound on bobbins of molded glass silicon resin material, with double glass insulated copper wire. Coils are impregnated with silicon varnish under vacuum condition. A wrapping of mica sheet is secured to the coil outside diameter. The coil assembly is a proven design used in many operating plants in the United States and Japan.

4.5.1.2 Austenitic Stainless Steel Components

Austenitic stainless steel base materials for CRDM applications are used in the solution annealed condition and are not heated above 800 °F after solution annealing, other than locally by welding operations, in accordance with the recommendations listed in RG 1.44. The welding materials used for joining the austenitic stainless steels meet the requirements of the welding material specification SFA 5.9 in ASME Code Section II. In addition, the above welding materials meet the requirements of ASME Code Section III. For design temperatures up to and including 800 °F, the minimum acceptance delta ferrite is 5FN (Ferrite Number).

Manufacturing process controls for preventing intergranular corrosion of stainless steel components are used in accordance with the guidance in RG 1.44 (Reference. 4.5-5). Furnace sensitized material is not allowed for the CRDM pressure housing, and methods described in the guide are followed for cleaning and protecting austenitic stainless steels from contamination during handling, storage, testing, and fabrication and for determining the degree of sensitization during welding.

Weld metals for the pressure boundary and non-pressure boundary of CRDM components are used in accordance with the guidance in RG 1.31 (Reference 4.5-9).

The process controls during manufacturing for abrasive work on austenitic stainless steel surfaces are designed to prevent contamination that may result in stress corrosion cracking. These controls are consistent with Regulatory Position C of RG 1.37 (Reference 4.5-6).

The final surfaces are required to meet the acceptance standards specified in ASME NQA-1 (Reference 4.5-7). Tools used on austenitic stainless steel surfaces are controlled to prevent materials that could contribute to stress corrosion cracking from contaminating these surfaces.

4.5.1.3 Other Materials

MIL-S23192 (Reference 4.5-8) is the standard that will be used for spring material made from X-750. This standard requires solution heat treatment and aging heat treatment to preclude SCC. This material has not observed stress corrosion cracking which is based on experience in operating plants.

Cobalt alloy for pins is ordered in the solution treatment and strain hardened condition. This material is used in the link pins, and has not observed stress corrosion cracking which is based on experience in operating plants.

Ferrite material is used for flux rings which are attached on the outer surface of the latch housing to make magnetic flux route.

4.5.1.4 Cleaning and Cleanliness Control

Cleaning and cleanliness tests are performed on all parts of the CRDM before assembling. Cleaning and cleanliness tests of the outer surface and the accessible area of the inner surface of subassemblies are performed after the functional test. Cleaning and cleanliness control shall comply with description in Subsection 5.2.3.4.1. Onsite cleaning and cleanliness control will be carried out in accordance with ASME NQA-1 and provisions of RG-1.37 (Reference 4.5-6).

4.5.2 Reactor Internals and Core Support Materials

This subsection addresses controls on welding and nondestructive examination. It then discusses fabrication and processing of austenitic stainless steel, including cleaning and contamination protection standards. It closes with a description of materials other than austenitic stainless steel that are used in the reactor internals and core support materials. Table 4.5-2 lists materials of interest. Description of the reactor internals and the core support structures are identified in Subsection 3.9.5.

Information in this subsection addresses relevant requirements of:

- GDC 1 of 10 CFR 50, Appendix A (Reference 4.5-1) as it relates to quality standards for structures, systems, and components important to safety; and

- 10 CFR 50.55a (Reference 4.5-2) as it relates to reactor internals and core support structures being designed, fabricated, tested, and inspected to quality standards commensurate with the importance of their safety function.

This subsection also demonstrates the adequacy of the materials selected for the construction of the reactor internals and core support structures in relation to Section III of the ASME Code (Reference 4.5-3) NG-1120.

The reactor internals and the core support structures in this subsection include all structures and components within the pressure vessel other than the fuel, in-core control components, and instrumentation.

4.5.2.1 Material Specifications

The material specifications for type 304 stainless steel used in core support structures and reactor internals are mostly forgings, plate, and bar. Other materials are also listed in table 4.5-2, as discussed in Subsection 4.5.2.5, used in limited applications are:

- Strain hardened type 316 stainless steel for threaded structural fasteners

- Alloy 690 for the radial support clevis inserts

- Type 403 F (modified) martensitic stainless steel for the hold-down spring

- Alloy X-750 for the radial support clevis insert bolts and springs
- Alloy X-750 or strain hardened type 316 stainless steel for guide tube support pins
- Stellite hardfacing of support keys and clevis inserts
- Type 316 stainless steel for incore instrumentation detector guide thimble and pressure retaining blocks of the incore instrumentation guide column
- Type 304 stainless steel casting or forging for guide funnel of the CRDM thermal sleeve
- Chrome plating is performed on the thread of the neutron reflector tie rods and on the alignment pins between the neutron reflectors.
- Hard facing cladding by Cobalt alloy is performed on the alignment pins and on the clevis inserts.

Threaded structural fasteners and bolts are mostly fabricated from strain hardened type 316 stainless steel except for the radial support clevis insert bolts, which are fabricated from Alloy X-750. The guide tube support pins are fabricated from Alloy X-750 or strain hardened type 316 stainless steel. Strain hardened austenitic stainless steels are controlled to have a 0.2 percent offset yield strength that is no greater than 90,000 psi, which reduces the probability of stress corrosion cracking in these materials. Locking devices are mostly fabricated from type 304L austenitic stainless steel. Additional programs for assuring the bolting and threaded fasteners structural integrity are discussed in Subsection 3.9.5.

Process controls are performed during all stages of component manufacturing and reactor internals construction to avoid sensitization and exposure to stainless steel contaminants. Additional information on contaminant controls are discussed in Subsection 5.2.3.

Materials used in reactor internals and core support structures comply with the ASME Code, Section II supplemented by ASME Code Cases N-4, as approved in RG 1.84 (Reference 4.5-4). An additional material requirement is to closely control the amount of cobalt in the austenitic stainless steels and hard-facing.

Material requirements in NG-2000, design requirements in NG-3000, fabrication and installation requirements in NG-4000, and examination requirements in NG-5000 of ASME code are complied with in the US-APWR reactor internals and core support structures design specification.

The US-APWR reactor internals and core support structures materials and material specifications are listed in Tables 4.5-2. All the materials have had successful operational experience in the United States and Japanese PWRs, as noted previously.

4.5.2.2 Controls on Welding

Welding of reactor internals and core support structures follows the rules of NG-2000, NG-4000, and NG-5000 and Section IX “Welding and Brazing Qualifications” of the ASME Code. The discussions provided in Subsection 5.2.3 are applicable to the welding of reactor internals and core support components which are in accordance with ASME Code Section III Subsection NG-4000. For design temperatures up to and including 800 °F, the minimum acceptance delta ferrite is 5FN.

4.5.2.3 Non-destructive Examination

Acceptance criteria of the nondestructive examination are in accordance with the requirements of ASME Code Section III, NG-5300. The nondestructive examination of wrought seamless tubular products and fittings is in accordance with ASME Code Section III, NG-2500.

4.5.2.4 Fabrication and Processing of Austenitic Stainless Steel Components

Regulatory Guide 1.44 provides acceptance criteria for preventing intergranular corrosion of stainless steel components. In accordance with this guide, furnace sensitized material is not allowed by fabrication process controls. The methods described in RG 1.44 are incorporated in the cleaning and protection of austenitic stainless steel from contamination during handling, storage, testing, fabrication, and minimizing the degree of sensitization that might occur during welding. The discussion provided in Subsection 5.2.3 verifies conformance of reactor internals and core support structures with RG 1.44 (Reference 4.5-5).

The discussions provided in Subsection 5.2.3 verify conformance of reactor internals and core support structure materials with RG 1.31 (Reference 4.5-9).

The discussions provided in Subsection 5.2.3 related to contamination protection and cleaning of austenitic stainless steel are applicable to the reactor internals and core support structures and verify conformance with ASME code NQA-1 (Reference 4.5-7).

4.5.2.5 Other Materials

As noted in Subsection 4.5.2.1 there are several other specialized materials used in the reactor internals and are summarized in Table 4.5-2. The application of each of these specialized materials is discussed below. These materials have been successfully used in many operating plants in the United Sates and Japan.

Alloy 690 is used for clevis inserts that are bolted to the reactor vessel radial support . The clevis insert coefficient of thermal expansion is compatible with the reactor vessel material and bolting material, thereby reducing the thermal expansion differences and subsequent thermal stresses on the bolts. This material also has proven resistance against stress corrosion cracking.

Type 403 F (modified) martensitic stainless steel has been a standard material in operating PWR plants and is used for the hold-down spring which has high yield strength at operating temperatures.

Alloy X-750 is used for the radial support clevis insert bolts and springs, and may be used for the guide tube support pins. The application for the radial support clevis insert bolts is thermally compatible with the clevis insert and reactor vessel low alloy steel base metal. The application for the guide tube support pins is due to its high strength and its resistance to stress corrosion cracking. Strain hardened type 316 SS is an alternative material for the guide tube support pins and nuts.

Stellite hardfacing is applied to the clevis inserts, pins, and keys to minimize wear and fretting from flow-induced vibration effects.

4.5.3 Combined License Information

No additional information is required to be provided by a COL Applicant in connection with this section.

4.5.4 Reference

4.5-1 General Design Criteria for Nuclear Power Plants, NRC Regulations Title 10, Code of Federal Regulations, 10 CFR Part 50, Appendix A.

4.5-2 Codes and Standards, NRC Regulations Title 10, Code of Federal Regulations, 10 CFR 50.55a.

4.5-3 Design Stress Intensity Values, Allowable Stresses, Material Properties, and Design Fatigue Curves, ASME Boiler and Pressure Vessel Code Division 1, Section III Appendix I, 2001 Edition.

4.5-4 Design and Fabrication Code Case Acceptability ASME Section III Division 1, Regulatory Guide 1.84 Revision 33, August 2005.

4.5-5 Control of the Use of Sensitized Stainless Steel, NRC Regulatory Guide 1.44, May 1973.

4.5-6 Quality Assurance Requirements for Cleaning of Fluid Systems and Associated Components of Water-cooled Nuclear Power Plants, NRC Regulatory Guide 1.37, March 2007.

4.5-7 Quality Assurance Requirements for Nuclear Facility Applications, ASME Boiler and Pressure Vessel Code NQA-1 1994 Edition.

4.5-8 Springs, Helical, Age-hardenable Nickel-Chromium-Iron Alloy(UNS N07750), MIL-S-23192, November 1978

4.5-9 Control of Ferrite Content in Stainless Steel Weld Metal, NRC Regulatory Guide 1.31 Revision 3, April 1978.

Table 4.5-1 Summary of Control Rod Drive System Structural Materials

Component	Material Specification(1)	Environment
CRDM pressure housing material in contact with reactor coolant on the inside surface	SA-182 Grade F316(4), F316LN	Inside surface exposed to reactor coolant water
Flux Ring	ASTM A519 Gr.1015	Not exposed to reactor coolant water
Latch assembly - magnetic poles, plungers, and keys	SA-479 Type 410	Exposed to reactor coolant water
Latch assembly - springs	Alloy X-750 (ASME SB637 N07750)(2)	Exposed to reactor coolant water
Latch assembly - link pins	Cobalt alloy (HAYNES No. 25 or equivalent material(3))	Exposed to reactor coolant water
Latch assembly - other parts	SA-479 Type 304 SA-213 Grade TP 304	Exposed to reactor coolant water
Latch assembly - cladding on latch arm tips and pin holes	Cobalt alloy (Stellite No.6 or equivalent material(3))	Exposed to reactor coolant water
Latch assembly - plating on sliding surfaces	Chrome plate	Exposed to reactor coolant water
Latch assembly - coating on tips of latch arms	Chrome carbide	Exposed to reactor coolant water
Drive rod assembly - drive rod,	SA-268 TP410	Exposed to reactor coolant water
Drive rod assembly - unlatch button, protection sleeve	SA-479 Type 410	Exposed to reactor coolant water
Drive rod assembly - coupling	SA-479 Type 403	Exposed to reactor coolant water
Drive rod assembly - springs	Alloy X-750 (ASME SB637 N07750)(2)	Exposed to reactor coolant water
Locking button in the drive rod assembly and pins in the latch assembly	Cobalt alloy (HAYNES No. 25 or equivalent material(3))	Exposed to reactor coolant water
Drive rod assembly other parts	SA-479 Type 304	Exposed to reactor coolant water
Coil assembly - housing	ASTM A536 Grade 60-40-18	Not exposed to reactor coolant water
Coil assembly - coil bobbins	Glass silicone resin	Not exposed to reactor coolant water
Coil assembly - wire	Double glass insulated copper	Not exposed to reactor coolant water
Welding material used in CRDMs housing	SFA-5.9 ER316L EC316L	Inside surface exposed to reactor coolant water

Notes: (1) Additional information appears in the text of Section 4.5 and Subsection 5.2.3.
(2) Additional stringent specification, MIL-S-23192, is applied.
(3) Equivalent material is a substitute material having the same chemistry and properties as the preferred material. The same requirements would be specified in the procurement requirements.
(4) Maximum carbon content will be controlled under 0.05% (heat analysis) and 0.06% (product analysis) when standard grade stainless steel is used.

Table 4.5-2 Summary of Reactor Internals and Core Support Materials

Component	Material Specification(1)
Reactor vessel internals - primary material	SA-182 Grade F304 SA-336 Grade F304 SA-240 Type 304 SA-479 Type 304/ Type 304L SA-213 Grade TP 304 SA-312 Type 304
Reactor vessel internals - radial support clevis inserts	Alloy 690 (SB-166 N06690)
Reactor vessel internals - hold-down spring	ASME Code Case N-4-11 (AISI Type 403 Modified)
Reactor vessel internals - most threaded fasteners and bolts	SA-193 Class 2 B8M SA-479 Type 316 Strain hardened
Reactor vessel internals - radial support clevis insert bolts and spring	Alloy X-750 (ASME SB637 N07750)(2)
Reactor vessel internals - guide tube support pins	ASME SB637 N07750 SA-193 Class 2 B8M
Incore instrumentation detector guide thimble	SA-213 Grade TP 316
Pressure retaining block of the incore instrumentation support column	SA-479 Type 316
Guide funnel of the CRDM thermal sleeve	SA-182 Type 304 SA-351 CF8
Tie rods of neutron reflector	SA-479 Type 316 Strain hardened (with chrome plating on thread)
Alignment pins and clevis inserts	SA-182 Grade F304 SA-479 type 304 SA-240 type 304 (with cladding cobalt alloy, Stellite No.6 or equivalent material)
Reactor vessel internals - welding material	SFA-5.9 ER308L SFA-5.9 ER316L SFA-5.4 E308L

Notes: (1) Additional information appears in the text of Section 4.5 and Subsection 5.2.3.

(2) Additional stringent specification, MIL-S-23192, is applied for spring.

4.6 Functional Design of Reactivity Control System

This section demonstrates that the control rod drive system (CRDS) provides the required functional performance and is properly isolated from other equipment. The required functional performance involves the capability to effect a safe shutdown, respond within acceptable limits during anticipated operational occurrences, and prevent or mitigate the consequences of anticipated operational occurrences and postulated accidents.

This section describes how the design of the CRDS conforms to the requirements of the following General Design Criteria (GDC) of 10 CFR 50, Appendix A (Reference 4.6-1): 4, 23, 25, 26, 27, 28, and 29, as well as to the requirements of 10 CFR 50.62. (Reference 4.6-2)

Information in this section is organized into subsections that provide information on the CRDS (Subsection 4.6.1), describe evaluations of this system (Subsection 4.6.2), describe testing and verification of the system (Subsection 4.6.3), provide information on combined performance of reactivity systems (Subsection 4.6.4), and describe evaluations of combined performance of these systems (Subsection 4.6.5). This section refers to other chapters and sections for certain information to avoid duplication.

The reactivity control systems for the US-APWR include both the mechanical reactivity control of the control rods and the chemical reactivity control of the emergency core cooling system (ECCS). No credit for the reactivity control capabilities of the chemical and volume control system (CVCS) is taken for anticipated operational occurrences and postulated accidents described in Chapter 15.

4.6.1 Information for Control Rod Drive System

Subsection 3.9.4 describes the control rod drive mechanism (CRDM) in detail. This section includes drawings of the CRDM, component descriptions and characteristics. The rod control cluster assembly (RCCA) is inserted in the core by gravity, if electrical power of the CRDM coils is cut off. Electrical power to the CRDM coils is cut off by the reactor trip breakers which have under voltage attachment as the fail safe actuation device. Hydraulic systems are not used in the control of the CRDS.

The instrumentation and controls for reactor trip and reactor control are described in Sections 7.2 and 7.7 respectively. The cooling system for the CRDS is described in Subsection 9.4.6.

4.6.2 Evaluations of the CRDS

The CRDS is part of the reactor trip system. Detail of the failure mode and effects analysis (FMEA) on the CRDS is described in Reference 4.6-3. FMEA of the reactor trip system is described in Section 7.2. These analyses demonstrate that the CRDS performs a reactor trip when plant parameters exceed the reactor trip setpoint. By this performance, the reactor is placed in a subcritical condition with any assumed credible failure of any single active component, in compliance with GDC 25.

The pressure housing of the CRDM is designed, fabricated and inspected in accordance with the ASME Code. Failure of the pressure housing is not credible.

The essential elements of the CRDS, those are required to ensure a reactor trip, are isolated from the nonessential portions of the CRDS, as described in Section 7.2. The essential components of the CRDS are protected from the effects of postulated moderate and high energy water line breaks and associated missiles that are generated as a result, as described in Subsection 3.5.1.2.

In compliance with GDC 29, it has been confirmed that the probability of a common cause failure impairing the ability of the reactor trip system to perform its safety function is extremely low, because failure of the power supply to the CRDM leads to a reactor trip (Reference 4.6-3).

In addition, the US-APWR diverse actuation system (DAS) provides the anticipated transient without scram (ATWS) mitigation system that is diverse from the reactor trip system. The DAS automatically initiates the auxiliary feedwater system and a turbine trip under conditions indicative of an ATWS. These ATWS mitigation functions are mandated for Westinghouse type PWR plants by 10 CFR 50.62. The DAS also initiates a diverse reactor trip as described in Section 7.8. Therefore, the ATWS requirements are met. The US-APWR ATWS core damage frequency is discussed in Chapter 19 which describes the probabilistic risk assessment (PRA). The US-APWR design meets the ATWS rule (10 CFR 50.62) and its ATWS core damage frequency safety goal basis.

The design of the CRDM is such that failure of the CRDM cooling system will, in the worst case, result in an individual control rod trip or a full reactor trip.

4.6.3 Testing and Verification of the CRDS

The CRDS is tested in several phases. These tests may be categorized as follows:

- Prototype test of components
- Production tests of components following manufacture in shop
- Initial startup tests
- Periodic in-service tests

These tests, which are performed to verify the proper function of CRDS, are described in Subsection 3.9.4.4 and Section 14.2. They include rod insertion and withdrawal tests, scram test, and hydrostatic tests.

4.6.4 Information for Combined Performance of Reactivity Systems

As discussed in Chapter 15, the only postulated events which assume credit for two reactivity control systems to render the plant subcritical are the steam line break (SLB) and loss-of-coolant accident (LOCA).The reactivity control systems, for which credit is taken in these accidents, are the reactor trip system and the ECCS.

Additional information on the CRDS is presented in Subsection 3.9.4 and information on the safety injection system (SIS) of the ECCS is presented in Section 6.3.

No credit is taken for the boration capabilities of the CVCS as a system in the analysis of transients presented in Chapter 15. CVCS capability information is provided in Subsection 9.3.4. Although no credit is taken for the reactivity control capabilities of the CVCS, the adverse boron dilution possibilities due to the operation of the CVCS are discussed in Subsection 15.4.6. Proper operation of the CVCS prior to transients has been assumed as an initial condition to evaluate the transients, and appropriate technical specifications have been prepared to ensure the correct operation of the CVCS or the taking of necessary remedial actions.

4.6.5 Evaluations of Combined Performance

As described in Subsection 4.6.4 and Chapter 15, only a limited number of postulated events assume the availability of two reactivity control systems to prevent or mitigate the accident. The evaluations for SLB and the LOCA, which assume the combined actuation of the CRDS and the ECCS, are described in Chapter 15.

All the equipment through sensors to logic which initiates the protective action is redundant. This equipment is described in detail in Sections 7.2 and 7.3. In particular, protection from equipment failures is provided by redundant equipment and periodic testing. The failure mode and effects analysis described in Chapter 7 verifies that any single failure will not have a deleterious effect upon the engineered safety feature system.

With the exception of large break LOCA, no credit is taken for reactivity control systems other than reactor trip to maintain the reactor core subcritical. For large break LOCA, reactor trip is not assumed following the event occurs, and the core power can be suppressed only by the negative reactivity insertion due to increase in core void fraction during the initial phase of the event. Then, the borated water from the accumulators and SIS provides the negative reactivity to maintain the shutdown margin during the refilling of the core. Control rod insertion is credited to provide additional shutdown margin during long-term cooling.

For small break LOCA, the reactor core fission power can be suppressed by the negative reactivity due to the reactor trip in addition to the core void increase, and the core is maintained under the subcritical state throughout the event. Borated water from the accumulators and the high head injection system is credited to provide additional shutdown margin during long-them cooling.

Adequacy of the ECCS performance under faulted conditions is verified in Section 6.3.

4.6.6 Combined License Information

No additional information is required to be provided by a COL Applicant in connection with this section.

4.6.7 References

4.6-1 General Design Criteria for Nuclear Power Plants, NRC Regulations Title 10, Code of Federal Regulations, 10 CFR Part 50, Appendix A.

4.6-2 Requirements for Reduction of Risk from Anticipated Transients without Scram (ATWS) Events for Light-Water-Cooled Nuclear Power Plants, NRC Regulations Title 10, Code of Federal Regulations, 10 CFR Part 50.62.

4.6-3 FMEA of Control Rod Drive Mechanism Control System, MUAP-07015, December 2007.